

**✓SYNTHESIS AND CONDUCTIVITY STUDIES ON  
POLYMER SOLID ELECTROLYTES BASED ON  
POLYACRYLATE AND POLYPHOSPHAZENE  
SYSTEMS  
AND  
STUDIES ON ORGANIC POLYMERS CONTAINING  
CYCLOPHOSPHAZENE PENDANT GROUPS**

*A Thesis Submitted*  
in Partial Fulfilment of the Requirements  
for the Degree of  
**DOCTOR OF PHILOSOPHY**

868628

*by*  
**I. IMMANUEL SELVARAJ**

*to the*  
**DEPARTMENT OF CHEMISTRY  
INDIAN INSTITUTE OF TECHNOLOGY KANPUR  
DECEMBER, 1993**

என் அன்பு அம்மாவிற்கு ...



To my beloved mother

CHM-1993-D-SEL-SY

1 3 JUN 1994

CENTRAL LIBRARY  
I. I. T. KANPUR

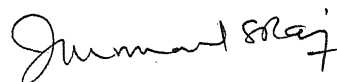
Acc. No. A. **117875**

TH  
504.7  
32498

### STATEMENT

I hereby declare that the matter embodied in this thesis entitled " SYNTHESIS AND CONDUCTIVITY STUDIES ON POLYMER SOLID ELECTROLYTES BASED ON POLYACRYLATE AND POLYPHOSPHAZENE SYSTEMS AND ORGANIC POLYMERS CONTAINING CYCLOPHOSPHAZENE PENDANT GROUPS ", is the result of investigations carried out by me in the Department of Chemistry, Indian Institute of Technology, Kanpur, India, under the supervision of Dr. V. Chandrasekhar.

In keeping with the general practice of reporting scientific observations, due acknowledgement has been made wherever the work described is based on the findings of other investigators.

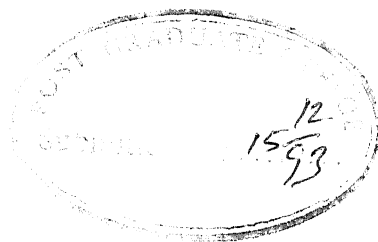


( I. IMMANUEL SELVARAJ )

KANPUR

DECEMBER 1993

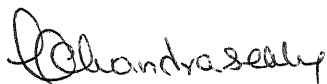




### CERTIFICATE

It is certified that the work contained in this thesis entitled " **SYNTHESIS AND CONDUCTIVITY STUDIES ON POLYMER SOLID ELECTROLYTES BASED ON POLYACRYLATE AND POLYPHOSPHAZENE SYSTEMS AND ORGANIC POLYMERS CONTAINING CYCLOPHOSPHAZENE PENDANT GROUPS** ", by **I.IMMANUEL SELVARAJ**, has been carried out under my supervision and the same has not been submitted elsewhere for a degree.

DECEMBER, 1993.

  
(Dr. V. Chandrasekhar)  
Thesis Supervisor  
Department of Chemistry  
IIT, Kanpur 208 016  
INDIA.

DEPARTMENT OF CHEMISTRY  
INDIAN INSTITUTE OF TECHNOLOGY  
KANPUR 208 016, INDIA

CERTIFICATE OF COURSE WORK

This is to certify that **Mr. I. IMMANUEL SELVARAJ** has satisfactorily completed all the courses required for the Ph.D degree. The courses include:

Chm 605	Principles of Organic Chemistry
Chm 624	Modern Physical Methods in Chemistry
Chm 625	Principles of Physical Chemistry
Chm 626	Solid State Chemistry
Chm 645	Principles of Inorganic Chemistry
Chm 668	Advanced Inorganic Chemistry II
Chm 800	General Seminar
Chm 801	Special Seminar
Chm 900	Post-Graduate Research

**Mr. I. IMMANUEL SELVARAJ** was admitted to the candidacy of the Ph.D degree in March, 1990 after he successfully completed the written and oral qualifying examinations.

*N. Sathyanurthy*  
HEAD  
Department of Chemistry  
IIT, Kanpur 208 016

*N. Sathyanurthy*  
CONVENOR, DPGC  
Department of Chemistry  
IIT, Kanpur 208 016

## ACKNOWLEDGEMENT

With utmost joy and sincerity I express my immense gratitude to my mentor Dr. V. Chandrasekhar, for his exemplary guidance, unstinted support and complete freedom. The faith he vested in me and the affection he showered upon me can never be forgotten and would serve as a tonic when tide strikes high in posterity. The association with him for the past few years will constitute the pleasant and cherishing memories of my life.

Two other good samaritans who deserve a place in my heart are Dr. T.K. Chandrashekar and Dr. N.S. Gajbhye. They have regarded me their younger brother and offered valuable suggestions; and their labs and offices were ever open to me.

It is my privilege to thank Dr. P.S. Venkataramani and Dr. P.T. Rajagopalan, Joint Directors, DMSRDE\*, Kanpur for making available all possible facilities of their labs, for their constant encouragement and benevolence.

I feel honoured to thank Dr. K. Shahi and Dr. K.N. Rai, Materials Science Programme, IIT Kanpur, for letting me use their Impedance Analyzer and for rendering all possible help; and Dr. Christopher W. Allen, Dept. of Chemistry, Univ. of Vermont, Burlington, USA for providing me the code for Mortimer-Tidwell method, making the computation possible.

I express my sincere gratitude to the following people for providing me with the Thermal data, reported in this thesis.

- Prof. (Mrs.) I.K. Verma, Centre for Materials Science and Technology, IIT Delhi.
- Dr. S. Sivaram, Head, Polymer Division, National Chemical Laboratory, Pune.
- Dr. Kulkarni, Dept. of Materials Science, IIT Bombay.
- Dr. Chakraborty, Dept. of Chemistry, IIT Bombay.
- Dr. D. Kunzru, Dept. of Chemical Engg., IIT Kanpur.

I gratefully acknowledge Dr. Ashok Khanna, Dept. of Chemical Engg., IIT Kanpur and M/s Asian Paints Ltd. Bombay, for the GPC data.

It gives great pleasure to recall the association with Dr. P. Manoravi, Physics Dept., Anna University, Madras; and Dr. S. Chaklanobis, Dept. of Physics, IIT Kanpur, towards conductivity studies. Here, I also mention my lab mates; Messrs. Murali, Rengarajan, Justin, Vivek, Venky, Dr. Tharmaraj, and Dr. E. Sampath Kumar for their cooperation and understanding.

---

\* - Defence Materials and Stores Research and Development Establishment

The camaraderie and devoted friendship of Jobie, Christie, Ilango, Kasi, Tamil, Thols, Kotts, Moorthi and Dr.V.Govindaraju is gratefully acknowledged. The inspiration and optimism, shown by them helped boost my morale when "going was tough".

I also thank the following friends for making me rich by their company: Gundu, Anbu, Dr.Ponnusamy, Dr.S.R.Pandian, Capt.Radha, Turbo, Pandimani, KVK, Victor, Uday, Nettayan, Haja, Suri-Pandian, Yogi, Alphonse, Raghu, Mansoor, Arul, Srini, Baga, Panju-Thalayan, Dr. D. Reddy, Ravikant, Kundu, Bhishma, Dada, Capt.Haddock, Raman, Urichaks, CKR, Rsel, Periyappa, Gundu-payyan, Umamahesh, Kullan, Thadiyan, Ramesh, Kuppi, Jeebu, Rasesu, Solai, Thirumathi, Ravi, Raghuraman, Naray, Jayshankar, Ramani, and fellow colleagues and faculty members of the Dept. of Chemistry.

I can never forget the hospitality and the culinary expertise of Mrs. Andal Ramesh, Mrs. Chitra Manoravi, and Mrs. Mohan.

The help of the following friends in the thesis preparation is gratefully acknowledged: Srini (Chief Engineer), Arumugam, Guru, Uma, Sivaguru, Tamil, Kasi, Ilango, and Sivarasan.

I gratefully acknowledge the financial assistance awarded by CSIR/UGC, which made this endeavour possible.

I thank Mr. Pant who typed the manuscript, Mr. Ganguly and Mr. Bajpai for the neat drawings and other employees of the institute who have helped me from time to time.

I use this opportunity to pay tributes to my father (late) Mr. G. Iyckiam, and my sister (late) Rani Akka. I also thank my family members; my mother, my brothers, my sisters, Jaya chithi and chithappa. Life wouldn't have been comfortable without their blessings and meticulous care.

It is with humility and sense of deep gratitude and a heavy heart, that I thank the crores of down-trodden fellow Indians, who by shedding their blood in poor living conditions, pay for the country's scientific research.

KANPUR  
DECEMBER 1993

I. IMMANUEL SELVARAJ

## SYNOPSIS

This thesis is divided into two parts viz., Part-A and Part-B.

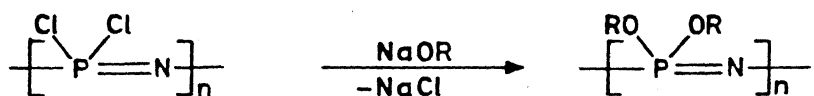
Part-A, consists of three chapters and deals with the "Synthesis and Conductivity Studies on Polymer Solid Electrolytes Based on Polyacrylate and Polyphosphazene Systems".

Part-B, deals with the "Studies on Organic Polymers Containing Cyclophosphazene Pendant Groups".

### Part-A

Polymer solid electrolytes are materials of high technological promise in several electrochemical applications such as high energy density batteries, gas sensors, electrochemical devices, etc.

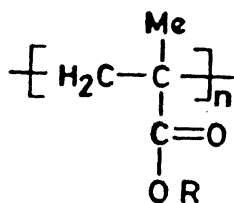
Chapter-I gives an overall review on polymer solid electrolytes including a brief note on conventional solid electrolytes. The most widely studied systems such as poly ethylene oxide, (PEO) and poly [bis(methoxy ethoxy ethoxy)phosphazene], (MEEP), have been reviewed in detail. Aspects such as conductivity measurements, phase diagram studies, mechanism of ion transport, and some of the applications of these electrolytes have been discussed. The limitations of these polymer electrolytes have also been pointed out. Thus PEO-alkali metal salt complexes show poor ionic conductivities at room temperature because of the high crystallinity of PEO. The polyphosphazene, MEEP, has poor mechanical properties and has a liquid like flow at ambient temperatures making its application in practical devices difficult. Further the purification of MEEP is cumbersome owing to the solubility of this material in water. MEEP is synthesised by a nucleophilic substitution reaction of the P-Cl bonds in poly(dichloro phosphazene) by the sodium salt of methoxy ethoxy ethanol.



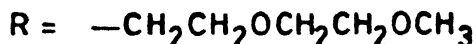
The sodium chloride formed in the reaction has to be separated from MEEP along with the unreacted sodium salt of the alcohol by a cumbersome dialysis procedure. In view of these limitations new synthetic strategies are required to make better polymer electrolytes. Keeping this in mind we have designed and assembled two types of polymer electrolytes, one based on an organic back bone Poly(MEEMA) and other on an inorganic back bone PP-I and PP-II.

Chapter II, describes the synthesis of Poly(MEEMA) and the conductivity studies of Poly(MEEMA)-alkali metal salt complexes.

Poly(MEEMA) is an acryloyl back bone containing polymer.



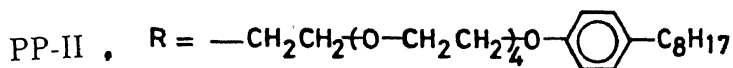
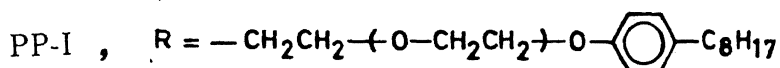
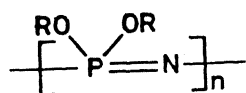
**Poly MEEMA**



The etheroxy side chain  $-\text{CH}_2\text{CH}_2\text{OCH}_2\text{CH}_2\text{OCH}_3$  has been chosen since in the polyphosphazene, MEEP, this side chain has been shown to be responsible for the high conductivities seen therein. It was felt that the more rigid acrylic back bone would increase the  $T_g$  of the polymer to have better mechanical properties at ambient temperatures in comparison with MEEP. Several Poly(MEEMA)-metal salt complexes were made by varying the O:Li ratios using  $\text{LiCF}_3\text{SO}_3$ ,  $\text{LiClO}_4$ , and  $\text{LiBF}_4$ . The polymer salt complexes were obtained as thin films and their conductivities studied over a wide temperature range (room temperature to

80° C) by complex impedance spectroscopy. Poly(MEEMA)-Li salt complexes show high room temperature conductivities. The highest conductivity at room temperature was observed for Poly(MEEMA)- LiBF<sub>4</sub> complex with O:Li ratio of 5:1 ( $7.9 \times 10^{-5} \Omega^{-1} \text{ cm}^{-1}$ ). This is among the highest conductivity displayed by polymer electrolytes. The conductive behaviour has been found to be obeying the VTF equation. By curve fitting analysis, parameters such as pseudo activation energy for the conduction of ions and  $T_0$  values (closely related to glass transition temperature) have been compiled. A comparison of these systems with literature data is made. It is found that the amorphous nature of Poly(MEEMA), ( $T_g$  -26.5°C) enables good ionic conductivities in Poly(MEEMA)-alkali metal salt complexes.

Chapter III, describes the synthesis and conductivity studies on PP-I and PP-II.

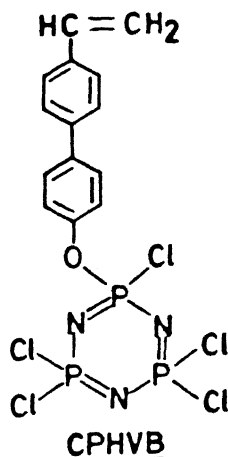


The rationale for the choice of the side chains is as follows. The alkyl chain substituted phenyl groups are expected to increase the glass transition temperatures of these polymers in comparison with MEEP. Further the long alkyl chains while rendering hydrophobicity would also make the polymer soluble in a wide range of organic solvents. These expecta-

tions have been realised in the synthesis of PP-I and PP-II. The small molecule  $N_3P_3(OR)_6$ ,  $R = -CH_2CH_2OCH_2CH_2O - C_6H_4 - C_8H_{17}$ , have also been synthesised. This served as a model reaction for the synthesis of PP-I and PP-II. PP-I.LiClO<sub>4</sub> complexes did not show good ionic conductivity, whereas PP-II.LiBF<sub>4</sub> complexes showed high conductivity values at higher temperatures. These aspects are discussed in this Chapter.

## Part-B

Chapter IV, describes about cyclophosphazene pendant polymers. The synthesis of a cyclophosphazene monomer, CPHVB, and copolymerization studies of CPHVB with other organic monomers viz., methylacrylate, ethylacrylate, methylmethacrylate, and styrene are presented in this chapter.



The results obtained from the analysis of the copolymers suggest the following conclusions:

- (i) the cyclophosphazene ring is intact in all copolymers,



- (ii) there is no structural change occurring in cyclophosphazene ring in any copolymer irrespective of the organic comonomer,
- (iii) even small incorporation of CPHVB in the copolymer gives extremely good thermal stabilities and the char yields of the copolymers in general are more than 60% at 600°C,
- (iv) all copolymers are flame retardant materials presumably due to the presence of P-Cl bonds present in the cyclophosphazene ring of CPHVB,
- (v) the molecular weight of the copolymers increase with an increased content of CPHVB in the copolymer,
- (vi) the reactivity ratios have been evaluated by Finemann- Ross and Mortimer-Tidwell methods, suggest that all copolymers form "Block" copolymers, i.e.,  $r_2(\text{CPHVB}) > 1$ ,
- (vii) using the  $r_1$  and  $r_2$  values obtained from the copolymerization Q and e parameters have been obtained for CPHVB, the large Q values suggest that the olefin functionality in the monomer is stabilized by conjugation, and negative e values obtained suggest that the  $\sigma$ -electron withdrawing effect of cyclophosphazene ring is not felt at vinyl centre of the monomer. These results are compared with other cyclophosphazene pendant monomers.

# CONTENTS

## PART I

### SYNTHESIS AND CONDUCTIVITY STUDIES ON POLYMER SOLID ELECTROLYTES BASED ON POLYACRYLATE AND POLYPHOSPHAZENE SYSTEMS

#### CHAPTER I INTRODUCTION

1.1	General Requirements for a Polymer Electrolyte	29
1.2	Electrical Measurements and Ion Transport in Polymer Electrolytes	56
1.2.1	Electrical Measurements	56
1.2.2	Phenomenological Models	77
1.2.3	Arrhenius Model	77
1.2.4	Free Volume Model	88
1.3	Polymer Solid Electrolytes	99
1.3.1	Linear Polymers	99
1.3.2	Poly(ethylene oxide)	121
1.3.3	Comb like Polymers	166
1.3.4	Polyphosphazenes	199
1.3.5	Pendant Oligo-oxo-ethylene Cyclophosphazene Containing Polymers	234
1.3.6	Dimensionally Stable Polyphosphazenes	255
1.4	Recent Developments	298
1.5	Research Problem Undertaken in this Thesis	299
	REFERENCES	381

#### CHAPTER II SYNTHESIS, CHARACTERIZATION AND IONIC CONDUCTIVITY STUDIES ON POLY(MEEMA) AND POLY(MEEMA)-LiX ( $X^- =$ $ClO_4^-$ , $CF_3SO_3^-$ , $BF_4^-$ ) COMPLEXES

2.1	Introduction	36
2.2	Experimental	38
2.2.1	Materials	38

2.2.2	Measurements	38
2.2.3	Thin Film Preparation	39
2.2.4	Electrical Measurements	40
2.2.5	Synthesis of Methoxy Ethoxy Ethyl Methacrylate, (MEEMA) and Poly(Methoxyethoxyethylmethacrylate), Poly(MEEMA)	41
2.2.5.1	Methacryloyl Chloride	41
2.2.5.2	Methoxyethoxyethylmethacrylate, (MEEMA)	42
2.2.5.3	Poly(Methoxyethoxyethylmethacrylate), Poly(MEEMA)	42
2.2.5.4	Poly(MEEMA)-Alkali Metal Salt Complexes	43
2.3	Results and Discussion	44
2.3.1	Synthesis and Characterization of MEEMA and Poly(MEEMA)	44
2.3.2	Characterization of Poly(MEEMA)-Alkali Metal Salt Complexes	53
2.3.3	Conductivity Studies on Poly(MEEMA)-Metal Salt Complexes	59
2.3.4	Comparison of Conductivities of Poly(MEEMA)-LiX complexes with other systems	77
2.4	Conclusions	78
	REFERENCES	80

## CHAPTER III SYNTHESIS, CHARACTERIZATION, AND IONIC CONDUCTIVITY STUDIES ON POLYPHOSPHAZENES, PP(I) & PP(II) AND THEIR METAL SALT COMPLEXES

3.1	Introduction	81
3.2	Experimental	82
3.2.1	Materials	82
3.2.2	Measurements	83
3.2.3	Thin Film Preparation	84
3.2.4	Electrical Measurements	84
3.2.5	Synthesis of $N_3P_3(OR)_6$ , $R = CH_2CH_2O-(CH_2CH_2O)_4-C_6H_4-C_8H_{17}$	85
3.2.6	Synthesis of Poly [bis{4'-n-octyl-4-phenoxy(oligoethoxy) phosphazenes}]	85
3.2.6.1	Poly(dichlorophosphazene)	85
3.2.6.2	Poly[bis{4'-n-octyl-4-phenoxyethoxyethoxy}phosphazene] PP(I)	86
3.2.6.3	Poly[bis{4'-n-octyl-4-phenoxy(oligoethoxy)phosphazene] PP(II)	87

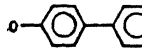
3.3	Results and Discussion	88
3.3.1	Synthesis and Characterization of PP(I) and PP(II)	88
3.3.2	Polymer-Metal Salt Complexes	100
3.3.3	Conductivity Studies of Polymer-Salt Complexes	100
3.3.3.1	General	100
3.3.3.2	Conductivity Studies on PP(I)-LiClO <sub>4</sub> System	102
3.3.3.3	Conductivity Studies on P(II)-LiBF <sub>4</sub> System	105
3.3.3.4	Comparison of the Present System with Other Known Systems	108
3.4	Conclusions	110
	REFERENCES	112

## PART B

### STUDIES ON ORGANIC POLYMERS CONTAINING CYCLOPHOSPHAZENE PENDANT GROUPS

## CHAPTER IV    COPOLYMERIZATION OF 2-(4'-VINYL-4-BIPHENYLYLOXY) PENTACHLOROCYCLOTRIPHOSPHAZENE WITH METHYLACRYLATE, ETHYLACRYLATE, METHYLMETHACRYLATE, AND STYRENE

4.1	Introduction	114
4.1.1	Polyphosphazenes	114
4.1.2	Cyclophosphazene Pendant Polymers	117
4.1.2.1	Homopolymerization of Cyclophosphazene Containing Organic Monomers	117
4.1.2.2	Copolymers of Cyclophosphazene Substituted Derivatives with Other Organic Monomers	120
4.1.2.2.1	Copolymers	120
4.1.2.2.2	Copolymerization Equation	121
4.1.2.2.3	Evaluation of Monomer Reactivity Ratios	122
4.1.2.2.4	Q-e Scheme	124
4.1.2.2.5	Copolymers Containing Cyclophosphazene Pendant Groups	126
4.1.2.3	Properties of the Cyclophosphazene Containing	

Copolymers	129
4.1.2.4 Statement of the Problem Undertaken in this Thesis	129
4.2 Experimental	130
4.2.1 Materials	130
4.2.2 Measurements	130
4.2.3 Synthesis of 2-(4'-vinyl-4-biphenyloxy)	
Pentachlorocyclotriphosphazene (CPHVB)	131
4.2.3.1 4-Acetoxy-4'-acetyl biphenyl (AAB)	131
4.2.3.2 4-Hydroxy-4'-hydroxyethyl biphenyl (HEB)	131
4.2.3.3 4-Hydroxy-4'-vinyl biphenyl (HVB)	132
4.2.3.4 2-(4'-vinyl-4-biphenyloxy) Pentachloro	
Cyclotriphosphazene (CPHVB)	132
4.2.3.5 Copolymerization of CPHVB with Methylacrylate	133
4.3 Results and Discussion	136
4.3.1 Synthesis of $N_3P_3Cl_5$ (  ),	
CPHVB (4)	136
4.3.2 Synthesis of Copolymers	139
4.3.3 Characterization of CPHVB Copolymers	142
4.3.4 Thermal Analysis	147
4.3.5 Molecular Weight Measurements for CPHVB Copolymers	151
4.3.5.1 Dilute Solution Viscosity	151
4.3.5.2 Gel Permeation Chromatography	154
4.3.6 Reactivity Ratios	158
4.3.7 Q-e Scheme	160
4.3.8 Conclusions	163
REFERENCES	164

*PART A*

SYNTHESIS AND CONDUCTIVITY STUDIES ON POLYMER SOLID  
ELECTROLYTES BASED ON POLYACRYLATE AND POLYPHOSPHAZENE SYSTEMS

## CHAPTER I

### INTRODUCTION

Solid state materials that exhibit high ion transport properties are of interest from both academic as well as an applied point of view<sup>1-3</sup>. These materials are also commonly known in literature as solid electrolytes, super ionic conductors or fast ion conductors. The conductivity range of typical solid electrolytes lies between  $10^{-6} < \sigma < 10^{-1} \text{ Scm}^{-1}$ ; this is comparable to that of dilute aqueous ionic solutions. The several potential applications envisaged for these materials include gas sensors<sup>4,5</sup>, electrochromic display devices<sup>6-8</sup>, high temperature heating elements<sup>9</sup>, intercalation electrodes<sup>10,11</sup>, power sources<sup>12</sup>, membranes for ion-selective electrodes<sup>13</sup>, fuel cells<sup>14,15</sup>, and high energy density batteries<sup>16,17</sup>.

The various materials known to function as solid electrolytes encompass hard refractory ceramic materials such as sodium  $\beta$ -alumina  $[(\text{Na}_2\text{O})_x \cdot 11\text{Al}_2\text{O}_3]$ , soft materials such as AgI, glassy materials such as  $\text{Ag}_2\text{GeSe}_3$  as well as metal salt complexes of organic and inorganic polymers. The polymeric materials have attracted attention more recently and currently hold great promise in this area<sup>18-21</sup>.

Investigations on the conduction mechanisms<sup>21-24</sup> in the solid electrolytes suggest that in the hard refractory materials ion hopping mechanism among various energetically favourable lattice subsites leads to the exhibited ionic conductivity. In the softer materials, the conductivity could result as a result of a similar ion hop, or via an order-disorder phase transition, or by a liquid like diffusion of one ionic sublattice. The conductivity mechanism in the polymer electrolytes would be discussed later.

The main difficulty in the use of conventional solid electrolytes in applications such as all solid state batteries, is the loss of contact between the electrodes and electrolyte arising out of dimensional changes of electrodes during charge-discharge cycles<sup>25,26</sup>. To a large extent this problem is overcome by operating these batteries at high temperatures, so that the electrodes are molten (eg. Sodium/Sulfur batteries<sup>27</sup> using  $\beta$ -alumina as the electrolyte).

Alternatively, use of polymeric materials can ensure interfacial contact with the electrodes since polymers are soft materials and can deform to suit the dimensional changes occurring at the electrodes<sup>28,29</sup>. This can result in functioning of batteries at ambient temperatures. Further, since polymers can be cast into thin films and thin films while minimizing resistance of the electrolyte also reduce the volume and the weight, use of polymer electrolytes can increase the energy stored per unit weight and volume. In view of these attractive features, in recent years, there has been considerable focus on the development of both organic and inorganic polymers as electrolytes for ion transport. In this chapter a review on these developments is presented.

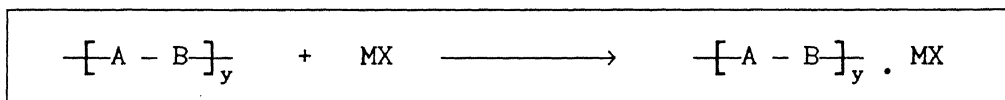
In 1973, Peter Wright and coworkers have first reported the ionic conductivity of poly(ethylene oxide),  $[\text{CH}_2\text{CH}_2\text{O}]_n$ , (PEO), with alkali metal salts<sup>30,31</sup>. This was followed by the pioneering suggestion of M. Armand for the use of PEO as a solid electrolyte system for the transport of ions<sup>29</sup>. Since then the area of polymer electrolytes has attracted considerable interest. In the following account first a discussion would be presented on the general characteristics of polymer electrolytes. This would be followed by an account on individual polymer electrolytes.

### 1.1 General Requirements for a Polymer Electrolyte

Since the polymer and the metal salt involved both are solid materials, the



preparation of a polymer salt complex is done by dissolution of the two materials in a common solvent such as acetonitrile, methanol, or THF followed by a slow removal of the solvent in vacuum. This results in either the bulk polymer-metal salt complex or a thin film depending upon the method of preparation. It is essential to ensure that no traces of moisture are present and hence the operations are carried out by using Schlenk techniques or glove box methods. The essential reaction that occurs in the formation of a polymer-metal salt complex can be written as



where  $\text{---[A - B]---}_y$  is a polymer chain and MX is an alkali metal salt or a transition metal halide. Divalent metal salts have also been used.

Just as the dissolution of ionic salts in a solvent system requires that the solvation energy of the ions in solution overcome the lattice energy of the ionic salt, similarly, polymer-metal salt complex formation proceeds, provided the polymer matrix effectively solvates the ions and overcomes the lattice energy of the ionic salt. Armand<sup>18b</sup> has described three essential criteria for this process:

- (a) Electron pair donicity (DN),
- (b) Acceptor Number (AN), and
- (c) an Entropy term.

The DN term measures the effectiveness of the solvent to function as a Lewis base in its ability to solvate the cation, a Lewis acid. Similarly, the AN term describes the solvation of the anion, the Lewis base. PEO, a polyether, can be considered similar to 1,2-dimethoxy ethane (DN, 22; AN, 10.2) or even THF (DN, 20; AN, 8)<sup>32</sup>. Thus PEO can effectively solvate cations possessing counter

anions that are bulky delocalized anions such as  $\text{I}^-$ ,  $\text{ClO}_4^-$ ,  $\text{BF}_4^-$ , or  $\text{CF}_3\text{SO}_3^-$  which require little or no solvation. The third term (entropy) has been related to the spatial disposition of the solvating unit and it has been shown that the ethyleneoxy ( $\text{CH}_2\text{CH}_2\text{O}$ ) containing polymers such as PEO have the most favourable spatial orientation of the solvating units.

While small ions such as  $\text{Li}^+$  which can be strongly solvated, lead to formation of polymer salt complexes even upto LiCl (with a lattice energy of  $853 \text{ KJmol}^{-1}$ ) other larger cations such as  $\text{Na}^+$ ,  $\text{K}^+$ , etc., require bulky counter anions such as  $\text{I}^-$ ,  $\text{SCN}^-$ , or  $\text{CF}_3\text{SO}_3^-$  in order to be solvated by PEO.

In addition to the above factors it has also been recognised that the polymer should possess a low cohesive energy and a high flexibility in order to effectively solvate the ions. This latter feature is indicated by a low glass transition temperature of the polymer.

In view of the above requirements, the important polymers that have been studied as polymer solid electrolytes include:

- (a) poly (ethylene oxide)
- (b) poly (propylene oxide)
- (c) poly siloxanes
- (d) poly phosphazenes
- (e) poly acrylates
- (f) poly (vinyl pyrrolidone)
- (g) poly (ethylene succinate)
- (h) poly (vinyl alcohol)
- (i) poly (ethylene imine)
- (j) poly (alkylene sulphides)

While oxygen containing polymers (a to h) have received more attention, other hetero atom containing polymers (i and j) have also been studied.

## 1.2 Electrical Measurements and Ion Transport in Polymer Electrolytes

### 1.2.1 Electrical Measurements

The basic and most useful information in the electrical measurements of a polymer electrolyte is the total ionic conductivity. In polymer electrolytes the conductivity occurs by the migration of ions and the measurement of total ionic conductivity is not straightforward, because of the resistance to ion flow at the electrode-electrolyte interface. To circumvent this problem, conductivity measurements are often made by ac impedance spectroscopy<sup>33,34</sup>, which minimizes the effects of cell polarization. The measurements are often made with the electrolyte sandwiched between a pair of electrochemically inert electrodes such as platinum or stainless steel electrodes. While the methodology involved in ac impedance method has been thoroughly reviewed<sup>35</sup>, a brief description of the method is given below:

Impedance spectroscopy is a powerful method of characterizing many of the electrical properties of materials. The dynamics of bound or mobile charge carriers in the bulk or interfacial regions of any kind of solid or liquid materials such as ionic, semiconducting, mixed electronic-ionic and even insulators (dielectrics) can be derived from impedance spectroscopy. Any intrinsic property that influences the conductivity of an electrode-material system can be studied by impedance spectroscopy. In this technique the impedance is directly measured in the frequency domain by applying a single frequency voltage to the interface and measuring the phase shift and amplitude or real and imaginary parts of current at that particular frequency.

When a sinusoidal potential,  $v(t) = V_m \sin(\omega t)$ , is applied, the magnitude ( $I_m$ ) and the phase shift ( $\theta$ ) of the current( $i$ ) which are measured with time ( $t$ ) are given by

$$i(t) = I_m \sin(\omega t + \theta)$$

where  $\omega$  is the frequency and  $\theta$  is the phase difference between the voltage and current.

This measurement is repeated from  $10^{-4}$  Hz to 10 MHz. The phase difference  $\theta$  is zero for purely resistive behaviour. Impedance is a more general concept than resistance, defined as below:

$$Z(\omega) = v_t / i_t$$

$Z(\omega)$  is a vector quantity and may be plotted in the plane with either rectangular or polar coordinates. The magnitude is

$$|Z(\omega)| = V_m / I_m(\omega).$$

The ac current vector is expressed in terms of real ( $i'_t$ ) and imaginary ( $i''_t$ ) parts i.e.,

$$i^* = i + ji, \text{ where } j = \sqrt{-1}$$

Similarly, ac potential is given by

$$v_t^* = v'_t + v''_t$$

and ac impedance can also be expressed in real and imaginary parts.

$$\text{i.e., } Z^* = Z' + j Z'', \text{ where } Z' = v'_t / i'_t$$

In a Cole-Cole plot, otherwise called the impedance spectrum (Fig.1.1) the real part of the impedance ( $Z'$ ) is plotted, against the imaginary part ( $Z''$ ) for data collected at a series of frequencies.

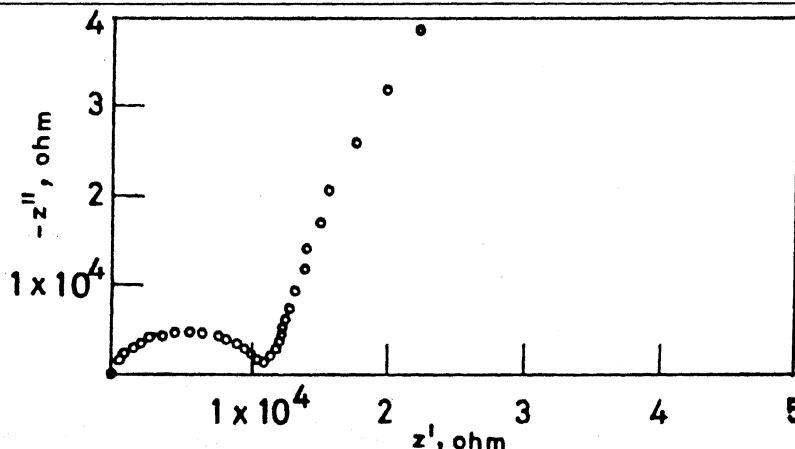


Fig.1.1. Room temperature complex impedance spectrum for 55 MEEP / 45 PEO- ( $\text{LiBF}_4$ )<sub>0.13</sub>. Ref.99.

The bulk resistance of the electrolyte ( $R_b$ ) with thickness of the sample and electrode area yields the resistivity of the sample and from this value the conductivity of the material is computed. The conductivity,  $\sigma$ , is given by ,  $\sigma = g / R_b$ , where  $g$  is the geometric factor (in  $\text{cm}^{-1}$  unit) and  $R_b$  is the bulk resistance.

### 1.2.2 Phenomenological Models

The conductivity of any material can be given by the following expression:

$$\sigma = \sum_i \mu_i n_i q_i$$

where  $\sigma$  is the ionic conductivity,  $\mu_i$  is the mobility of the  $i$  species,  $n_i$  is the concentration of carriers of the  $i$  species, and  $q_i$  is the charge of the  $i$  species.

As the polymer electrolytes contain no significant conjugation within the polymer backbone and also the salts used to form complexes with the polymer have negligible electronic conductivities, the conductivity observed is purely ionic. Moreover, Dupon and coworkers have shown experimentally that electrons and electron holes do not contribute to the total conductivity observed<sup>36</sup>. However, both cations and anions contribute but the problem of finding out the relative mobilities (the transference numbers) of the cationic and anionic carriers remain unsolved. The temperature dependence of conductivity can be explained by two models viz., (i) Arrhenius model (ii) the free volume model. The description of the models is given below:

### 1.2.3 Arrhenius Model

The Arrhenius equation which fits to the conduction in solid electrolytes, (crystalline and slightly disordered ones), is given as:

$$\sigma = A \exp (- E_A / kT )$$

where  $E_A$  is the activation energy and  $k$  is Boltzmann constant. The Arrhenius type plots, in which  $\log \sigma T$  is plotted against  $T^{-1}$  show straight lines. For highly crystalline polymeric materials such as PEO-alkalimetal salts, it is observed that the curve obtained in the plot of  $\log \sigma$  Vs  $T^{-1}$  is a straight line. This shows crystalline polymers are like any other solid electrolytes which follow the Arrhenius behaviour.

#### 1.2.4 Free Volume Model

Quantitative description of the conductivity behaviour in amorphous polymer solid electrolytes can be obtained from the empirical Vogel-Tamann-Fulcher equation<sup>37</sup> which is given below:

$$\sigma = A \exp [-B / k(T-T_0)]$$

where  $T_0$  is a parameter to be determined (in many cases, however, it is found that  $T_0$  is very close to  $T_g$ , the glass transition temperature),  $B$  is a constant called the pseudo activation energy differing from the actual activation energy, and  $k$  is Boltzmann constant.

In this model, the liquid phase which is obtained above glass transition temperature,  $T_g$ , can lose configurational entropy rapidly when temperature is lowered. This restricts the phase space felt by the cations resulting in an increase in the local activation energy and decrease in conductivity. This suggests that in highly disordered polymer electrolytes, above  $T_g$  the local structure is more like liquid and also the highest conductivity is achieved for the material with the lowest  $T_g$ .

### 1.3 Polymer Solid Electrolytes

Given below is an account of the various polymer systems that have been studied as polymer electrolytes.

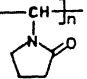
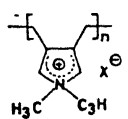
### 1.3.1 Linear polymers

Linear polymers such as poly(ethylene oxide) contain the donor oxygen atoms in the main back bone. Several such polymers are known to function as polymer electrolytes. These are tabulated in Table 1.1. A discussion on PEO is presented separately.

Table 1.1 Other polymer systems studied

Polymer	Metal Salt	O:Li ratio	Maximum Conductivity $\text{Scm}^{-1}$ (K)	Ref
PPO	LiBr, LiI		$\sim 10^{-6}$	38
Poly(propyleneOxide)	$\text{NaB}(\text{C}_6\text{H}_5)_4$		$\sim 10^{-6}$	39
	$\text{LiCF}_3\text{SO}_3$	9:1	$2.2 \times 10^{-5}$ (312)	
	$\text{NaCF}_3\text{SO}_3$		$\sim 10^{-6}$	
$\left[ \begin{array}{c} \text{CH} \\   \\ \text{CH}_3 \end{array} - \text{CH}_2 - \text{O} \right]_n$				
Poly( $\beta$ -propiolactone)	$\text{LiClO}_4$	20:1	$3.5 \times 10^{-5}$	40
$\left[ \text{CH}_2 - \text{CH}_2 - \underset{\text{O}}{\underset{  }{\text{C}}} - \text{O} \right]_n$				
Poly(ethylenesuccinate)	$\text{LiClO}_4$	33:1	$\sim 10^{-5}$ (363)	41
	$\text{LiBF}_4$	12:1	$3.4 \times 10^{-6}$ (288.2)	42
$\left[ \text{O} - \left( \text{CH}_2 \right)_2 - \text{O} - \underset{\text{O}}{\underset{  }{\text{C}}} - \underset{\text{O}}{\underset{  }{\text{C}}} - \left( \text{CH}_2 \right)_2 - \right]_n$				
Poly(ethylene adipate)	$\text{LiCF}_3\text{SO}_3$	16:1	$\sim 10^{-6}$	43
$\left[ \text{OCH}_2\text{CH}_2\text{O} - \underset{\text{O}}{\underset{  }{\text{C}}} - \left( \text{CH}_2 \right)_4 - \underset{\text{O}}{\underset{  }{\text{C}}} \right]_n$				

Table 1.1 (continued...)

Polymer	Metal Salt	O:Li ratio	Maximum Conductivity $\text{Scm}^{-1}$ (K)	Ref
Poly(ethyleneimine) $\text{---}[\text{CH}_2\text{CH}_2\text{---NH}]_n\text{---}$	$\text{NaSO}_3\text{CF}_3$	6:1 <sup>(a)</sup>	$\sim 10^{-7}$	44
Poly (alkylene sulphide)s $\text{---}[(\text{CH}_2)_x\text{---S}]_n\text{---}$	$\text{AgNO}_3$ $n = 5$	4:1 <sup>(b)</sup>	$9 \times 10^{-8}$ (318)	45
Poly (vinyl pyrrolidone) $\text{---}[\text{CH}_2\text{---CH}]_n\text{---}$ 	$\text{LiCF}_3\text{SO}_3$	3:1:6 <sup>(e)</sup>	$5 \times 10^{-5}$ (353 )	49
Poly (diallyl dimethyl ammonium chloride) 	$x = \text{Cl}^-$	0.67:1 <sup>(d)</sup>	$1 \times 10^{-5}$ (299 )	47
	$x = \text{CF}_3\text{SO}_3^-$	0.67:1 <sup>(d)</sup>	$1.5 \times 10^{-5}$ (371 )	48
Poly (vinylidone fluoride) $\text{---}[\text{C}(\text{F})=\text{C}]_n\text{---}$	$\text{LiClO}_4$	-	$5 \times 10^{-5}$ (373 ) <sup>(c)</sup>	46

(a) O : Na ratio

(b) O : Ag ratio

(c) conductivity obtained in presence of PEG as Plasticizer

(d)  $\text{X}^-$  : OH of PEG mole ratio(e) PVP :  $\text{LiCF}_3\text{SO}_3$  : PEG



### 1.3.2 Poly (ethylene oxide)

PEO is prepared by the ring opening polymerization of ethylene oxide. High molecular weight polymers upto  $5 \times 10^6$  are available commercially. PEO is a semicrystalline material, about 60% of the bulk is crystalline at room temperature and rest is present in an amorphous phase. The melting point of the crystalline phase ( $T_m$ ) is  $65^\circ\text{C}$  and the glass transition temperature of the amorphous phase ( $T_g$ ) is  $-60^\circ\text{C}$ . PEO forms metal-salt complexes with a wide range of systems<sup>18b</sup>. Some of these are listed in Table 1.2.

In order to understand the nature of the PEO-metal salt complexes, attempts have been made to obtain and study phase diagrams. Unlike for simple inorganic systems, for polymers, obtaining phase diagrams is complicated as a result of slow crystallizations as well as presence of chain ends and defects. These result in an apparent violation of the Gibbs rule. In spite of these complications phase diagram information is available for some PEO-metal salt compositions<sup>55-58</sup>. The techniques used for obtaining this information are mainly polarized light microscopy<sup>59</sup>, differential scanning calorimetry<sup>59,60</sup>, X-ray diffraction, and NMR<sup>61-64</sup>.

The maximum stoichiometry of the polymer-metal salt complexes ( $\text{CH}_2\text{CH}_2\text{O}$  : metal salt) as shown by NMR and DSC studies is 3:1 for smaller metal ions such as  $\text{Li}^+$  or  $\text{Na}^+$ . Ions such as  $\text{K}^+$  or  $\text{NH}_4^+$  tend to form 4:1 complexes. Bulky symmetrical anions such as  $\text{ClO}_4^-$  and  $\text{AsF}_6^-$  favour 6:1 complexes. A eutectic or a quasi eutectic exists between pure PEO and PEO-metal salt complexes. For example, the 3:1 complex between PEO and  $\text{LiCF}_3\text{SO}_3$  shows a eutectic point which is very close to that of pure PEO itself in composition and melting temperature (30:1 and  $60^\circ\text{C}$ ). In contrast the 6:1 PEO.  $\text{LiClO}_4$  complexes show a lower salt concentration (18:1 and  $42^\circ\text{C}$ ). As an example of the phase diagrams studied, the PEO- $\text{LiClO}_4$  phase diagram is shown in Fig.1.2. Use of multinuclear NMR ( $^1\text{H}$ ,  $^7\text{Li}$ ,

and  $^{19}\text{F}$ ) has corroborated evidence from DSC towards phase information. Thus faster relaxation times ( $T_2$ ) have been associated with crystalline phases and while longer  $T_2$  values have been attributed to amorphous solid solutions<sup>61</sup>.

Table 1.2<sup>(a)</sup>

Cation Anion	$\text{Li}^+$	$\text{Na}^+$	$\text{K}^+, \text{Rb}^+$ $\text{Cs}^+, \text{NH}_4^+$	$\text{Mg}^{2+}$	$\text{Ca}^{2+}$	$\text{Zn}^{2+}$	$\text{Cu}^{2+}$
$\text{F}^-$	-	-	-	-	-	-	-
$\text{Cl}^-$	+	-	-	+	-	+	+
$\text{Br}^-$	+	+	-	+	+	+	+
$\text{I}^-$	+	+	+	+	+	+	+
$\text{NO}_3^-$	+	-	-	+	x	x	x
$\text{SCN}^-$	+	+	+	+	+	+	+
$\text{ClO}_4^-$	+	+	+	+	+	+	+
$\text{CF}_3\text{SO}_3^-$	+	+	+	+	+	+	+
$\text{BPh}_4^-$	+	+	+	+	+	-	-

(a) Table taken from Ref. (18b); + indicates the complexes studied ; - not studied. The other PEO-salt complexes known are as follows:  $\text{HgCl}_2$ ,  $\text{PbBr}_2$ ,  $\text{PbCl}_2$ ,  $\text{PbBr}_2^{(51)}$ ,  $\text{CoBr}_2$ ,  $\text{CoBr}_2 \cdot 6\text{NH}_2$ ,  $\text{CoBr}_2 \cdot 28\text{H}_2\text{O}$ ,  $\text{NiBr}_2$ ,  $\text{NiBr}_2 \cdot 6\text{NH}_2$ ,  $\text{NiBr}_2 \cdot 30\text{H}_2\text{O}$ ,  $\text{MnBr}_2$ ,  $\text{FeCl}_2/\text{FeCl}_3 (1:1)^{(52)}$ ,  $\text{Cu}(\text{CF}_3\text{SO}_3)_3^{(54)}$

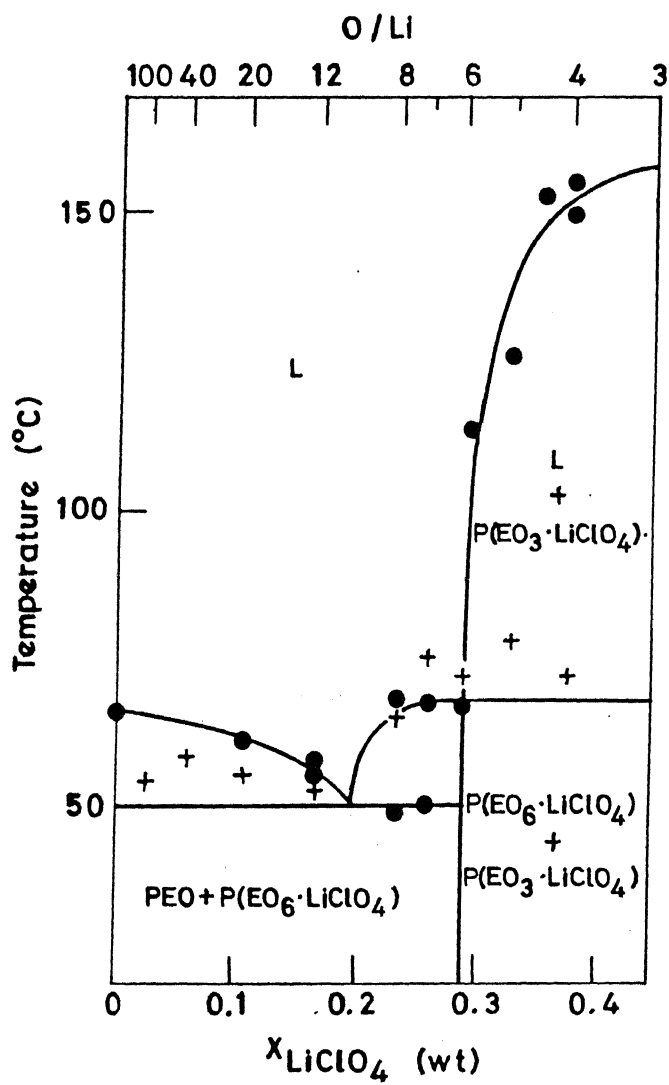


Fig.1.2. Phase diagram of PEO-LiClO<sub>4</sub> complexes. (Ref.56)

IR, Raman, and NMR studies on polymer solid electrolytes give substantial amount of information about the structure and dynamics. Vibrational spectroscopy gives the direct evidence of the cation-polymer interaction. Far IR studies confirm that the cation is coordinated to the ether oxygen atoms in PEO<sup>65-68</sup> and other comb like acrylate polymers (vide infra) having short oligo oxyethylene side chains. The mechanism of conduction of ions involves local, liquid like motions of the solvent (poly ether in case of PEO) with the ions then moving in the amorphous, locally disordered (liquid) phase. This implies curved plots,  $\log \sigma T$  Vs  $1/T$  over the entire temperature range with no discontinuities, much weaker stoichiometry dependence, and increase in conduction with decreased glass transition temperature.

IR and Raman studies on PEO- $\text{NaBF}_4$  and PEO- $\text{NaBH}_4$  systems reported by Dupon and coworkers<sup>66</sup>, indicate that extensive ion pairing occurs in  $\text{NaBH}_4$  complexes leading to low conductivity values. Absence of such pairing in  $\text{NaBF}_4$  complexes leads to enhanced conductivity.

NMR measurements and conductivity study correlations with phase diagrams have clearly established that the amorphous elastomeric phase in PEO is primarily responsible for the ionic conductivity.

Typical conductivity Vs composition and temperature plots for PEO- $\text{LiClO}_4$  and PEO- $\text{LiCF}_3\text{SO}_3$  are shown in Fig. 1.3. Usually the conductivities are in the range of  $10^{-3}$  to  $10^{-4} \text{ Scm}^{-1}$  at  $100^\circ\text{C}$  and fall to  $10^{-6}$  to  $10^{-8} \text{ Scm}^{-1}$  at room temperature. The molecular weight of the polymer changes the conductivity values. However, after a certain molecular weight the conductivities are invariant with increase in molecular weight of PEO. The highest conductivities are seen for the  $\text{Li}^+$  salts while the least conductive are the sodium salts. Both free volume and configurational entropy models have been used to describe the temperature and concentration dependent behaviour of the conductivity.

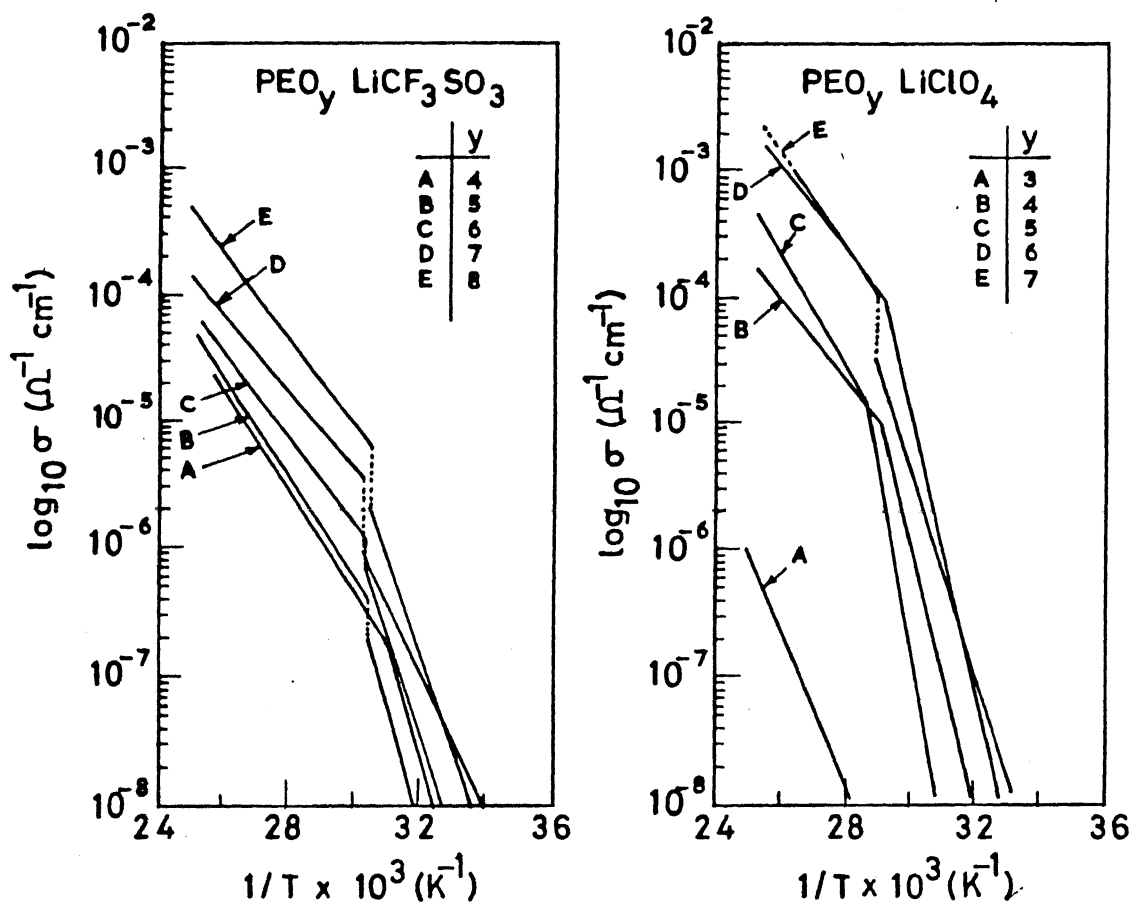


Fig.1.3. The conductivity plots ( $\log \sigma$  vs  $10^3/T$ ) of PEO-LiX complexes: (a) PEO-LiCF<sub>3</sub>SO<sub>3</sub> system and (b) PEO-LiClO<sub>4</sub> system. (Ref. 56)

In general the conductivity of the PEO polymer electrolyte varies with the concentration of the dissolved salt with the maximum conductivity being observed for an intermediate salt concentration. This is understood qualitatively by applying the VTF relation for conductivity, given as

$$\sigma = A T^{-1/2} \exp \left[ -E_a / (T - T_0) \right]$$

Here the pre-exponential term is proportional to the charge carrier concentration and the  $E_a$  term is a pseudo activation energy of the ion transport. As discussed earlier, the  $T_0$  is a parameter closely related to the  $T_g$  of the sample. In the absence of all other effects, increase of salt concentration should increase  $A$  and hence the conductivity. However, as the salt concentration is increased there is a simultaneous increase in  $T_g$  and this leads to a decrease in conductivity. Therefore optimum salt concentrations are required for maximum conductivities. Generally, where phase diagrams have been studied it is shown that for the eutectic composition a single amorphous phase is formed above the congruent melting point. This leads to an enhanced conductivity which is explained by the VTF equation. Above the eutectic point variation of conductivity appears linear on the Arrhenius plot.

Attempts to obtain transport number information by various methods such as pulsed field gradient NMR<sup>64</sup>, radiotracer diffusion<sup>69</sup>, and potentiostatic polarization technique<sup>45</sup> have suggested that both cation and anion mobilities are important for the total ionic conductivity seen.

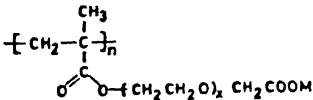
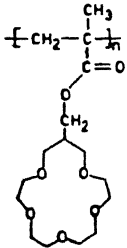
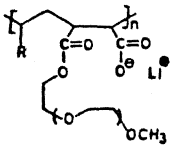
### 1.3.3 Comb like Polymers

In this type of polymers the backbone of the polymer itself does not possess atoms of sufficient basicity to complex with metal ions. However, the polymers possess side chains which contain the structural features to enable them to function as polymer electrolytes. Examples of comb like polymer electrolyte systems include polyphosphazenes, polyacrylates etc. Some of the comb like polymers and their metal salt complexes along with conductivity values are listed in Table 1.3. In the following a discussion on polyphosphazenes is presented.

Table 1.3

Polymer	Metal Salt	Maximum conductivity $\text{Scm}^{-1}(\text{K})$	Ref
Poly(methoxy poly ethyleneglycolmono methacrylate)  $\begin{array}{c} \text{CH}_3 \\   \\ \text{-(CH}_2\text{-C)-}_n \\   \\ \text{C=O-O-(CH}_2\text{CH}_2\text{O)}_x\text{CH}_3 \end{array}$			
x = 8,22	NaSCN NaCF <sub>3</sub> SO <sub>3</sub> LiCF <sub>3</sub> SO <sub>3</sub>		70
x = 22	LiCF <sub>3</sub> SO <sub>3</sub>	$6 \times 10^{-5}(373), 2 \times 10^{-5}(293)$	71
x = 9	LiCF <sub>3</sub> SO <sub>3</sub>	$3 \times 10^{-4}(373), \sim 10^{-6}(293)$	71
x = 3,7,12 & 17	LiClO <sub>4</sub>	$\sim 10^{-5}(298)$	72
x = 7	LiPF <sub>6</sub>	$\sim 10^{-5}(298)$	72
Poly[diethoxy(3) methyl itaconate]  $\begin{array}{c} \text{CH}_2\text{COO(CH}_2\text{CH}_2\text{O)}_x\text{CH}_3 \\   \\ \text{-(CH}_2\text{-C)-}_n \\   \\ \text{CH}_2\text{COO(CH}_2\text{CH}_2\text{O)}_x\text{CH}_3 \end{array}$	LiClO <sub>4</sub>	$5.6 \times 10^{-5}(333)$	73
Poly(di-poly(pro pylene glycol) itaconate)  $\begin{array}{c} \text{CH}_2\text{COO(CH}_2\text{CH}_2\text{O)}_x\text{CH}_3 \\   \\ \text{-(CH}_2\text{-C)-}_n \\   \\ \text{CH}_2\text{COO(CH}_2\text{CH}_2\text{O)}_x\text{CH}_3 \end{array}$	LiClO <sub>4</sub> NaClO <sub>4</sub> ZnCl <sub>2</sub> LiCl	$\sim 10^{-6}(303)$ $3.4 \times 10^{-7}(333)$ $1.2 \times 10^{-7}(333)$	74

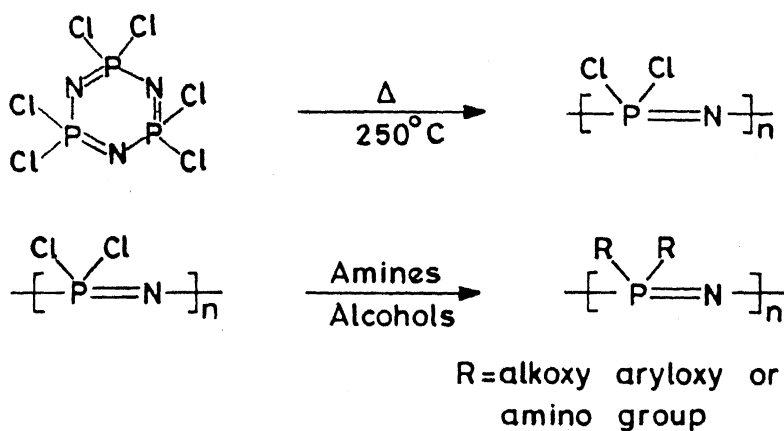
Table 1.3 (continued...)

Polymer	Metal Salt	Maximum conductivity $\text{Scm}^{-1}(\text{K})$	Ref
Poly[(w-carboxy) oligooxyethylene methacrylate]  	Li Na K	$8 \times 10^{-11}$ $7 \times 10^{-8}$ $2 \times 10^{-8}$	75
Poly(crown ether)  	Li Na K  $\text{LiClO}_4$	$3 \times 10^{-9}$ $3 \times 10^{-8}$ $1 \times 10^{-7}$ $2 \times 10^{-7} (333)$	75   76
Styrene-maleic anhydride copolymer with oligooxyethylene side chains 50:50 copolymer	$x=6, R=\text{Ph}$ $x=2, R=\text{Ph}$ $x=6, R=\text{H}$	$\sim 10^{-6} (370^\circ\text{C})$	77
			
Poly[oligo oxyethylene)methacrylate-CO-methacrylyl hexyl sulphonic acid alkali metal salt	Li	$2 \times 10^{-6} (298)$	78



### 1.3.4 Polyphosphazenes

Polyphosphazenes are inorganic macromolecules containing phosphorus and nitrogen atoms arranged alternately in the backbone. The phosphorus atom is pentavalent and tetracoordinate while nitrogen atom is trivalent and dicoordinate<sup>79</sup>. Poly(dichlorophosphazene), (2), which serves as starting material for all other polyphosphazenes, (3), is synthesized by a ring opening polymerization of hexachlorocyclotriphosphazene, (1), the six membered P—N heterocycle:



Replacement of the chlorines on phosphorus in poly (dichlorophosphazene) by a variety of nucleophilic reagents such as amines and alcohols is well documented<sup>80-82</sup>. Shriver and coworkers in collaboration with Allcock have synthesized the etheroxy side chain containing polyphosphazenes, MEEP and MEP<sup>83-85</sup>. MEEP is a completely amorphous polymer with a glass transition

temperature of  $-83.5^{\circ}\text{C}$  while MEP has a  $T_g$  of  $-75^{\circ}$ . MEEP has been shown to form complexes with a wide range of metal salts. The glass transition temperatures of the polymer-salt complexes increased with increasing salt concentration. The conductivity values first increase with an increase of salt concentrations and after attaining an optimum value begin to drop<sup>84</sup>. Some data are summarized in Table 1.4.

**Table 1.4 Glass transition Temperatures and Conductivities  
for Selected MEEP complexes**

Salt	M : P <sup>(a)</sup> (x:1)	$T_g^{(b)}$ ( $^{\circ}\text{C}$ )	$\sigma_{30^{\circ}\text{C}}$	$\sigma_{55^{\circ}\text{C}}$	$\sigma_{70^{\circ}\text{C}}$	$\sigma_{90^{\circ}\text{C}}$
			$\text{Ohm}^{-1}\text{cm}^{-1}$			
No salt	0.000	-83.5	$8.1 \times 10^{-8}$	$1.6 \times 10^{-7}$	$1.9 \times 10^{-7}$	$2.1 \times 10^{-7}$
$\text{AgSO}_3\text{CF}_3$	0.083	-78.3	$1.6 \times 10^{-4}$	$3.2 \times 10^{-4}$	$4.8 \times 10^{-4}$	$7.5 \times 10^{-4}$
$\text{AgSO}_3\text{CF}_3$	0.125	-74.3	$2.6 \times 10^{-4}$	$5.3 \times 10^{-4}$	$8.4 \times 10^{-4}$	$1.4 \times 10^{-4}$
$\text{AgSO}_3\text{CF}_3$	0.167	-68.7	-	$6.8 \times 10^{-4}$	$9.8 \times 10^{-4}$	--
$\text{AgSO}_3\text{CF}_3$	0.250	-60.0	-	$4.8 \times 10^{-4}$	$9.4 \times 10^{-4}$	$1.4 \times 10^{-3}$
$\text{AgSO}_3\text{CF}_3$	0.500	-35.2	$2.8 \times 10^{-4}$	$1.5 \times 10^{-4}$	$3.1 \times 10^{-4}$	$6.7 \times 10^{-4}$
$\text{AgSO}_3\text{CF}_3$	1.000	-11.6	$2.5 \times 10^{-6}$	$3.3 \times 10^{-5}$	$1.0 \times 10^{-4}$	$3.7 \times 10^{-4}$
$\text{AgSO}_3\text{CF}_3$	2.000	+11.4	$<10^{-9(c)}$	$<10^{-9(c)}$	$<10^{-9(c)}$	$<10^{-9(c)}$
$\text{LiCF}_3\text{SO}_3$	0.125	-69.4	$2.2 \times 10^{-5}$	$5.7 \times 10^{-5}$	$8.5 \times 10^{-5}$	$1.3 \times 10^{-4}$
$\text{LiCF}_3\text{SO}_3$	0.167	-65.4	$2.2 \times 10^{-5}$	$6.2 \times 10^{-5}$	$8.7 \times 10^{-5}$	$1.5 \times 10^{-4}$
$\text{LiCF}_3\text{SO}_3$	0.250	-62.4	$2.7 \times 10^{-5}$	$7.5 \times 10^{-5}$	$1.2 \times 10^{-5}$	$2.2 \times 10^{-4}$
$\text{LiCF}_3\text{SO}_3$	0.500	-58.9	$1.2 \times 10^{-5}$	$5.7 \times 10^{-5}$	$1.0 \times 10^{-5}$	$1.9 \times 10^{-4}$

The conductivity of  $\text{MEEP} \cdot (\text{LiCF}_3\text{SO}_3)_{0.25}$  is as high as  $10^{-5} \text{ Scm}^{-1}$  at room temperature. This is atleast three orders of magnitude higher than that observed for the analogous PEO-metal salt complexes<sup>85</sup>. It was reasoned by Shriver and coworkers that the high conductivity is largely due to the highly flexible backbone of the polymer leading to a large segmental motion. The high reorientational mobility of the backbone and the side groups as reflected by the glass transition temperature of MEEP allows for the observed conductivity. It has been suggested that the mode of transport of ions follows the free volume or excess entropy model and obeys the VTF equation (vide supra).

Blonsky and coworkers attempted to identify the nature of the carrier species and the transport numbers of the ions in the MEEP-metal salt complexes. Since virgin MEEP is an insulator it was assumed that in the MEEP-metal salt complexes the observed conductivity has no electronic component. Using potentiostatic polarization method the transference number were found for  $\text{Li}^+$  ions to be in the range of 0.34 to 0.42 for  $\text{MEEP-LiCF}_3\text{SO}_3$  complexes. However, Blonsky and coworkers conclude that the potentiostatic polarization technique does not provide reliable and straight forward results. The overall picture was that both the cations and anions contribute to the ionic conductivity.<sup>85,86</sup>

Tonge and coworkers have investigated the effect of (side) chain length in a series of poly (alkoxy phosphazenes),  $\{ \text{NP} [\text{O}(\text{CH}_2\text{CH}_2\text{O})_x\text{CH}_3]_2 \}$ , (where  $x = 1, 2, 7, 12$ , and  $17$ ), on the conductivity of their complexes with lithium trifluoromethane sulphonate. The maximum conductivity at  $30^\circ\text{C}$  ( $5.3 \times 10^{-5} \text{ Scm}^{-1}$ ) was observed when  $x = 7$ . It was also noted that while the glass transition temperatures of the pure polymers increased with increasing chain length, the  $T_g$ 's of the polymer-metal complexes showing an optimum conductivity of  $2 \times 10^{-4} \text{ Scm}^{-1}$  at  $70^\circ\text{C}$  was nearly constant at  $220\text{K}$ <sup>87</sup>. Table 1.5 summarizes selective

conductivity data for MEEP and other polyphosphazene polymer electrolytes that have been studied.

Table 1.5

Polymer	Metal Salt	O:Li ratio	Conductivity $\text{Scm}^{-1}$	Ref
$[\text{NP}(\text{OCH}_2\text{CH}_2\text{OCH}_2\text{CH}_2\text{OCH}_3)_2]_n$ , MEEP.	-	-	$8.1 \times 10^{-8}$ (303) $2.1 \times 10^{-7}$ (363)	85
	$\text{AgCF}_3\text{SO}_3$	48:1	$2.6 \times 10^{-4}$ (303) $1.4 \times 10^{-3}$ (363)	85
	$\text{LiCF}_3\text{SO}_3$	24:1	$2.7 \times 10^{-5}$ (303) $2.2 \times 10^{-4}$ (363)	85
	$\text{LiBF}_4$	36:1	$5.2 \times 10^{-5}$ (303) $8.7 \times 10^{-4}$ (363)	86
	$\text{LiBr}$	36:1	$8.4 \times 10^{-6}$ (303)	86
	$\text{LiNO}_3$	36:1	$1.1 \times 10^{-5}$ (303)	86
	$\text{LiSCN}$	36:1	$9.1 \times 10^{-6}$ (303)	86
	$\text{NaCF}_3\text{SO}_3$	21:1 <sup>(a)</sup>	$6.1 \times 10^{-5}$ (303)	86
	$\text{I}_2$	2.5:1	$< 10^{-3}$ (303)	92
$[\text{NP}(\text{OCH}_2\text{CH}_2\text{OCH}_3)_2]_n$ $[\text{NP}\{(\text{OCH}_2\text{CH}_2)_x\text{OCH}_3\}]_n$ $x = 7$ , ME7P	$\text{LiCF}_3\text{SO}_3$	16:1	$6.0 \times 10^{-5}$ (303) $6.0 \times 10^{-5}$ (363)	86
$x = 12$ , ME12P	$\text{LiCF}_3\text{SO}_3$	95:1	$2.4 \times 10^{-5}$ (303) $1.1 \times 10^{-4}$ (363)	86, 87
$x = 17$ , ME17P	$\text{LiCF}_3\text{SO}_3$	24:1	$1.4 \times 10^{-5}$ (303) $1.5 \times 10^{-4}$ (354)	86
	$\text{LiCF}_3\text{SO}_3$	222:1	$1.2 \times 10^{-6}$ (305) $6.2 \times 10^{-5}$ (343)	86, 87
MEEP-PEG <sup>(b)</sup> crosslinked	$\text{LiCF}_3\text{SO}_3$	6.4 <sup>(c)</sup>	$4.1 \times 10^{-5}$ (303) $1.7 \times 10^{-4}$ (343)	88
MEEP-PEG <sup>(d)</sup> crosslinked	$\text{LiCF}_3\text{SO}_3$	8.9 <sup>(c)</sup>	$3.0 \times 10^{-5}$ (303) $1.0 \times 10^{-4}$ (343)	88
Crosslinked MEEP <sup>(e)</sup>	$\text{LiCF}_3\text{SO}_3$	24:1	$7.0 \times 10^{-5}$ (295) $7.0 \times 10^{-4}$ (373)	89

Table 1.5 (continued...)

Polymer	Metal Salt	O:Li ratio	Conductivity Scm <sup>-1</sup>	Ref	
EEP-PEO Blend	LiBF <sub>4</sub>	114 : 0.033	4.0x10 <sup>-6</sup> (298) --	90	
	LiBF <sub>4</sub>	20.83 : 0.18	1.3x10 <sup>-6</sup> (298) --	90	
	LiClO <sub>4</sub>	53.57 : 0.07	1.2x10 <sup>-5</sup> (298) --	90	
	LiCF <sub>3</sub> SO <sub>3</sub>	28.85 : 0.13	< 10 <sup>-6</sup> (298) < 10 <sup>-4</sup> (373)	90	
	LiAlCl <sub>4</sub>	28.85 : 0.13	~ 10 <sup>-7</sup> (298) --	90	
	LiAsF <sub>6</sub>	28.85 : 0.13	< 10 <sup>-6</sup> (298) < 10 <sup>-4</sup> (373)	90	
	Li-- N(CF <sub>3</sub> SO <sub>2</sub> ) <sub>2</sub>	28.85 : 0.13	6.7x10 <sup>-3</sup> (298)	91	
	$\text{N}_3\text{P}_3[\text{O}(\text{CH}_2\text{CH}_2\text{O})_x\text{CH}_3]_5-\text{O}-\text{C}_6\text{H}_4-\text{C}_6\text{H}_4-\text{CH}(\text{CH}_3)-\text{CH}_2-]_n$	x=2, PDEP	LiClO <sub>4</sub>	30:1	7.6x10 <sup>-6</sup> (313), 6.5x10 <sup>-5</sup> (363)
		LiClO <sub>4</sub>	15:1	1.2x10 <sup>-4</sup> (363)	93
x=3, PTEP		LiClO <sub>4</sub>	30:1	3.6x10 <sup>-5</sup> (313) 2.9x10 <sup>-4</sup> (363)	93
		LiClO <sub>4</sub>	15:1	1.1x10 <sup>-4</sup> (333)	93
$\text{N}_3\text{P}_3[\text{O}(\text{CH}_2\text{CH}_2\text{O})_x\text{CH}_3]_5-\text{O}-\text{C}_6\text{H}_4-\text{CH}(\text{CH}_3)-\text{CH}_2-]_n$	x=2, Poly SDEP	LiClO <sub>4</sub>	21:1	1.8x10 <sup>-5</sup> (303) 2.6x10 <sup>-4</sup> (373)	94
	x=3, Poly STEP	LiClO <sub>4</sub>	20:1	1.8x10 <sup>-5</sup> (303) 3.9x10 <sup>-4</sup> (373)	94
	x=3, Poly STEP	NaSCN			
		KSCN			
		CsSCN	28.57:1	9x10 <sup>-5</sup> , 6.46x10 <sup>-4</sup>	95
		LiClO <sub>4</sub>	80:1	~10 <sup>-6</sup> (344)	96
		NaClO <sub>4</sub>	80:1	~10 <sup>-6</sup> (333)	96

(a) O : Na ratio

(b) 1 mole % PEG

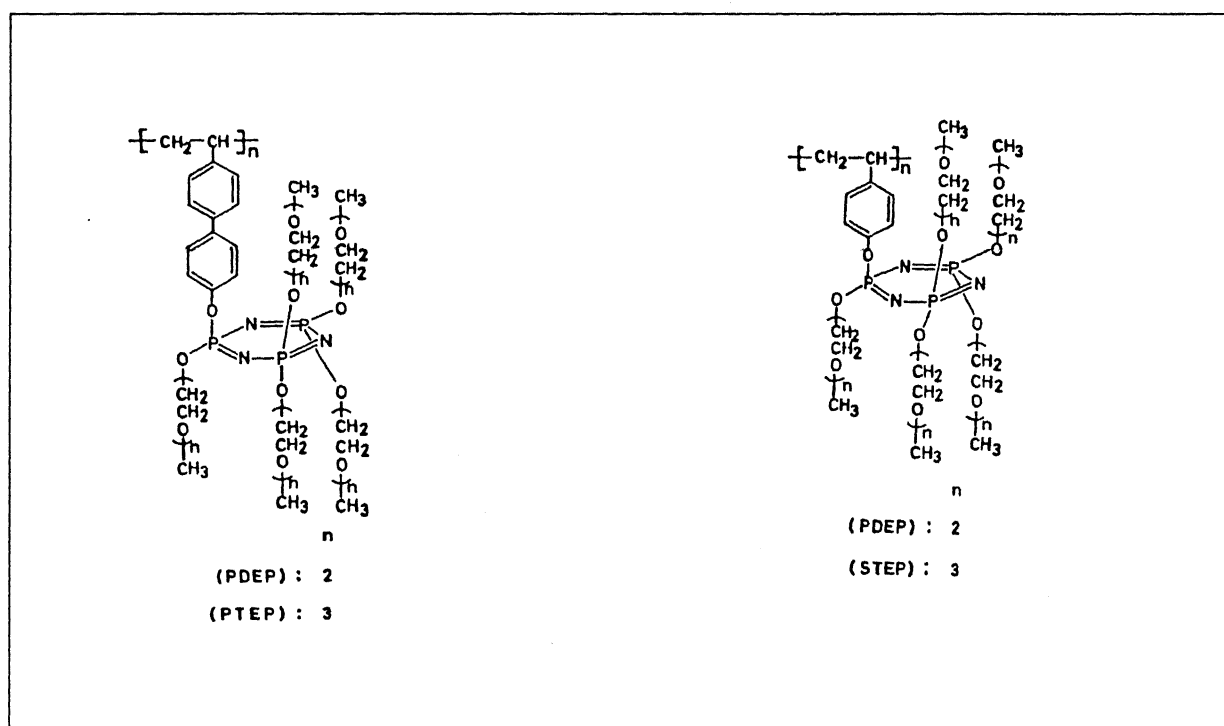
(c) Wt % of the salt

(d) 10 mole % PEG

(e) cross linking by  $\gamma$ -radiation

### 1.3.5 Pendant Oligooxy Ethylene Cyclophosphazene Containing Polymers

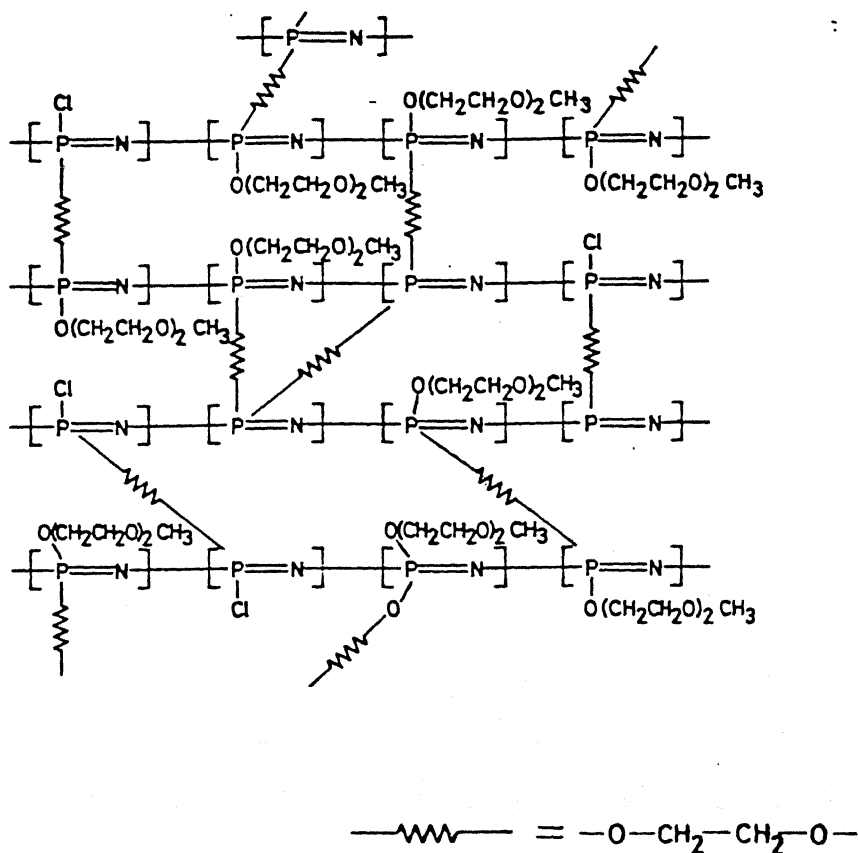
Recently Inoue and coworkers have assembled polymers containing rigid skeletal backbones which formed metal salt complexes and showed excellent conductivities in contrast to the flexible MEEP system<sup>93-95</sup>. They have synthesized poly styrene and poly ethylene biphenoxy derivatives with pendant oligo(oxyethylene) cyclotriphosphazenes. The polymers PDEP, PTEP, poly(SDEP), and poly(STEP) all form complexes with  $\text{LiClO}_4$  and show good conductivities at room temperature (refer Table 1.5). The conductivities of the complexes exhibit a non-Arrhenius



temperature dependence analogous to that of MEEP indicating that the ion transport occurs in the amorphous phase. The authors attribute the high conductivities as due to an ion transport through a continuous conducting phase consisting of oxyethylene chains. Also it is speculated that the ion transport, governed by ion dipole interactions between the  $\text{Li}^+$  and inter oxyethylene chain strands, does not require a flexible polymer backbone with high segmental motion such as what was suggested in the case of MEEP.

### 1.3.6 Dimensionally Stable Polyphosphazenes

Although MEEP-metal salt complexes show high ionic conductivities, the liquid like nature of these polymer electrolyte systems precludes their use in applications such as batteries. To overcome this problem one approach has been to synthesize dimensionally stable polyphosphazenes by crosslinking poly [(chloro)(methoxyethoxyethoxy)phosphazene] with polyethylene glycol<sup>88</sup>. If some of the chlorines in poly(dichlorophosphazenes) are left unreplaced by the initial reaction with the sodium salt of methoxy ethoxy ethanol, these can be reacted further with the difunctional PEG affording crosslinking:



A marked increase in the stability of the crosslinked materials was noted and there was no flow of the polymer even at  $140^{\circ}\text{C}^{88}$ . The overall conductivity of (PEG crosslinked MEEP)- $\text{LiCF}_3\text{SO}_3$  complexes compares favourably with parent MEEP.

Alternative methods of increasing the mechanical properties of MEEP have included crosslinking by irradiation of pure MEEP or  $\text{MEEP}-(\text{LiX})_{0.25}$  complexes with  $^{60}\text{Co}$   $\gamma$ -rays and the use of porous fibre glass support matrices<sup>89</sup>. More recently physical blends of MEEP with various polymers such as poly (ethylene oxide), poly (propylene oxide), poly (ethylene glycol diacrylate), and poly (vinylpyrrolidone) have been made<sup>99</sup>. These blends were shown to possess better mechanical properties than pure MEEP, while showing comparable conductivities. For example, a mixed  $(\text{MEEP})(\text{PEO})_5-(\text{LiBF}_4)_{0.033}$  complex shows a conductivity of  $4.0 \times 10^{-6} \text{Scm}^{-1}$  at room temperature<sup>99</sup>. Comparable magnitude of ionic conductivity is shown by  $\text{PEO}-(\text{LiBF}_4)_{0.125}$  only at  $57^{\circ}\text{C}$ . Similarly,  $(\text{MEEP})(\text{PEO})_5-[\text{LiN}(\text{CF}_3\text{SO}_2)_2]_{0.013}$  showed a high conductivity of  $6.7 \times 10^{-5} \text{Scm}^{-1}$  at  $25^{\circ}\text{C}^{99}$ . Some of these data are tabulated in Table 1.5. Abraham and coworkers have also recently reported that  $\text{MEEP-LiAlCl}_4$  system itself is mechanically stable presumably owing to the  $\text{AlCl}_4^-$  anions serving as crosslinks between the polymer chains involving the  $\text{P}=\text{N}$  bonds.

DSC studies on MEEP-PEO composite system clearly suggests a multiphase character in the composite with both amorphous MEEP-like and crystalline PEO-like phases being present<sup>100</sup>.  $^7\text{Li}$  NMR studies based on  $T_1$  measurements and linewidths have been helpful in distinguishing between lithium ions present in the crystalline and amorphous phases. Thus  $\text{Li}^+$  ion in a crystalline phase is associated with a longer  $T_1$  than that in an amorphous phase. Further, it is expected that enhanced ionic mobility ( $\text{Li}^+$ ) in polymer electrolytes leads to a line narrowing in the  $^7\text{Li}$  NMR spectrum of the corresponding ion. Arrhenius



plots of  $^7\text{Li}$  NMR line widths (full widths at half maximum, fwhm) for several MEEP-PEO composites (Fig. 1.4) clearly shows that the onset of line narrowing corresponding to onset of ionic mobility correlates with the  $T_g$  of the material<sup>100</sup>.

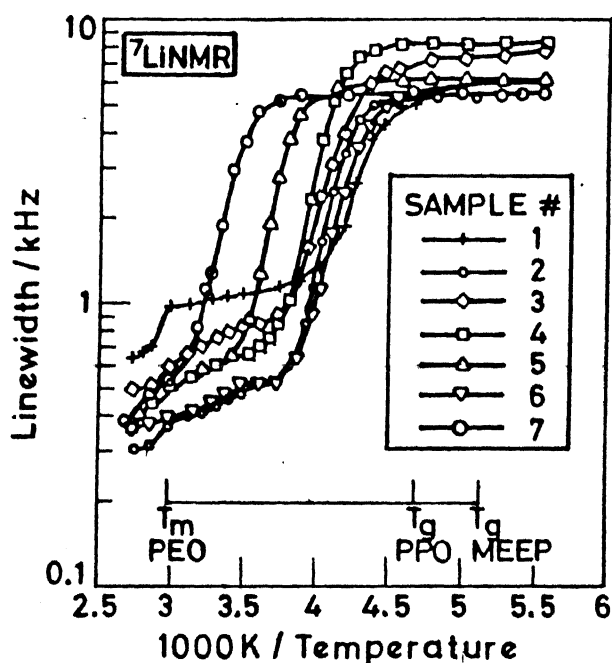


Fig.1.4. Arrhenius plots of  $^7\text{Li}$  NMR line widths. (Ref.100)

Sample 1, MEEP:PEO: $\text{LiClO}_4$ , 46:38:16

Sample 2, MEEP:PEO: $\text{LiClO}_4$ , 60:26:14

Sample 3, MEEP:PEO: $\text{LiBF}_4$ , 47:38:15

Sample 4, MEEP:PEO: $\text{LiBF}_4$ , 62:26:12

Sample 5, MEEP:PPO: $\text{LiClO}_4$ , 48:39:13

Sample 6, MEEP: $\text{LiClO}_4$ , 92:8

Sample 7, PPO: $\text{LiClO}_4$ , 81:19

(All the compositions are in weight percentage)

Attempts have been made to use MEEP-PEO- $\text{LiBF}_4$  polymers as polymer electrolytes in  $\text{Li} / \text{TiS}_2$  batteries. It was shown that the polymer electrolyte

was stable over a 200 cycle period, suggesting the potential uses of these materials.

#### 1.4 Recent Developments

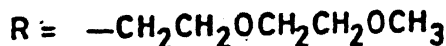
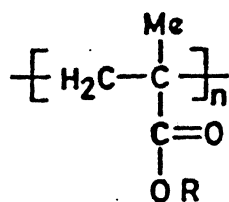
In the preceding discussion it was shown that in the polymer electrolytes, ionic conductivity is realised as a result of doping of metal salts in the host polymer. Very recently a new approach was found by Angell and coworkers<sup>101</sup>. Instead of doping polymers with metal salts they have tried doping into a salt mixture an elastomeric polymer. Among the several salt mixtures studied the highest conductivity was observed when a 50LiI-30LiOAc-20LiClO<sub>4</sub> (mole percentage) is doped with a small amount of polypropylene oxide (conductivity is  $\sim 10^{-4} \text{ Scm}^{-1}$  at room temperature) These materials have glass transitions low enough to remain rubbery at room temperature while preserving good lithium ion conductivities and high electrochemical stability.

### 1.5 Research Problem Undertaken in this Thesis

The aim of the present work is to design new polymeric materials based on inorganic and organic backbones which would form complexes with alkali metal salts and exhibit favourable ionic conductivity. As discussed previously the most widely studied polymer electrolyte PEO suffers from a poor room temperature conductivity in most of the metal salt complexes that it forms. On the other hand the etheroxy containing polyphosphazene,  $\left[ \begin{array}{c} \text{RO} \quad \text{OR} \\ \diagdown \quad \diagup \\ \text{P}=\text{N} \end{array} \right]_n$ , (MEEP, R =  $\text{CH}_2\text{CH}_2\text{OCH}_2\text{CH}_2\text{OCH}_3$ ) although readily forms complexes with several salts which show high ambient temperature ionic conductivity, suffers from certain disadvantages, (a) MEEP-metal salt complexes have poor mechanical strength; this rules out their use in a practical device (b) MEEP is water soluble making its separation from NaCl (formed in the reaction) and purification complicated. Further, the hydrophilicity of MEEP requires stringent anhydrous conditions for its study and eventual end use.

In this thesis the design of both organic and inorganic polymers which can function as polymer electrolytes is described. The rationale behind the design of the polymer structural motifs is as follows:

#### (a) Poly(MEEMA)

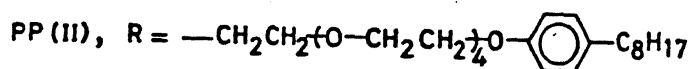
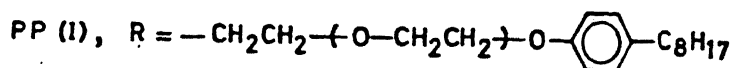
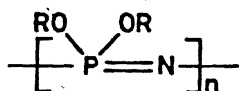


**Poly MEEMA**

In this polymeric system we have incorporated a short etheroxy side chain on to a more rigid organic acryloyl backbone. This choice while retaining the basic structural unit (responsible for complexation and transport of ions) as in

MEEP, with its relatively rigid backbone would render the eventual polymer electrolyte more stable mechanically. Further, all previous studies on acrylate polymers involved long side chains.

**(b) Polyphosphazenes, PP(I) and PP(II)**



In this system the etheroxy side chain on the polyphosphazene is terminated by a long alkyl (chain) substituted aromatic group. This structural feature while increasing the  $T_g$  should also simultaneously render the polymers water-insoluble making their purification and separation easier.

The next two chapters describe the synthesis and characterization of these polymers, along with the conductivity studies carried out with a few alkali metal salts.

## REFERENCES

1. "Solid State Ionics-91", Nicholson, P.S.; Whittingham, M.S.; Farrington, G.C.; Smeltzer, W.W.; Thomas, J. Eds. North-Holland, Amsterdam, 1992.
2. "Solid State Ionics, Materials and Applications", Chowdari, B.V.R.; Chandra, S.; Shri Singh; Srivastava, P.C., Eds. World Scientific, Singapore, 1992.
3. "Fast Ion Transport in Solids", Vashishta, P.; Mundy, J.N.; Shenoy, G.K. Eds. North-Holland, New York, 1979.
4. Rao, N.; Van den Bleck, C.M.; Schoonman, J.; Sorensen, O.T. Ref. 1, p. 30.
5. Liaw, B.J.; Liu, J.; Menne, A.; Weppner, W. Ref. 1. p. 39.
6. Passerini, S.; Scrosati, B. Ref. 1. p. 520.
7. Bange, K.; Gambke, T. *Adv. Mater.* 1990, 2, 10.
8. Visco, S.J.; Liu, M.; Doeff, M.M.; Ma, Y.P.; Lampert, C.; De Jonghe, C. *Solid State Ionics*, 1993, 60, 175.
9. Anthony, A.M. in "Solid Electrolytes, General principles, characterization, Materials, Applications", Hagenmuller, P.; Van Gool, W. Eds. Academic Press, New York, 1978.
10. "Lithium Batteries", Gabano, Ed., Academic Press, London, 1983.
11. "Modern Batteries", Vincent, C.A.; Bonino, F.; Lazzari, M.; Scrosati, B. Edward Arnold, London, 1983.
12. Hagenmuller, P.; Van Gool, W. Ref. 9. p. 235.
13. Cullander, C.; Guy, R.H. Ref. 1. p. 197.
14. Kleywept, G.J.; Driessen, W.L. *Chem. Br.*, 1988, 24, 447.
15. Rickert, H. *Angew Chem. Int. Ed. Engl.*, 1978, 17, 37.
16. (a) Owens, B.B.; Skarstad, P.M. Ref. 1. p. 665.  
(b) Yde Anderson, S.; Koksang, R.; Lundsgaard, J.S. Ref. 1. p. 673.
17. Bonino, F.; Ottaviani, M.; Scrosati, B.; Pistoia, G. *J. Electrochem. Soc.*, 1988, 135, 12.
18. (a) Shriver, D.F.; Ratner, M.A. *Chem. Rev.*, 1988.  
(b) "Polymer Electrolyte Reviews - I", Mac Callum, J.R.; Vincent, C.A. Eds. Elsevier Applied Science, New York, 1987.  
(c) "Polymer Electrolyte Reviews - II", Mac Callum, J.R.; Vincent, C.A. Eds. Elsevier Applied Science, New York, 1989.
19. *Solid State Ionics*, 1993, 60. "Proceedings of the Conference on Polymer Ionics", Gothenberg, Sweden, 1992.

20. *Electrochim. Acta*. 1992, **37**, 1468-1745. Third International Symposia on "Polymer Electrolytes", Armand, M.; Gandini, S. Eds. Pergamon Press, 1992.
21. Linford, R.G.; Hackwood, S. *Chem. Rev.*, 1981, **4**, 347.
22. Geller, S. *Top. Appl. Phys.*, 1977, **21**, 1.
23. Salamon, S.B. *Top. Curr. Phys.*, 1979, **15**, 1.
24. Dupon. R.; Papke. B.L.; Ratner. M.A.; Whitmore. D.H.; Shriver. D.F. *J. Am. Chem. Soc.*, 1982, **104**, 6247.
25. Johnson, R.T., Jr.; Morosin, B.; Knotek, M.L.; Biefeld, R.M. *Phys. Letts*, 1975, **54A**, 403.
- 26 Karvamoto, Y.; Nagura, N.;Tsuchihashi,S. *J. Am. Ceram. Soc.*, 1974, **57**,489
27. Yau, Y.Y.; Kummer, J.T. *J. Inorg. Nucl. Chem.* 1967, **29**, 2453.
28. Worrell, W.L. *Pure and Applied Chem.* 1984, **56**, 1577.
29. Armand, M.; Chabagno, J.M.; Duclot, M.J. "Fast Ion Transport in Solids", Vashishta, P.; Mundy, J.N.; Shenoy, G.K. Eds. North-Holland, New York, 1978, p. 131.
30. Fenton, D.E.; Parker, J.M.; Wright, P.V. *Polymer*, 1977, **14**, 589.
31. Wright, P.V. *Br. Poly. J.* 1975, **7**, 319.
32. Gutmann, V. "The Donor Acceptor Approach to Molecular Interactions", Plenum Press, New York, 1978.
33. Cole, S.; Cole, R.H. *J. Chem. Phys.* 1941, **9**, 341.
34. Macdonald, J.R. *J. Chem. Phys.*, 1973, **58**, 4982.
35. Macdonald, J.R. in "Superionic conductors"; Mahan, G.D.; Roth, W.L. Eds. Plenum Press, New York, 1976.
36. Dupon, R.; Whitmore, D.M.; Shriver, D.F. *J. Electrochem. Soc.* 1981, **128**, 716.
37. Fulcher, J. *Am. Chem. Soc.* 1925, **8**, 339 ; Vogel, H. *Phys. Z.* 1921, **22**, 645.
38. Armand, M.B. *Solid State Ionics*, 1983.9/10, 745.
39. Watanabe,M.;Rikukawa ; Sanui, K.; Ogata, N.; Kato, H.; Kobayashi, T.; Ohtaki, Z. *Polymer J.* 1983, **15**, 65.
40. Watanabe. M.; Togo. M.; Sanui, K.; Ogata, N.; Kobayashi, T.; Ohtaki, Z. *Macromolecules*, 1984, **17**, 2908.
41. Watanabe. M.; Ritukwa. M.; Sanui, K.; Ogata, N.; Kato. H.; Kobayashi,

- T.; Ohtaki, Z. *Macromolecules*, 1984, **17**, 2902.
42. Dupon, R.; Papke, B.L.; Ratner, M.A.; Shriver, D.F. *J. Electrochem. Soc.*, 1987, **131**, 586.
  43. Armstrong, R.D.; Clarke, M.D.; *Electrochim. Acta*, 1984, **29**, 1443.
  44. Harris, C.S.; Shriver, D.F.; Ratner, M.A. *Macromolecules*, 1986, **19**, 987.
  45. Clancy, S.; Shriver, D.F.; Ochrymowycz, L.A. *Macromolecules*, 1986, **19**, 606.
  46. Tsuchida, E.; Ohno, H.; Tsunemi, E. *Electrochim. Acta*, 1983, **28**, 833.
  47. Hardy, L.C.; Shriver, D.F. *Macromolecules*, 1984, **17**, 975.
  48. Hardy, L.C.; Shriver, D.F. *J. Am. Chem. Soc.*; 1985, **104**, 3823.
  49. Splinder, R.; Shriver, D.F. *Macromolecules*, 1986, **19**, 347.
  50. Bruce, P.G.; Krok, F.; Evans, J.; Vincent, C.A. *Solid State Ionics*, 1988, **27**, 81.; *Brit. Poly. J.*, 1988, **20**, 193.
  51. Jones, G.K.; Mc Ghie, A.R.; Farrington, G.C. *Macromolecules*, 1991, **24**, 3285.
  52. Wintersgill, M.C.; Fontanella, J.J.; Greenbaum, S.G.; Adamic, K.J. *Brit. Poly. J.* 1988, **20**, 195.
  53. Vincent, C.A. *Proc. Solid State Chem.*, 1987, **17**, 145.
  54. Smith, M.J.; Silva, C.J.R. *Solid State Ionics*, 1992, **98**, 269.
  55. Chiang, C.K.; Davis, G.T.; Harding, C.A.; Takahashi, T. *Macromolecules*, 1985, **18**, 825.
  56. Robitaille, C.P.; Fauteux, D. *J. Electro Chem. Soc.*, 1983, **133**, 315.
  57. Lee, Y.L.; Crist, B. *J. Appl. Phys.* 1986, **60**, 2683.
  58. Stainer, M.; Hardy, L.C.; Whitmore, D.H.; Shriver, D.F. *J. Electrochem. Soc.*, 1984, **131**, 784.
  59. Hibma, T. *Solid State Ionics*, 1983, **9/10**, 1101.
  60. Parker, J.M.; Wright, P.V.; Lee, C.C. *Polymer*, 1981, **22**, 1305.
  61. Berthier, C.; Gorecki, W.; Minier, M.; Armand, M.B.; Chabagno, J.M.; Rigand, P. *Solid State Ionics*, 1983, **11**, 91.
  62. Minier, M.; Berthier, C.; Gorecki, W. *Solid State Ionics*, 1983, **9/10**, 1125.
  63. Gorecki, W.; Andreani, R.; Berthier, C.; Armand, M.B.; Mali, M.; Roos, J.; Brinkmann, D. *Solid State Ionics*, 1986, **18/19**, 295.

64. Bhattacharja, S.; Smoot, S.W.; Whitmore, D.H. *Solid State Ionics*, 1986, **18/19**, 306.
65. Papke, B.L.; Ratner, M.A.; Shriver, D.F. *J. Electrochem. Soc.*, 1982, **129**, 1694.
66. Dupon, R.; Papke, B.L.; Ratner, M.A.; Whitmore, D.H.; Shriver, D.F. *J. Am. Chem. Soc.*, 1982, **104**, 6247.
67. Teeters, D.; Frech, R. *Solid State Ionics*, 1986, **18/19**, 271.
68. Papke, B.; Ratner, M.A.; Shriver, D.F. *J. Electrochem. Soc.*, 1982, **129**, 1434.
69. Chadwick, A.V.; Strange, J.H.; Worboys, M.R. *Solid State Ionics*, 1984, **9/10**, 1155.
70. Xia, D.W.; Soltz, D.; Smid, J. *Solid State Ionics*, 1984, **14**, 221.
71. Bannister, D.J.; Davies, G.R.; Ward, I.M.; Mc Intyre, J.E. *Polymer*, 1984, **25**, 1600.
72. Kobayashi, N.; Uchigama, M.; Shigehara, Tsuchida, E. *J. Phys. Chem.*, 1985, **89**, 987.
73. Cowie, J.M.G.; Martin, A.C.S. *Polymer Commun.*, 1985, **25**, 298.
74. Cowie, J.M.G.; Martin, A.C.S. *Polymer*, 1987, **28**, 627.
75. Tsuchida, E.; Ohno, H.; Kobayashi, N.; Zshizaka, H. *Macromolecules*, 1989, **22**, 1771.
76. Peramunage, D.; Fernandez, J.E.; Garcia Rubio, L.H. *Macromolecules*, 1989, **22**, 2845.
77. Rietman, E.A.; Kaplan, M.L. *J. Polym. Sci., Part C, Polym. Lett.* 1990, **28**, 187.
78. Zhang, S.; Deng, Z.; Wan, G. *J.M.S-Pure Appl. Chem.*, 1992, **A29**, 77.
79. Allcock, H.R. "Phosphorus - Nitrogen Compounds", Academic Press, New York, 1972.
80. Allcock, H.R. "Encyclopedia of Polymer Science and Engineering", Mark, Bikales, Overberger, Menger. Eds. 198, **13**, 31.
81. Allcock, H.R. *Chem. & Eng. News*, 1985, **22**.
82. Potin, Ph.; De Jaeger, R. *Eur. Polym. J.*, 1991, **27(4/5)**, 341.
83. Allcock, H.R.; Austin, P.E.; Neenan T.X.; Sisko, J.T.; Blonsky, P.M.; Shriver, D.F. *Macromolecules*, 1986, **19**, 1508.
84. Blonsky, P.M.; Shriver, D.F.; Austin, P.; Allcock, H.R. *J. Am. Chem. Soc.* 1984, **106**, 6854.



85. Blonsky, P.M.; Shriver, D.F.; Austin, P.; Allcock, H.R. *Solid State Ionics*, 1986, 18 & 19, 258.
86. Blonsky, P.M. Ph.D. Dissertation, North Western University, 1986.
87. Tonge, J.S.; Blonsky, P.M.; Shriver, D.F.; Allcock, H.R.; Austin, P.E.; Neenan, T.X.; Sisko, J.T. *Proc. Symp. on Lithium Batteries*, 1987, 87-1, 533.
88. Tonge, J.S.; Shriver, D.F.; *J. Electrochem. Soc.*, 1987, 134, 269.
89. Nazri, G.A.; Meibuhr, S.G. *J. Electrochem. Soc.* 1989, 136, 2450.
90. Abraham, K.M.; Alamgir, M.; Perrotti, S.J. *J. Electrochemical. Soc.* 1988, 105, 535.
91. Abraham, K.M. Ref. 2. p. 277.
92. Lerner, M.M.; Tipton, A.L.; Shriver, D.F.; Dembek, A.A.; Allcock, H.R. *Chem. Mater.*, 1991, 3, 1117.
93. Inoue, K.; Nishikawa, Y.; Tanigaki, T. *Macromolecules*, 1991, 24, 3464.
94. Inoue, K.; Nishikawa, Y.; Tanigaki, T. *J. Am. Chem. Soc.*, 1991, 113, 7609.
95. Inoue, K.; Nishikawa, Y.; Tanigaki, T. *Solid State Ionics*, 1992, 58, 217.
96. Cowie, J.M.G.; Sadaghianizadeh, K. *Macromol. Chem., Rapid Commun.*, 1988, 9, 387.
97. Andrei, M.; Cowie, J.M.G.; Prosperi, P. *Electrochim. Acta*, 1992, 37, 1545.
98. Cowie, J.M.G.; Anderson, A.T.; Andrei, M.; Martin, A.C.S.; Roberts, *Electrochim. Acta*, 1992, 37, 1539.
99. Abraham, K.M.; Alamgir, M. *Chem. Mater.*, 1991, 3, 339.
100. Adamic, K.J.; Greenbaum, S.G.; Abraham, K.M.; Alamgir, M.; Winstersgill, M.C.; Fontanella, J.J. *Chem. Mater.*, 1991, 3, 534.
101. Angell, C.A.; Liu, C.; Sanchez, E.; *Nature*, 1993, 362, 137.

## CHAPTER II

SYNTHESIS, CHARACTERIZATION AND IONIC CONDUCTIVITY STUDIES ON POLY(MEEMA)  
AND POLY(MEEMA) - LiX ( $X^- = \text{ClO}_4^-, \text{CF}_3\text{SO}_3^-, \text{BF}_4^-$ ) COMPLEXES

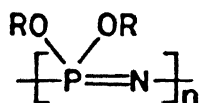
## 2.1 Introduction

Currently there is a widespread research interest in the area of polymer electrolytes and the phenomenon of ionic conduction in solvent free macro molecular systems<sup>1</sup>. This interest is largely due to potential application of these materials in electrochemical devices such as high energy density batteries<sup>2</sup>. The most widely studied polymer for this purpose is polyethylene oxide (PEO)<sup>3</sup>. High ionic conductivities have been achieved in the complexes formed between PEO and a number of mono and divalent cations such as  $\text{Li}^+$ ,  $\text{Na}^+$ ,  $\text{K}^+$ ,  $\text{Cs}^+$ ,  $\text{Ag}^+$ ,  $\text{Mg}^{2+}$ ,  $\text{Ca}^{2+}$ ,  $\text{Zn}^{2+}$ ,  $\text{Cu}^{2+}$  etc., with different counter anions such as  $\text{BPh}_4^-$ ,  $\text{CF}_3\text{SO}_3^-$ ,  $\text{ClO}_4^-$ ,  $\text{SCN}^-$ ,  $\text{I}^-$  etc. Most of the PEO-metal salt complexes are semi crystalline at ambient temperatures and higher conductivities are observed in the amorphous phase of the polymer which is attained only at higher temperatures. The crystallinity of PEO in its high conductivity region is a serious drawback for any practical electrochemical applications. Among the several approaches being currently tried towards the design of 'ideal' polymer electrolytes include (a) modification of PEO by plasticization or formation of crosslinked networks and (b) design of new macromolecular hosts capable of solubilizing ionic salts.

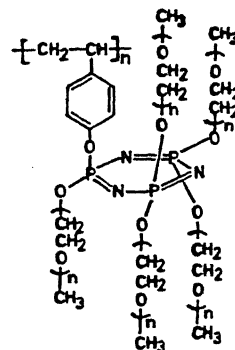
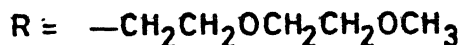
It has been shown recently that two structurally divergent polyphosphazenes (MEEP and SDEP) can complex with alkali metal ions<sup>4-7</sup>. These systems show high ionic conductivities at ambient temperatures. In polymer (MEEP) the  $\equiv \text{P} = \text{N}$  - back bone is flexible and shows large segmental motion

while in polymer (SDEP) the conductivity has to be a result of the segmental motion of the side groups on the pendant cyclophosphazene unit.

According to Inoue and coworkers who have studied (II) the oxyethylene chains form a continuous conducting phase around the rigid backbone<sup>6,7</sup>. Carrier ions could move in this phase irrespective of the rigidity of the back bone,



MEEP



(SDEP) : 2

and a high conductivity is therefore observed. Therefore, it appears that either backbone flexibility or segmental motion of the side groups can lead to highly conducting polymer electrolytes. Keeping these factors in mind we have chosen to design a simple, polyacrylate containing a short etheroxy side chain similar to the one found in MEEP and SDEP. Earlier studies on polyacrylates with oxyethylene side chains are limited and are confined to long chains and even these have not been carried out systematically<sup>8-13</sup> (Chapter I, Table 1.3). But in the case of polyacrylates containing oligooxyethylene side chains, their metal salt complexes show low conductivity levels. So we have designed a polyacrylate system where it contains a short oligooxyethylene side chain possible just as in the case of MEEP, where the side chain is methoxyethoxyethoxy group. In this chapter we describe the synthesis and

characterization of poly(MEEMA) and the ionic conductivity studies of poly(MEEMA) LiX ( $x^- = \text{ClO}_4^-, \text{CF}_3\text{SO}_3^-, \text{BF}_4^-$ ) complexes in detail.

## 2.2 Experimental

### 2.2.1 Materials

Methacrylic acid (Merck, Germany) and 2-(2-(methoxyethoxy) ethanol] (Aldrich, USA) were used as received. Thionylchloride and triethylamine (S.D. Fine chemicals, India) were distilled before use. All alkali metal salts viz.,  $\text{LiCF}_3\text{SO}_3$ ,  $\text{LiClO}_4$  (Aldrich, USA) and  $\text{LiBF}_4$  (Alfa products, USA) were dried in an oven by keeping them for 24 hours at  $100^\circ\text{C}$  prior to use. AIBN was recrystallized from methanol and vacuum dried before use. All organic solvents (employed in this work) were purified and dried by standard literature procedures<sup>14</sup>.

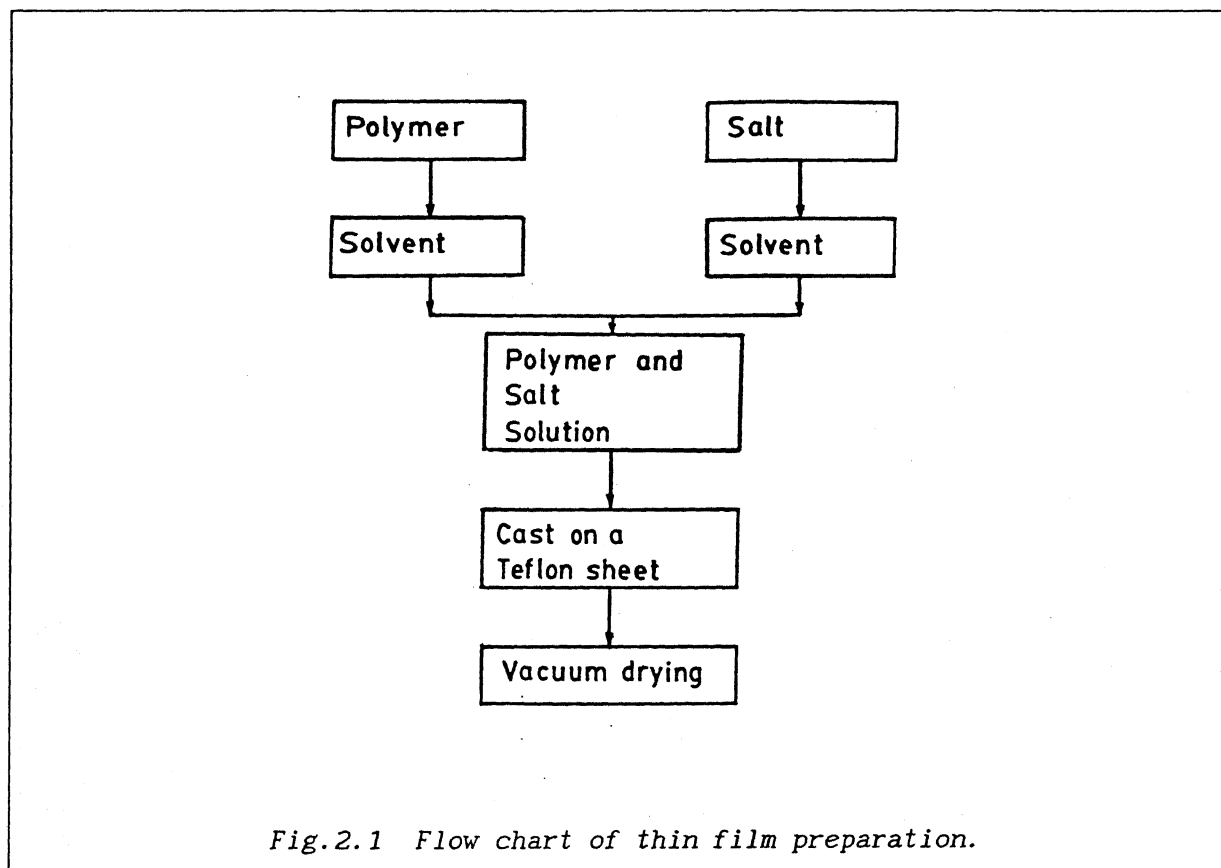
### 2.2.2 Measurements

$^1\text{H}$  and  $^{13}\text{C}$  NMR spectra were recorded on a Bruker WM 400 spectrophotometer operating at 400 MHz and 100 MHz for  $^1\text{H}$  and  $^{13}\text{C}$  respectively. All the spectra were taken in  $\text{CDCl}_3$  solvent using TMS as internal reference and the chemical shifts are reported in ppm. Upfield shifts are negative. Infrared spectra were recorded as neat or film in  $\text{CHCl}_3$  on Perkin-Elmer FT IR 1600 series model spectrophotometer. Thermal data were obtained on a Perkin-Elmer DSC 7 thermal analyzer and a Dupont 9900 thermal analyzer at a heating rate of  $10^\circ$  per minute. GPC measurements were carried out on a maxima 820 instrument using THF as solvent and poly styrene as standard calibrant. Dilute solution viscosity measurements were carried out on a Schott-Gerate Viscometer in dry benzene at  $26^\circ\text{C}$  using Ubbelohde Viscometer (Capillary size 0.46 mm). X-ray diffraction patterns of all the samples were recorded on a Rich Seifort (Iso Debye flex

2002D) counter diffractometer using a  $\text{CuK}_\alpha$  radiation, operating at 30 kV. All XRD studies were done at room temperature. The electron micrograph were taken with a JEOL scanning microscope (JSM-840A). Each sample was silver coated using sputtering unit (International Scientific instruments PS-2 coating unit) before loading in the system. The photographs were taken at 10 kV accelerating voltage. The system has a provision of 10X - 3,60,000X magnification of the images. The magnification was fixed according to the need.

### 2.2.3 Thin Film Preparation

Appropriate amounts of poly(MEEMA) and the alkali metal salt were dissolved in THF and allowed to form a homogeneous solution of polymer salt complex by



stirring at room temperature for 8 to 20 hours. The concentrated solution was cast on a teflon sheet and the solvent was removed by slow evaporation at room

temperature. The samples were dried completely by keeping in a vacuum oven at 40°C with a pressure of  $10^{-1}$  torr for 48 hours. The dried thin films (thickness 0.2 mm to 0.8 mm) were used to do the conductivity measurements. Fig. 2.1 shows the flow chart of thin film preparation.

#### 2.2.4 Electrical measurements

The conductivity studies were carried out using a HP 4194A impedance/gain phase analyzer with a slow heating rate. A dynamic vacuum of  $\sim 10^{-3}$  torr was maintained throughout the experiment to exclude trace amounts of moisture and solvent that might be present in the sample. The bulk resistance of the complexes at different composition of the polymer and salt were obtained using the complex impedance spectra at different temperatures. The dc conductivity was derived from the resistance, using the relation given below :

$$\sigma = \frac{g}{R_b}$$

where,  $\sigma$  is the total ionic conductivity of the sample,  $g$  is the geometric factor, depends on the thickness of the film (sample) area of the electrodes.  $R_b$  is the bulk resistance obtained from the impedance spectra.

Fig. 2.2 shows the block diagram of sample holder used to measure the impedance. The impedance of each sample as a function of frequency and temperature was measured with a slow heating rate. The dc conductivity was determined by complex impedance analysis which was analyzed by using a software package<sup>15</sup>.

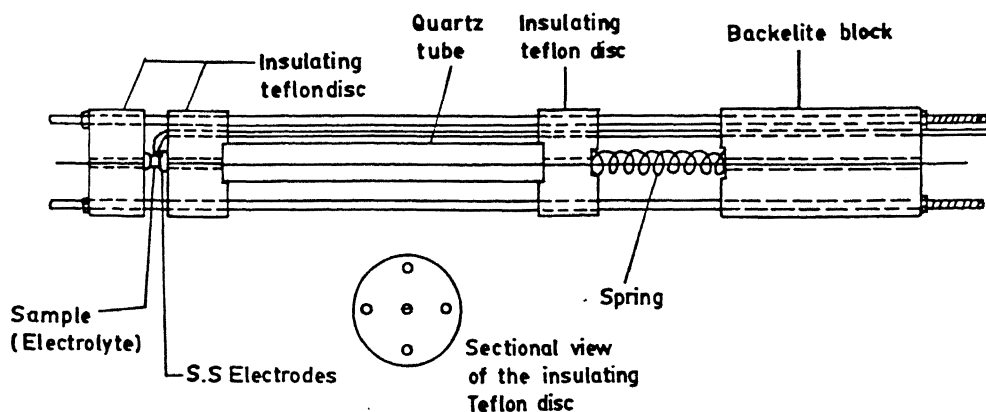


Fig.2.2. Block Diagram of Sample Holder Used for Electrical Measurements

## 2.2.5 Synthesis of Methoxy Ethoxy Ethyl Methacrylate (MEEMA) and Poly (methoxyethoxyethylmethacrylate), Poly (MEEMA)

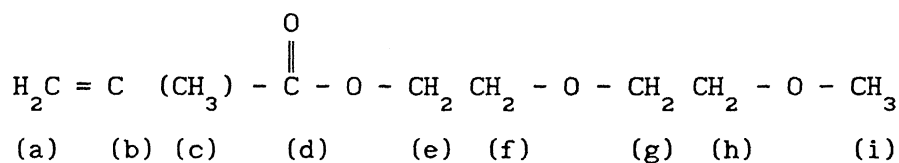
### 2.2.5.1 Methacryloyl Chloride

Thionylchloride (50.0 ml, 0.53 mol) was taken in a three necked RB flask, fitted with a reflux condenser. To this methacrylic acid (45.7 ml, 0.53 mol) was added dropwise over a period of 30 minutes with stirring. The reaction mixture was stirred for another 5 hours at room temperature. Fractional distillation of the mixture gave methacryloyl chloride (50.0 ml, 90%) b.p.  $96^{\circ}\text{C}$  (lit.  $96^{\circ}\text{C}$ ).

$^1\text{H NMR}$  ( $\text{CDCl}_3$ ) :  $\delta$ , 6.10; 5.58 ( $=\text{CH}_2$ ); 1.95 ( $-\text{CH}_3$ )

### 2.2.5.2 Methoxy ethoxy ethyl methacrylate, (MEEMA)

To a stirred ice cold solution of 2-[2-(methoxy ethoxy) ethanol] (59.2g, 0.49 mol) and triethylamine (55.5 g 0.55 mol) in dry benzene (250 ml), methacryloyl chloride (55.6 g, 0.53 mol) was added dropwise for a period of 45 minutes. After the addition was over the stirring was continued for four more hours. The resulting triethylamine hydrochloride was filtered and benzene was evaporated to afford an oil. This was distilled at reduced pressure (0.1 mm/82°C) to afford MEEMA (70.2 g, 70%)



$^1\text{H}$  NMR ( $\text{CDCl}_3$ ) :  $\delta$ , 6.14 (a); 5.58 (a); 4.31 (e); 3.76 (f); 3.67 (g); 3.57 (h); 3.4 (i); 1.95 (b)

$^{13}\text{C}$  NMR ( $\text{CDCl}_3$ ) :  $\delta$ , 167.07 (d); 135.96 (b); 125.44 (a); 71.71 (e); 70.32 (f); 68.95 (g); 63.64 (h); 58.8 (i); 18.06 (c)

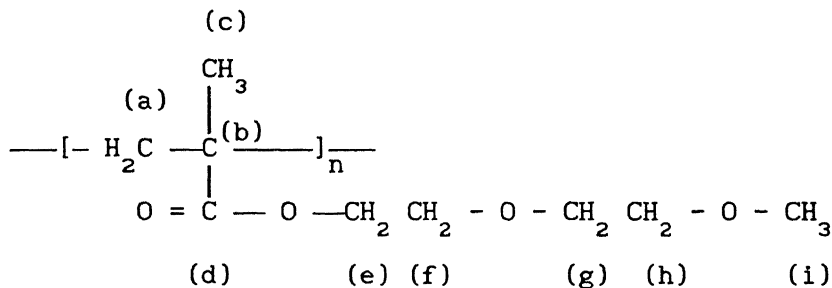
IR (neat,  $\text{cm}^{-1}$ ) : 2934.0 (m); 1770 (W); 1733.0 (vs); 1620 (m); 1440 (m); 1310 (s); 1290 (s); 1110.0 (s); 1040 (m); 930 (m), 800 (W).

### 2.2.5.3 Poly (Methoxyethoxyethylmethacrylate), Poly(MEEMA)

MEEMA (5.0g, 26.61 mmol) was taken in dry benzene (50 ml) with AIBN (43.6 mg. 0.27 mmol) in a thick walled glass ampoule. The solution was subjected to four freeze-thaw cycles by cooling to 77 K and allowing to come to room temperature under a vacuum of 0.1 torr. The tube was vacuum sealed and kept for polymerization at 65°C for 10 hours. The tube was broken and the contents were poured into a large excess of n-hexane precipitating the polymer. Reprecipitating was performed three times to afford poly(MEEMA), which was



dried at 50°C under vacuum (0.1 Torr) for 24 hours (4.0g, 80%)



$^1\text{H}$  NMR ( $\text{CDCl}_3$ ) :  $\delta$ , 4.12 (e); 3.69 (f); 3.64 (g); 3.57 (h); 3.42 (i); 1.83; 1.07 and 0.90 (a, c).

$^{13}\text{C}$  NMR ( $\text{CDCl}_3$ ) :  $\delta$ , 177.03 (b); 71.76 (e); 70.32 (f); 68.37 (g); 63.73 (h); 58.87 (i); 18.34; 16.53(a, c).

IR (neat,  $\text{cm}^{-1}$ ) : 3579.2 (w); 2934.0 (vs); 1733.8 (vs); 1458 (s); 1388.6 (m); 1245.7 (s); 1110.11 (vs); 862 (m), 741 (w)

#### 2.2.5.4 Poly(MEEMA) - Alkali metal Salt Complexes

A typical example for the preparation of a poly(MEEMA)-LiX complex film is given below :

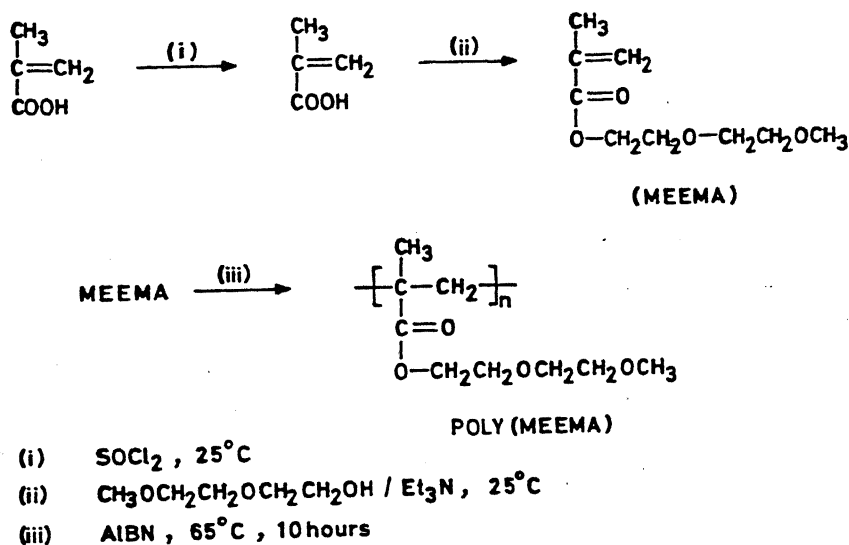
0.38g (2mmol) of poly(MEEMA) and 0.31g (2mmol) of  $\text{LiCF}_3\text{SO}_3$  was dissolved in dry THF (10ml) separately in different containers. The two THF solutions were mixed together to give a polymer-salt solution in THF. This mixture was stirred for 8 hours to get a homogeneous solution and then the solvent was evaporated at room temperature to give a concentrated solution. The concentrated solution was cast on a teflon sheet and the final trace of solvent was removed by keeping it in a vacuum oven ( $10^{-3}$  Torr) at 50°C for 24 hours. Thus the obtained film is a Poly(MEEMA)- $\text{LiCF}_3\text{SO}_3$  complex with a O:Li ratio of 4:1. The carbonyl oxygen has also been used for calculating O:Li ratio.

All the complexes studied have been prepared by analogous method.

## 2.3 Results and Discussion

### 2.3.1 Synthesis and characterization of MEEMA and poly(MEEMA)

The monomer, MEEMA and poly(MEEMA) are synthesized according to the scheme.



Scheme

The  $^1\text{H}$  and  $^{13}\text{C}$  NMR spectra of the monomer and polymer are shown in figure 2.3 and 2.4 respectively. As can be seen, the vinylic protons present in MEEMA are absent in poly(MEEMA) indicating complete polymerization (Fig. 2.3).  $^{13}\text{C}$  NMR spectra corroborate this fact. It should be mentioned that the polymerization of MEEMA requires stringent experimental conditions with a need to expunge to the extent possible - oxygen from the reaction medium. In order to ensure this a solution of MEEMA in benzene containing the initiator AIBN was subjected to four freeze-thaw cycles by cooling to 77 K and allowing to come to

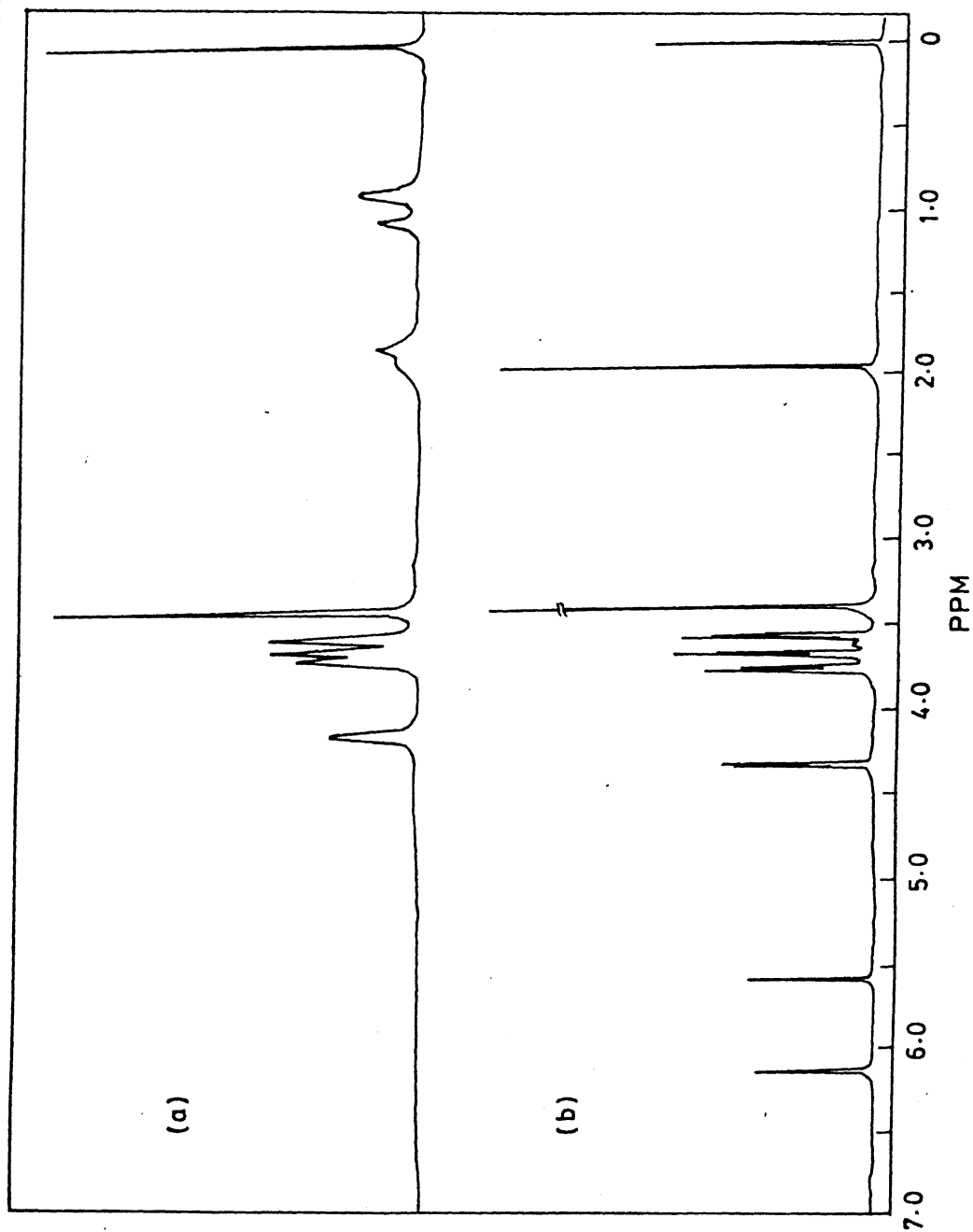


Fig.2.3.  $^1\text{H}$  NMR (400 MHz) of (a) Poly(MEEMA) and (b) MEEHA.

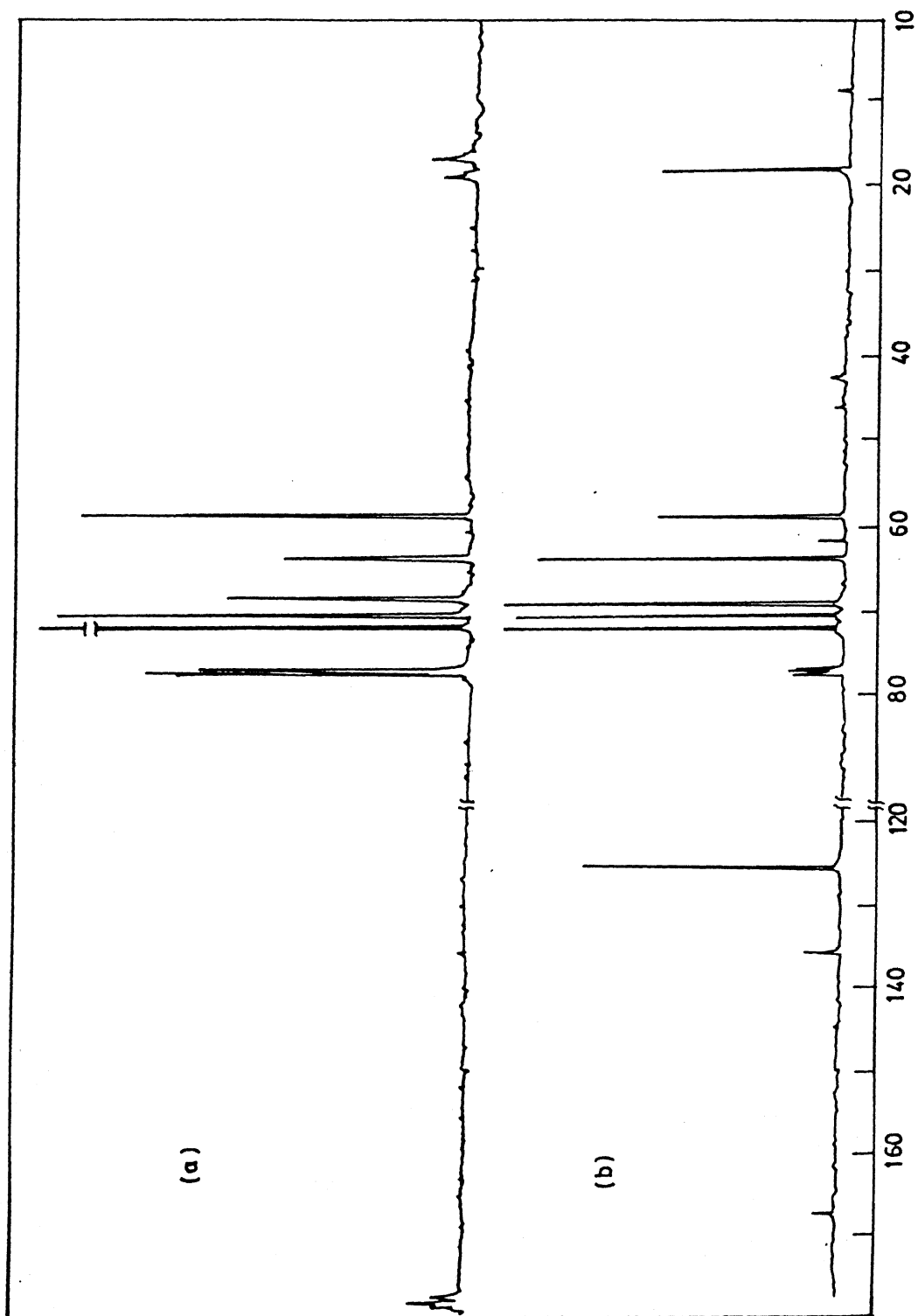


Fig. 2.4.  $^{13}\text{C}$  NMR (137 MHz) of (a) Poly(MEEMA) and (b) MEEMA.

room temperature under a vacuum of 0.1 torr. Polymerization vessels were vacuum sealed and kept for polymerization at a fixed temperature (See experimental).

Poly(MEEMA) is a colourless, transparent, elastomer and is readily soluble in several organic solvents such as benzene, THF, chloroform etc. However, Poly(MEEMA) has been found to be insoluble in straight chain hydrocarbons such as hexane, heptane and also in solvents like water. Poly (MEEMA) has a good shelf life; no significant changes in the polymeric material was observed when left for atleast 3 months at ambient temperatures. Poly(MEEMA) is a high molecular weight polymer. The molecular weight obtained from GPC measurements with polystyrene as the standard showed high molecular weight species is of  $2.4 \times 10^5$ , However, the polydispersity is high, 34.86. Dilute solution viscosity studies carried out on the polymer revealed that the intrinsic viscosity is  $17.35 \text{ cc g}^{-1}$ . Table 2.1 summarizes the data on  $\eta_{\text{relative}}$ ,  $\eta_{\text{specific}}$  and  $\eta_{\text{reduced}}$  at different concentration of poly(MEEMA). Fig. 2.5 shows the reduced viscosity vs concentration plot, from which the intrinsic viscosity value was obtained.

Table 2.1

S.No.	Relative Viscosity $\eta_r$	Specific Viscosity $\eta_{sp}$	Reduced Viscosity $\eta_{red}$	Concentration g/100 ml
1.	1.2136	0.2136	24.71	0.8646
2.	1.1507	0.1507	22.93	0.6571
3.	1.1068	0.1068	21.45	0.4980
4.	1.1151	0.1151	22.29	0.5163
5.	1.0809	0.0809	20.51	0.3947
6.	1.0544	0.0544	18.17	0.2995

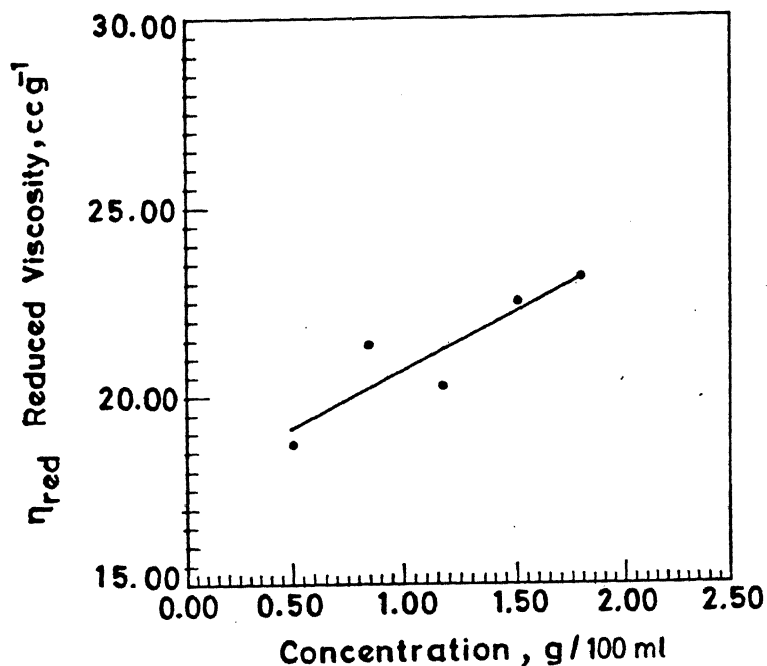
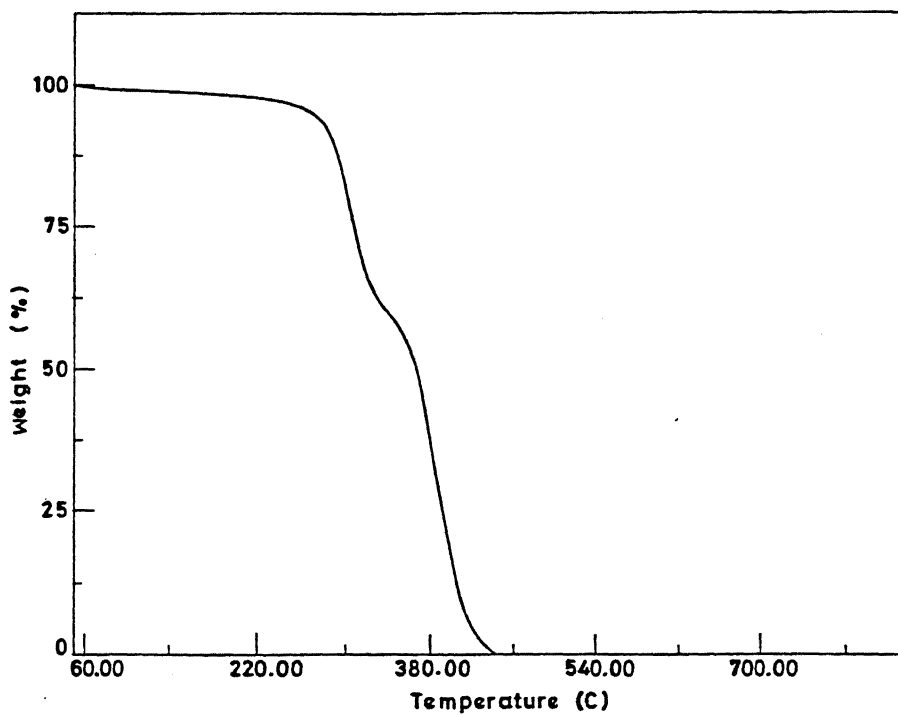


Fig.2.5. Reduced Viscosity vs Concentration Plot for Poly(MEEMA) at 26°C

Thermogravimetric analysis shows poly(MEEMA) has a 3 step decomposition process, with first decomposition occurring at 284°C, the second at 370°C, and complete decomposition takes place at 444°C (Fig. 2.6) DTA and DSC analysis from room temperature (25°C) to 450°C reveal only changes due to decomposition and none due to phase transition. Low temperature DSC shows an endotherm at -26.5°C which has been attributed to the glass transition temperature of the sample (Fig. 2.7). The amorphous nature of the polymer has also been confirmed



*Fig.2.6. Thermogram of Poly(MEEMA).*

by XRD studies (Fig. 2.8). No peaks due to any crystalline phase were detected. Similarly, the scanning electron microscopy (SEM) studies on poly(MEEMA) show the sample is amorphous with no crystalline domain (Fig. 2.9).

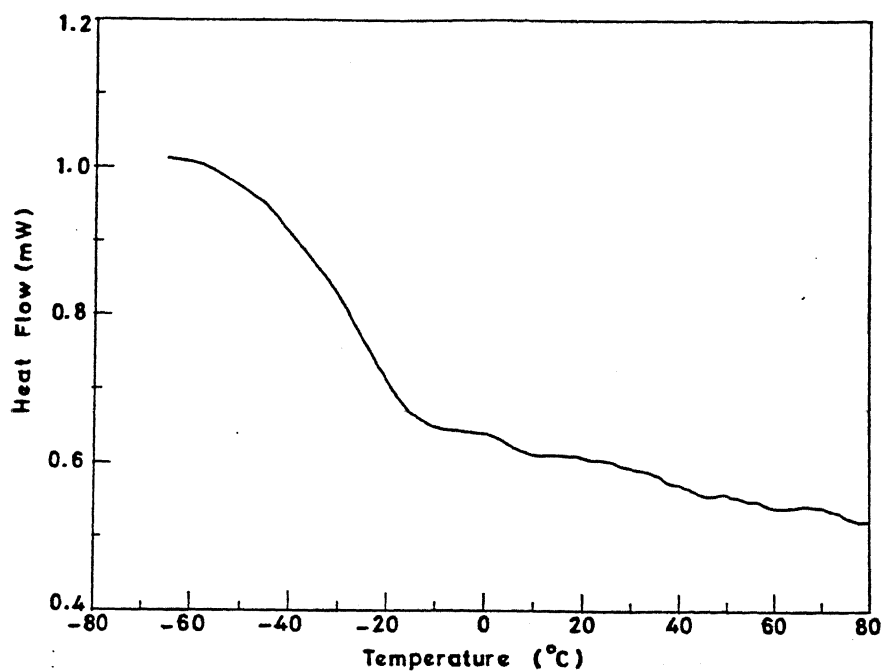


Fig.2.7. Low temperature DSC curve of Poly(MEEMA).



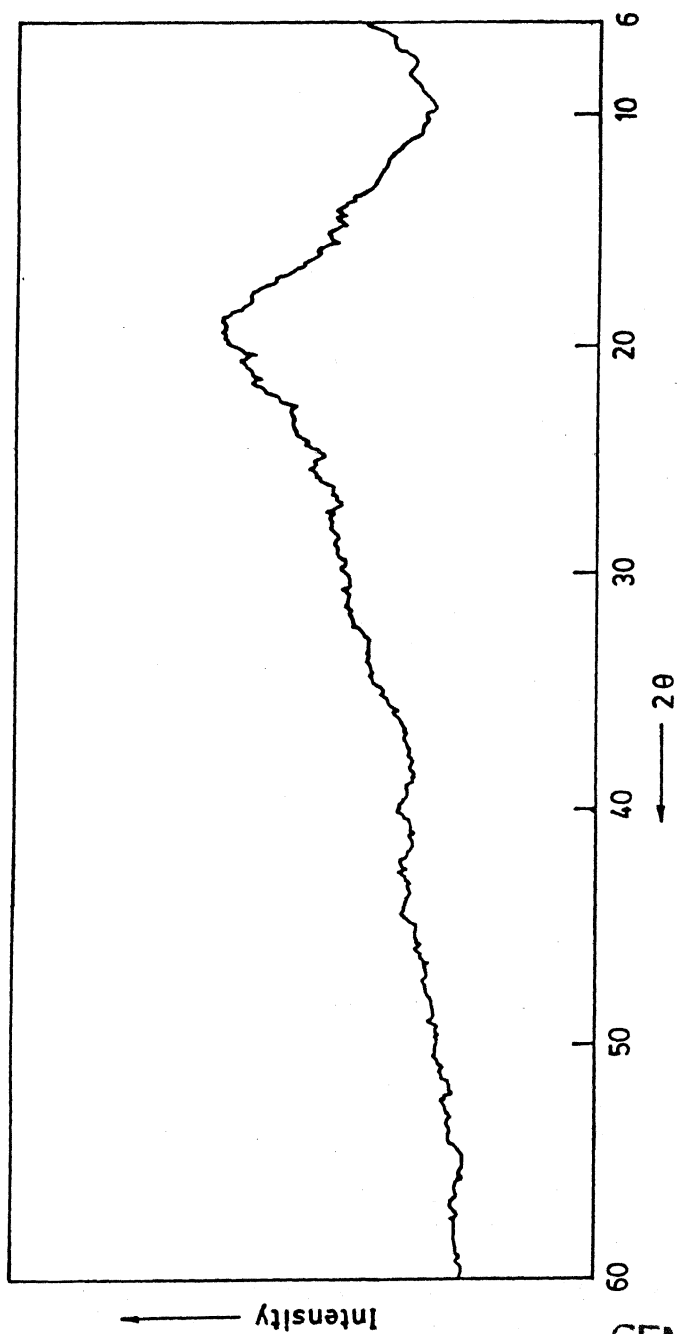
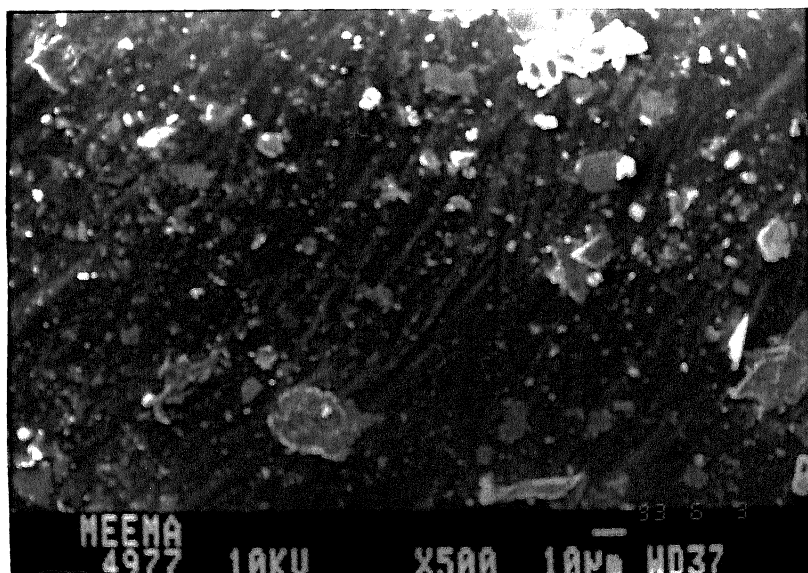


Fig.2.8. XRD plot of polymer , Poly(MEEMA).

CENTRAL LIBRARY  
I. I. T., KANPUR

Acc. No. A. 017875



*Fig.2.9. SEM photograph of Poly(MEEMA).*

### 2.3.2 Characterization of Poly(MEEMA) - Alkali Metal Salt Complexes

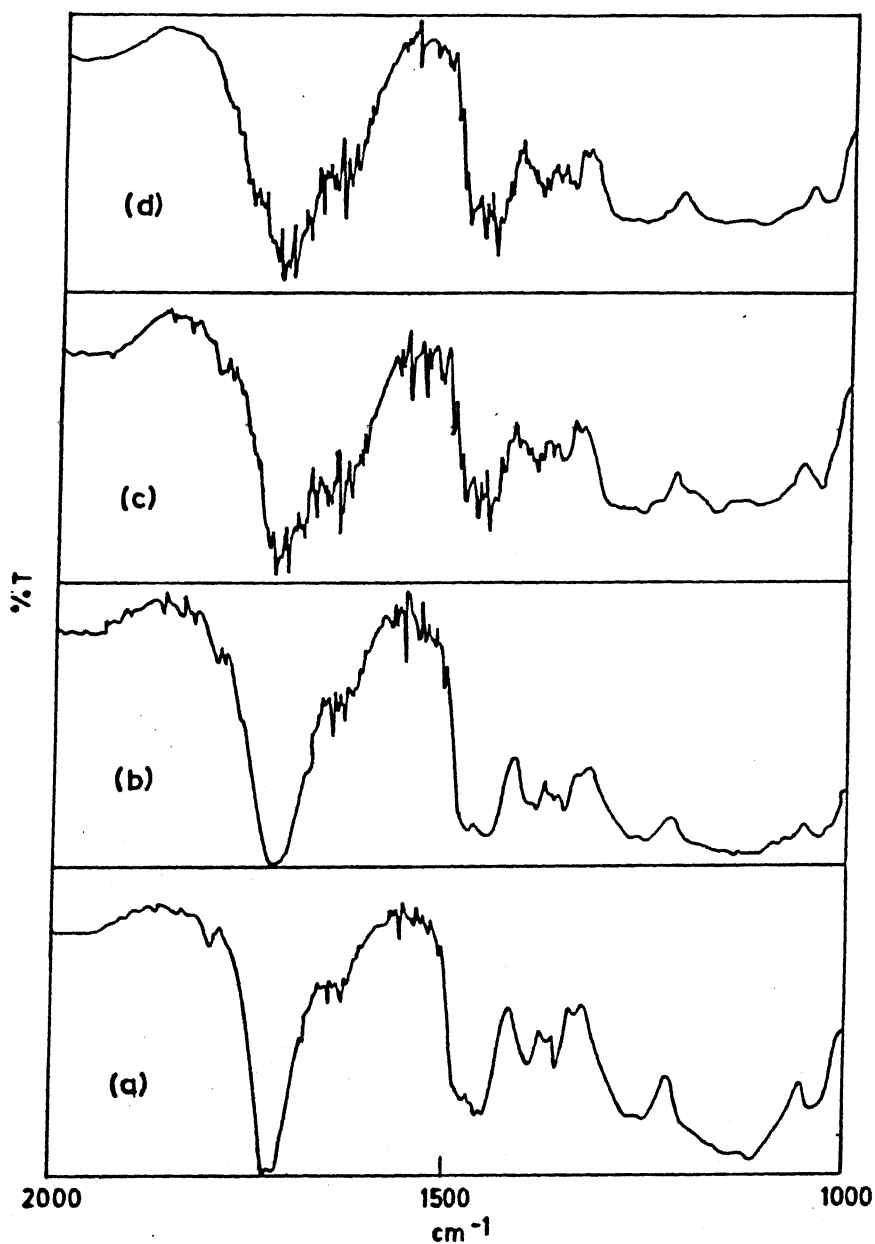
Poly(MEEMA) - LiX (  $X^- = \text{ClO}_4^-$ ,  $\text{CF}_3\text{SO}_3^-$ , and  $\text{BF}_4^-$  ) complexes were prepared using the procedure given in section 2.2.5.4. Characterization of the complexes is discussed below:

The infrared spectra of polymer-metal salt complexes with pure Poly(MEEMA) are given in Fig. 2.10 and the peak positions are tabulated in Table 2.2. The results obtained from infrared studies reveal that there is no

Table 2.2 Infrared spectral data for selected Poly(MEEMA)-LiX  
( $X^- = \text{CF}_3\text{SO}_3^-$ ,  $\text{ClO}_4^-$ ,  $\text{BF}_4^-$ ) complexes

Sample	O:Li Ratio	C = O stretching $\text{cm}^{-1}$	C—O—C stretching $\text{cm}^{-1}$
Poly(MEEMA)	1:0	1733.8(vs)	1110.1(vs)
Poly(MEEMA)- $\text{LiCF}_3\text{SO}_3$	8:1	1729.8(vs)	1164.9, 1037.3(b)
	12:1	1731.7(vs)	1167.7(b)
		1714.6(vs)	
	20:1	1724.1(vs)	1113.1(b)
	24:1	1731.9(vs)	1108.8(b)
		1715.4(vs)	
$\text{LiClO}_4$	8:1	1727.8(vs)	1111.9(b)
	10:1	1731.6(vs)	1113.8(b)
		1713.9(vs)	
	12:1	1725.4(vs)	1100.1(b)
$\text{LiBF}_4$	6:1	1731.7(vs)	1108.3(b)
		1714.8(vs)	
	20:1	1731.8(vs)	1104.1(b)
		1715.4(vs)	
(vs), Very Strong; (b), Broad			

drastic structural change observed because of the salt complexation. However, one can derive the following informations i.e., the peak position corresponding



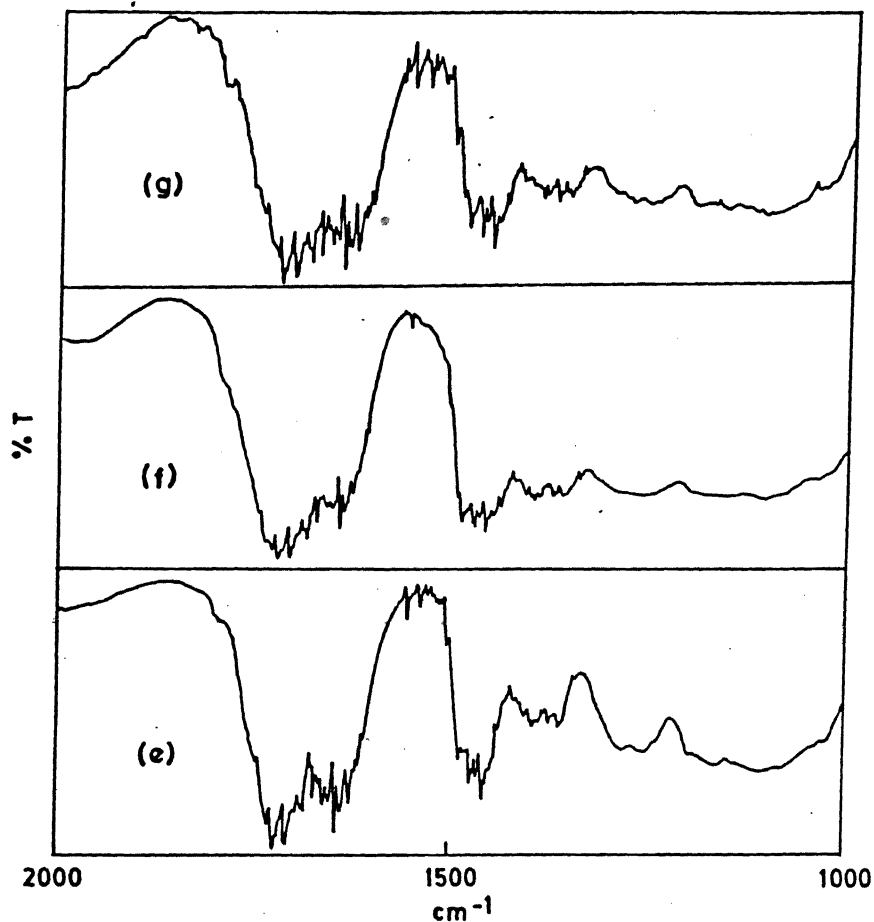


Fig. 2.10.

Infrared spectra of selected Poly(MEEMA)-metal salt complexes:

(a) Poly(MEEMA); (b) Poly(MEEMA)-LiCF<sub>3</sub>SO<sub>3</sub> (O:Li, 20:1); (c) Poly(MEEMA)-LiCF<sub>3</sub>SO<sub>3</sub> (O:Li, 12:1); (d) Poly(MEEMA)-LiCF<sub>3</sub>SO<sub>3</sub> (O:Li, 24:1); (e) Poly(MEEMA)-LiBF<sub>4</sub> (O:Li, 6:1); (f) Poly(MEEMA)-LiBF<sub>4</sub> (O:Li, 20:1); (g) Poly(MEEMA)-LiClO<sub>4</sub> (O:Li, 10:1).

to that of the carbonyl group,  $C = O$ , for pure poly(MEEMA) is shifted down by about  $15\text{--}20\text{ cm}^{-1}$ , suggesting that there is a weak interaction possibly between the carbonyl oxygen and the alkali metal of the salt used for complexation. Thus in the preparation of the polymer-alkali metal complexes at different Li : O ratios, the carbonyl oxygen has also been taken into account for the calculation of polymer and salt. The other changes are expected only in the C-O-C region. However, the peak due to C-O-C stretching frequency at  $\sim 1100\text{ cm}^{-1}$  is very broad in the virgin polymer and therefore the shift in values is not clearly seen upon complexation, although further broadening in this region is seen. However, from literature evidences of other polymer electrolytes, PEO-LiX, PEG-NaI, it is reasonable to propose that in the present instance the oxygens of the ethoxy side groups are also involved in interaction with the metal ion.

The scanning electron microscopic (SEM) studies reveal that the native polymer, Poly(MEEMA) as well as the polymer-metal salt complexes are amorphous in nature showing no spherulitic structure due to crystalline phase. However, for the polymer-salt complexes containing excess salt content, the salt forms a crystalline phase on the surface of the sample. The SEM photographs of selected polymer-salt complexes are given in Fig. 2.11.

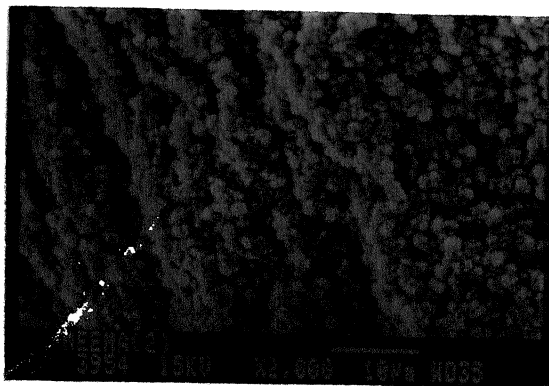
The amorphous nature and complete complexation of the polymer-metal salt complexes were further confirmed by X-ray diffraction (XRD) studies. In XRD also, no crystalline phase is detected showing the amorphous nature of the polymer as well as the metal salt complexes of the polymer, Poly(MEEMA). In principle the amorphous nature of the polymer metal salt complexes can be confirmed by low temperature DSC studies. DSC studies were done for all the complexes from room temperature ( $\sim 25^{\circ}\text{C}$ ) to  $400^{\circ}\text{C}$ . No peaks due to any phase transformation were observed. Low temperature DSC could not be done due



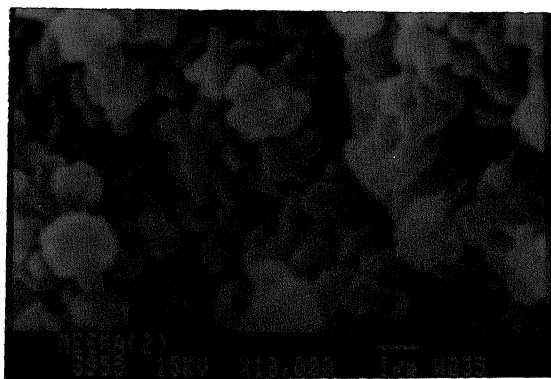
(a) Magnification, X 500



(a) Magnification, X 2000



(b) Magnification, X 2000



(b) Magnification, X 10000

**Fig.2.11. SEM Photographs of selected poly(MEEMA)-metal salt complexes:**  
 (a) Poly(MEEMA)-LiBF<sub>4</sub> (O:Li, 20:1) and  
 (b) Poly(MEEMA)-LiClO<sub>4</sub> (O:Li, 8:1)



to the non availability of this facility.

In conclusion the structural studies suggest that the polymer- metal salt complexes form a homogeneous amorphous phases at room temperature ( $\sim 25^{\circ}\text{C}$ ).

### 2.3.3 Conductivity Studies on Poly(MEEMA) - Metal salt complexes

By using the film casting technique, described in the experimental section, several poly(MEEMA) - alkali metal salt complexes in various compositions were made using  $\text{LiCF}_3\text{SO}_3$ ,  $\text{LiClO}_4$  and  $\text{LiBF}_4$  respectively. The choice of the metal salts has been dictated by the small size of cation and the large size of the anion. It was felt that the small cation would aid in increased ionic mobility. The large anion while showing a restricted mobility would also not form ion pairs with the alkali metal ion. Further this combination of ions leads to a low lattice energy for the salt enabling favourable solution of the cation as described in Chapter I.

The various compositions of the poly(MEEMA) - metal salt complexes were made by varying the O : Li ratios. In the calculation the carbonyl oxygen was also taken into consideration (see experimental, 2.2.5.4). The dried polymer-metal salt complexes were made into thin films and used for conductivity measurements. To avoid cell polarization ac impedance analysis was carried out using stainless steel as ion blocking electrodes. Block diagram of the sample holder is given in Fig. 2.2. The dc conductivity of each compositions at different temperature was measured by complex analysis in view of strong frequency dependent impedances of the sample. The impedance of all the composition of poly(MEEMA) :  $\text{LiX}$  ( $\text{X}^- = \text{CF}_3\text{SO}_3^-, \text{ClO}_4^-, \text{BF}_4^-$ ) at different O : Li ratios and temperatures were carried out (Chapter I). Figures 2.12, 2.13, and 2.14 show the representative impedance spectra of each metal salt complex of poly(MEEMA). The dc resistance of each sample at different temperature was

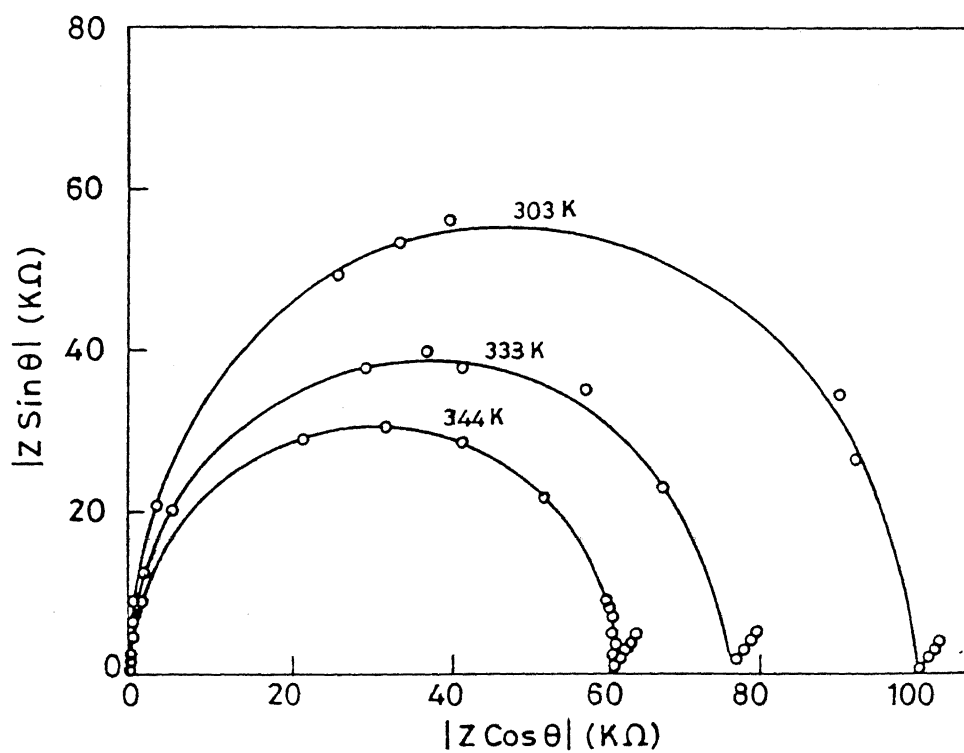


Fig.2.12. Representative impedance spectra of Poly(MEEMA)-LiCF<sub>3</sub>SO<sub>3</sub> complex (O:Li ratio 24:1) at 3 different temperatures

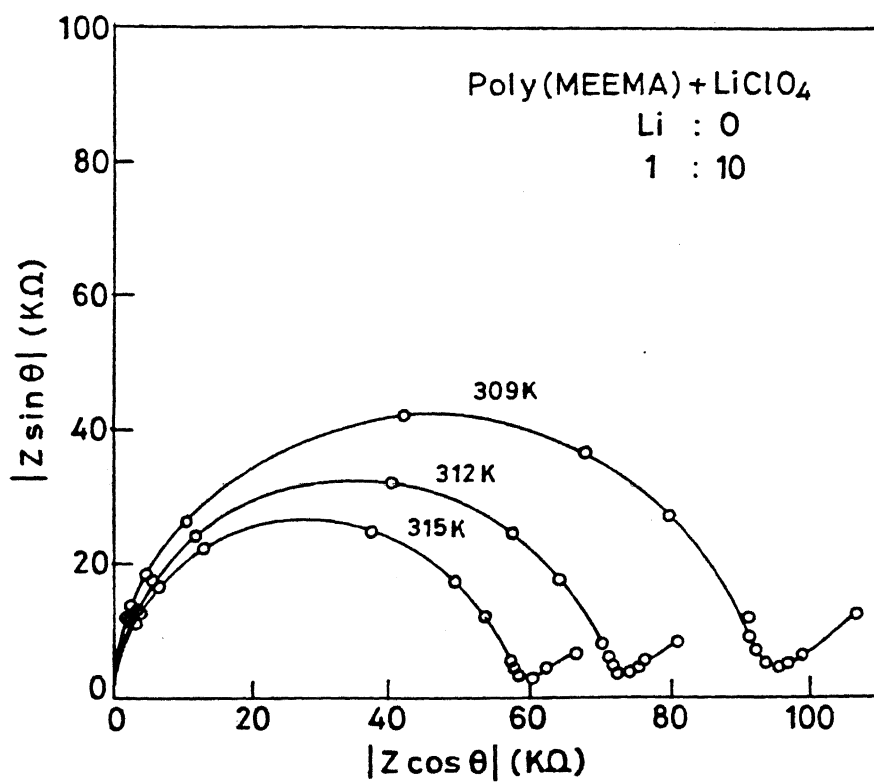


Fig.2.13. Representative impedance spectra of Poly(MEEMA)-LiClO<sub>4</sub> complex (O:Li ratio 10:1) at 3 different temperatures

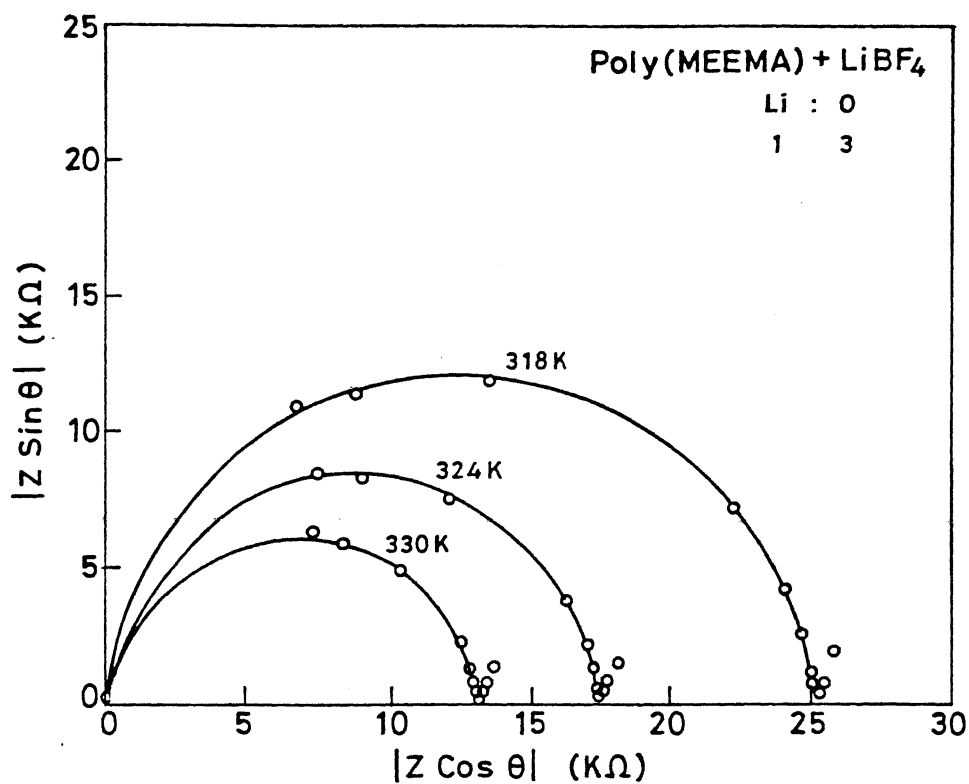


Fig.2.14. Representative impedance spectra of Poly(MEEMA)-LiBF<sub>4</sub> complex (O:Li ratio 3:1) at 3 different temperatures

obtained and the conductivity was computed according to the procedure described in the experimental (2.2.4). Figures 2.15, 2.16 and 2.17 show the conductivity plots ( $\log \sigma$  vs  $\frac{10^3}{T}$ ) obtained for Poly(MEEMA) - LiX complexes ( $X^- = CF_3SO_3^-$ ,  $ClO_4^-$ ,  $BF_4^-$ ). Tables 2.3, 2.4 and 2.5 summarize the dc conductivity of Poly(MEEMA) -  $LiCF_3SO_3$ , Poly(MEEMA) -  $LiClO_4$ , Poly(MEEMA) -  $LiBF_4$  complexes respectively at different O : Li ratio, and at three different temperatures. Several features emerge from the variable temperature conductivity studies.

The dc conductivity of virgin polymer, Poly(MEEMA) is  $1.38 \times 10^{-8} \text{ S.cm}^{-1}$ , indicating that the native polymer is a good insulator and compares well with ultra pure MEEP which shows a conductivity of  $8 \times 10^{-8} \text{ S.cm}^{-1}$  at  $25^\circ\text{C}$ . The conductivity plots of  $\log \sigma$  Vs  $\frac{10^3}{T}$  for a variety of polymer salt complexes, are gentle curves as expected for amorphous polymers due to the T, To temperature dependence. Upon addition of the metal salts the conductivity increases steadily at any given temperature reaches an optimum value and starts to drop as the metal ion concentration is increased. Also the conductivities experience an enhancement for any given polymer-salt complex with increase in temperature.

Among the various systems studied the conductivity trends can be summarized as follows :

- (a) The highest conductivity at room temperature is observed for Poly(MEEMA) -  $LiBF_4$  system for an O:Li ratio of 5:1, this system shows a conductivity of  $5.8 \times 10^{-5} \text{ Scm}^{-1}$  (300K) and  $3.3 \times 10^{-4} \text{ Scm}^{-1}$  (330K). The value is atleast 3 order of magnitude higher than that of the virgin polymer.
- (b) In the case of Poly(MEEMA)- $LiClO_4$  the conductivity values observed are lower than that observed for the  $LiBF_4$  system. The interesting feature of the conductivity behaviour of Poly(MEEMA) -  $LiClO_4$  complexes is that although at lower temperature different conductivities are seen for

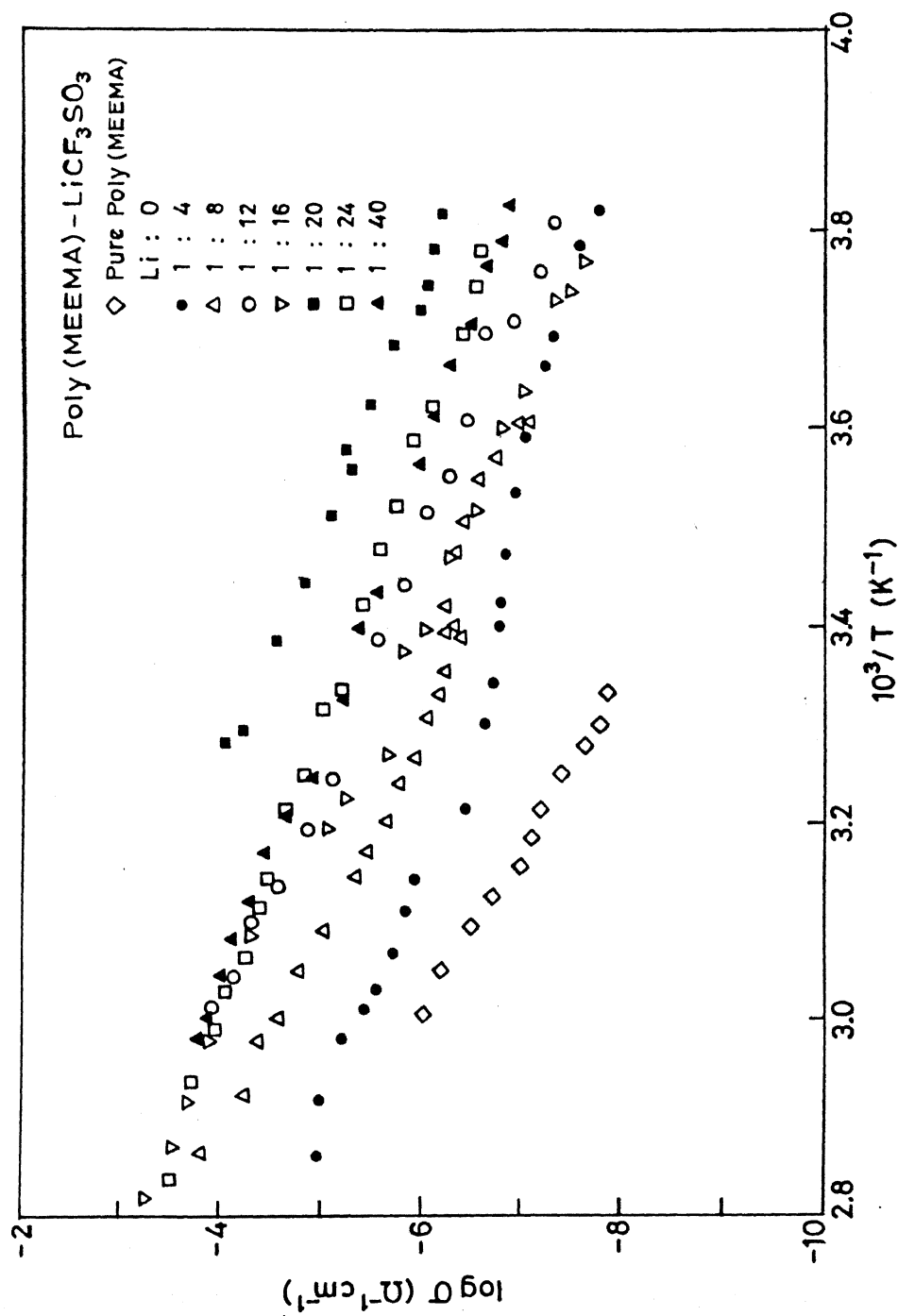


Fig.2.15. Conductivity plots ( $\log \sigma$  vs  $10^3/T$ ) of Poly(MEEMA)- $\text{LiCF}_3\text{SO}_3$  complex

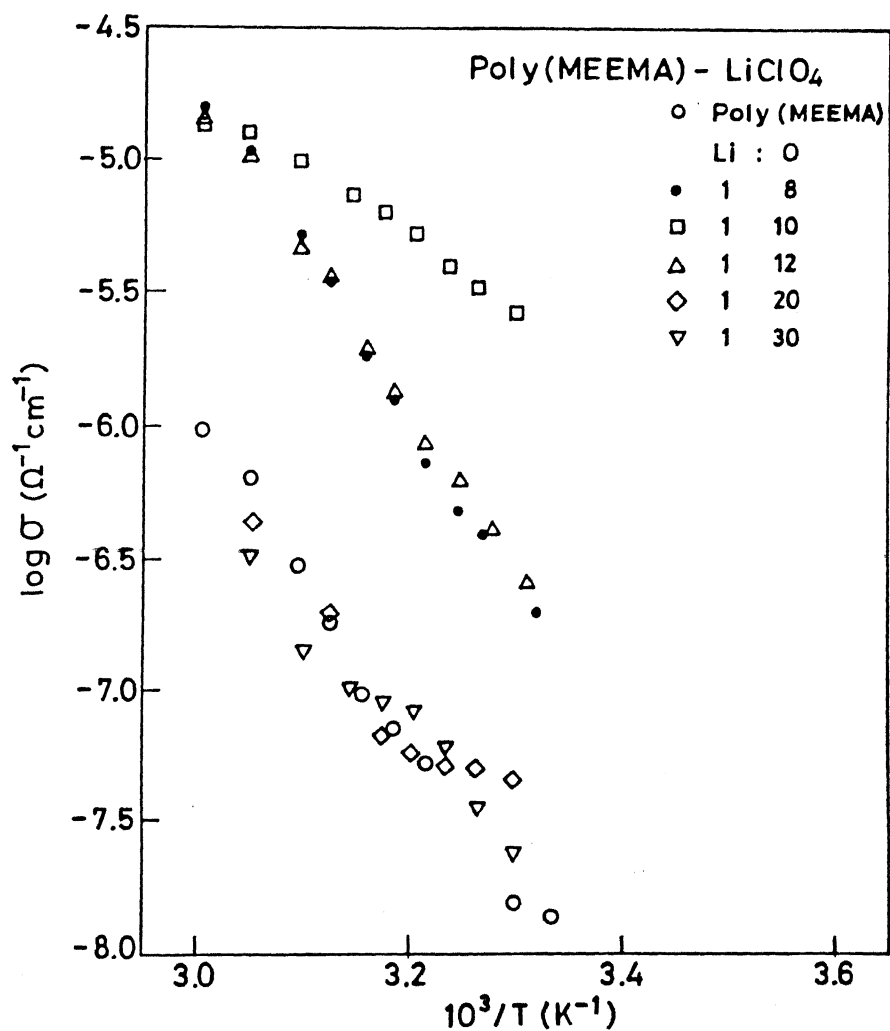


Fig. 2.16.

Conductivity plots ( $\log \sigma$  vs  $10^3/T$ ) of Poly(MEEMA)-LiClO<sub>4</sub> complex

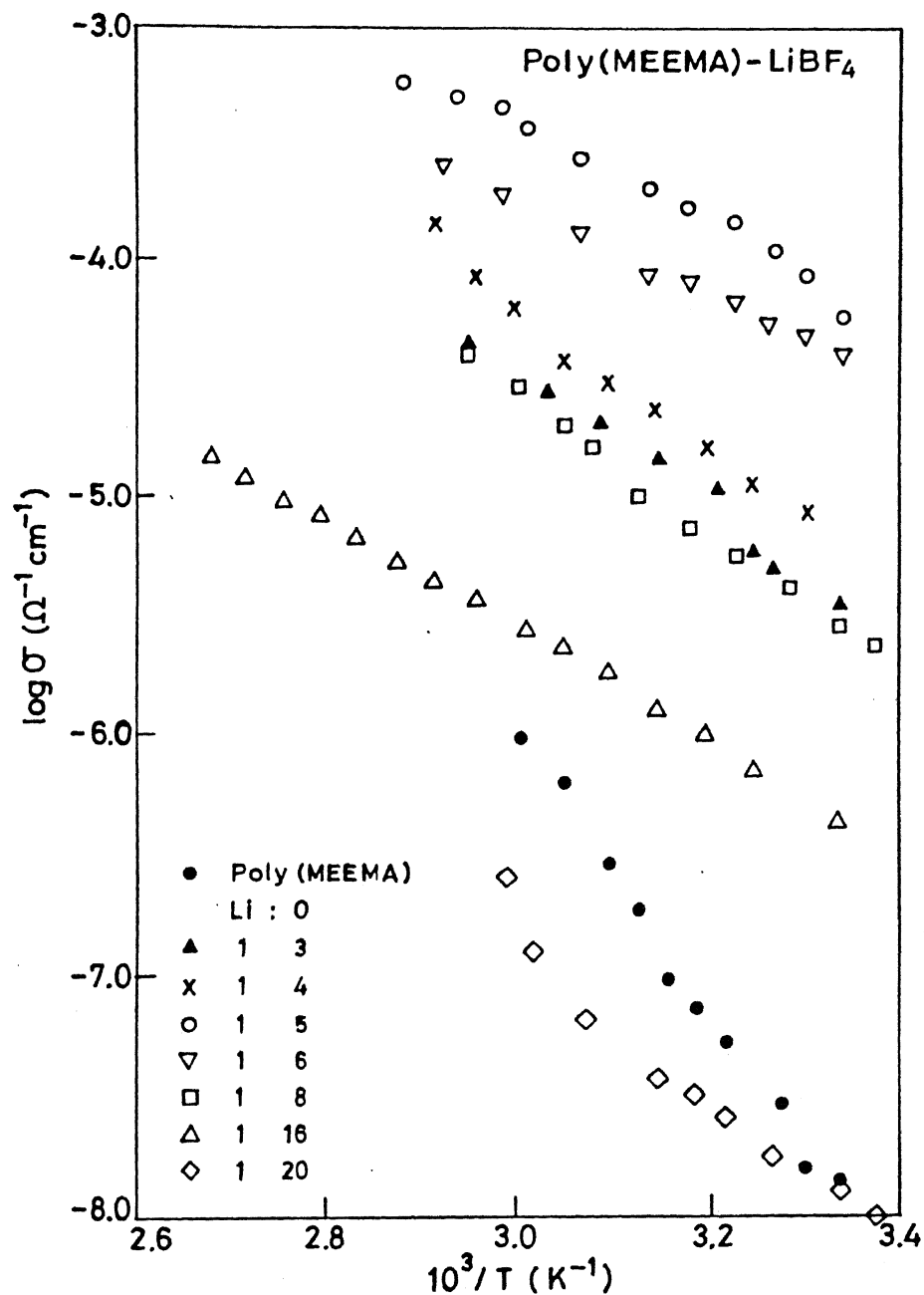


Fig.2.17. Conductivity plots ( $\log \sigma$  vs  $10^3/T$ ) of Poly(MEEMA)-LiBF<sub>4</sub> complex



Table 2.3 Poly(MEEMA) -  $\text{LiCF}_3\text{SO}_3$ 

Composition Li:O Ratio	$\sigma$ $\text{Scm}^{-1}$ (270K)	$\sigma$ $\text{Scm}^{-1}$ (303K)	$\sigma$ $\text{Scm}^{-1}$ (333K)
1:4	$4.5 \times 10^{-8}$	$2.7 \times 10^{-7}$	$3.7 \times 10^{-6}$
1:8	--	$8.3 \times 10^{-7}$	$2.9 \times 10^{-5}$
1:12	$2.1 \times 10^{-7}$	--	$1.0 \times 10^{-4}$
1:16	--	--	$1.2 \times 10^{-4}$
1:24	$3.8 \times 10^{-7}$	$1.0 \times 10^{-5}$	$1.0 \times 10^{-4}$
1:20	$2.3 \times 10^{-6}$	$6.1 \times 10^{-5}$	--
1:40	$4.8 \times 10^{-7}$	$6.1 \times 10^{-6}$	$1.2 \times 10^{-4}$

Table 2.4 Poly(MEEMA) -  $\text{LiClO}_4$ 

Composition Li:O Ratio	$\sigma$ $\text{Scm}^{-1}$ (305K)	$\sigma$ $\text{Scm}^{-1}$ (323K)	$\sigma$ $\text{Scm}^{-1}$ (333K)
1:8	$4.05 \times 10^{-7}$	$4.95 \times 10^{-6}$	$1.50 \times 10^{-5}$
1:10	$3.27 \times 10^{-6}$	$1.00 \times 10^{-5}$	$1.40 \times 10^{-5}$
1:12	$4.13 \times 10^{-7}$	$7.61 \times 10^{-6}$	$1.41 \times 10^{-5}$
1:20	$2.41 \times 10^{-7}$	$1.5 \times 10^{-6}$	$3.91 \times 10^{-6}$
1:30	$3.45 \times 10^{-8}$	$1.36 \times 10^{-7}$	—

Table 2.5 Poly(MEEMA) -  $\text{LiBF}_4$ 

Composition Li:O Ratio	$\sigma$ $\text{Scm}^{-1}$ (300K)	$\sigma$ $\text{Scm}^{-1}$ (318K)	$\sigma$ $\text{Scm}^{-1}$ (330K)
1:3	$3.35 \times 10^{-6}$	$1.46 \times 10^{-5}$	$2.66 \times 10^{-5}$
1:4	$8.26 \times 10^{-6}$	$2.30 \times 10^{-5}$	$2.66 \times 10^{-5}$
1:5	$5.81 \times 10^{-5}$	$2.03 \times 10^{-4}$	$3.25 \times 10^{-4}$
1:6	$3.98 \times 10^{-5}$	$7.94 \times 10^{-5}$	$1.52 \times 10^{-4}$
1:8	$2.71 \times 10^{-6}$	$8.21 \times 10^{-6}$	$1.55 \times 10^{-4}$
1:16	$4.44 \times 10^{-7}$	$1.26 \times 10^{-6}$	$2.43 \times 10^{-4}$
1:20	$1.26 \times 10^{-8}$	$3.47 \times 10^{-8}$	$1.00 \times 10^{-4}$

closely related compositions (with Li : O ratio 1:8, 1:10, 1:12), a same maximum conductivity value of  $1.5 \times 10^{-5} \text{ Scm}^{-1}$  is observed for all the three compositions at 333 K.

- (c) In Poly(MEEMA)- $\text{LiCF}_3\text{SO}_3$  system the highest conductivities observed is for 20:1 (O:Li)  $2.98 \times 10^{-5} \text{ Scm}^{-1}$  at 298 K.

Plots of  $\log \sigma$  vs Li/O ratios for various Poly(MEEMA)-metal salt complexes are shown in Figures 2.18, 2.19, and 2.20. It can be clearly seen that increase

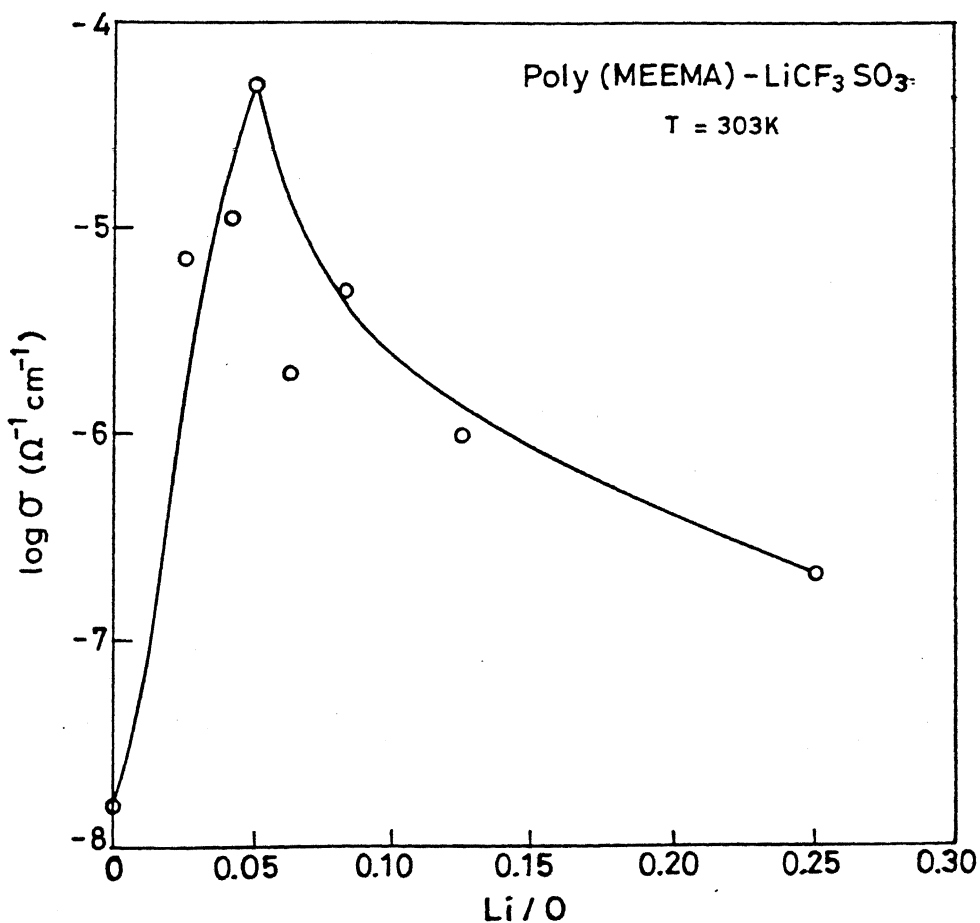


Fig.2.18. Plot of  $\log \sigma$  vs Li/O ratios for Poly(MEEMA)- $\text{LiCF}_3\text{SO}_3$  complexes

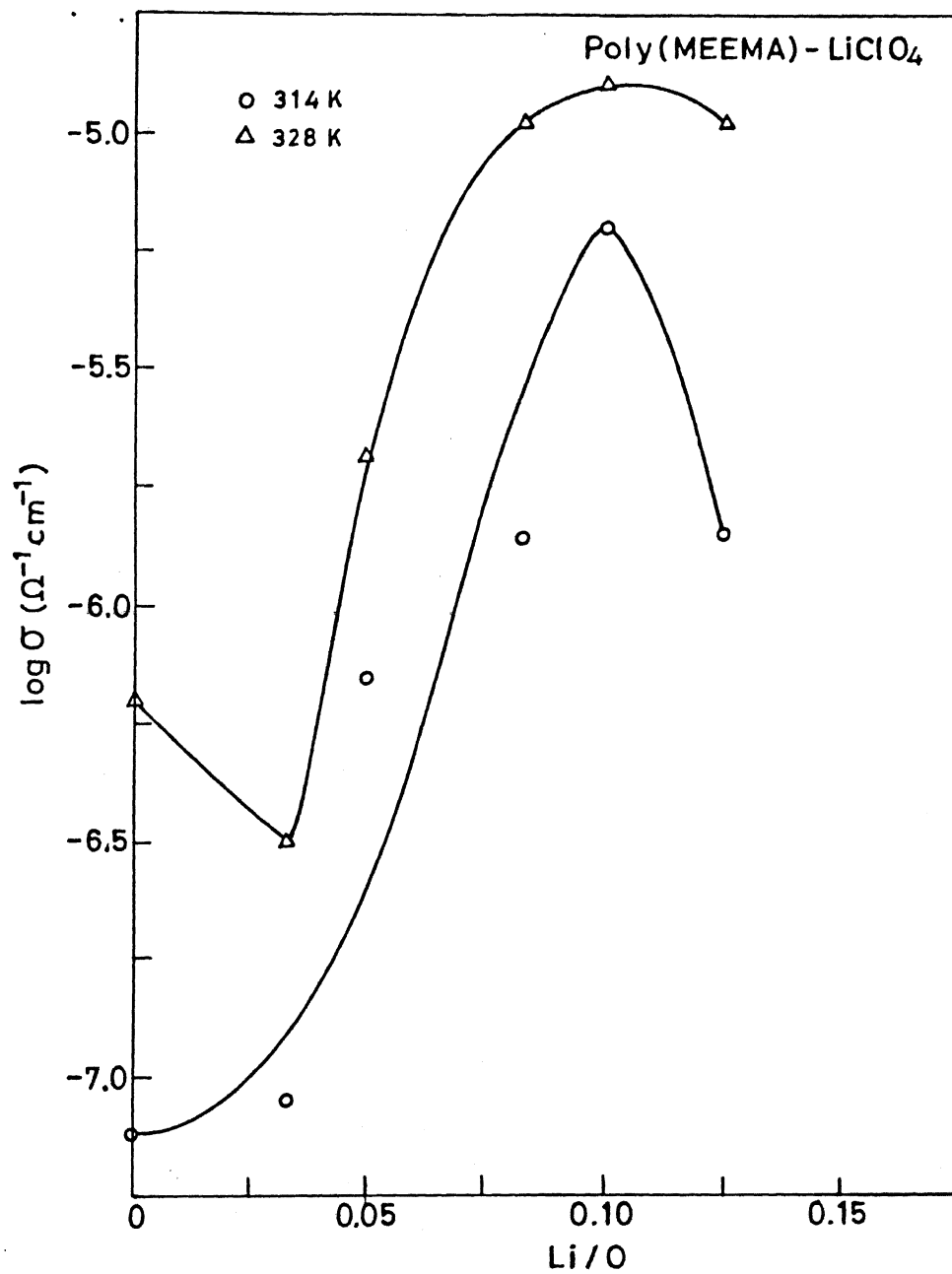


Fig.2.19. Plot of  $\log \sigma$  vs Li/O ratios for Poly(MEEMA)-LiClO<sub>4</sub> complexes

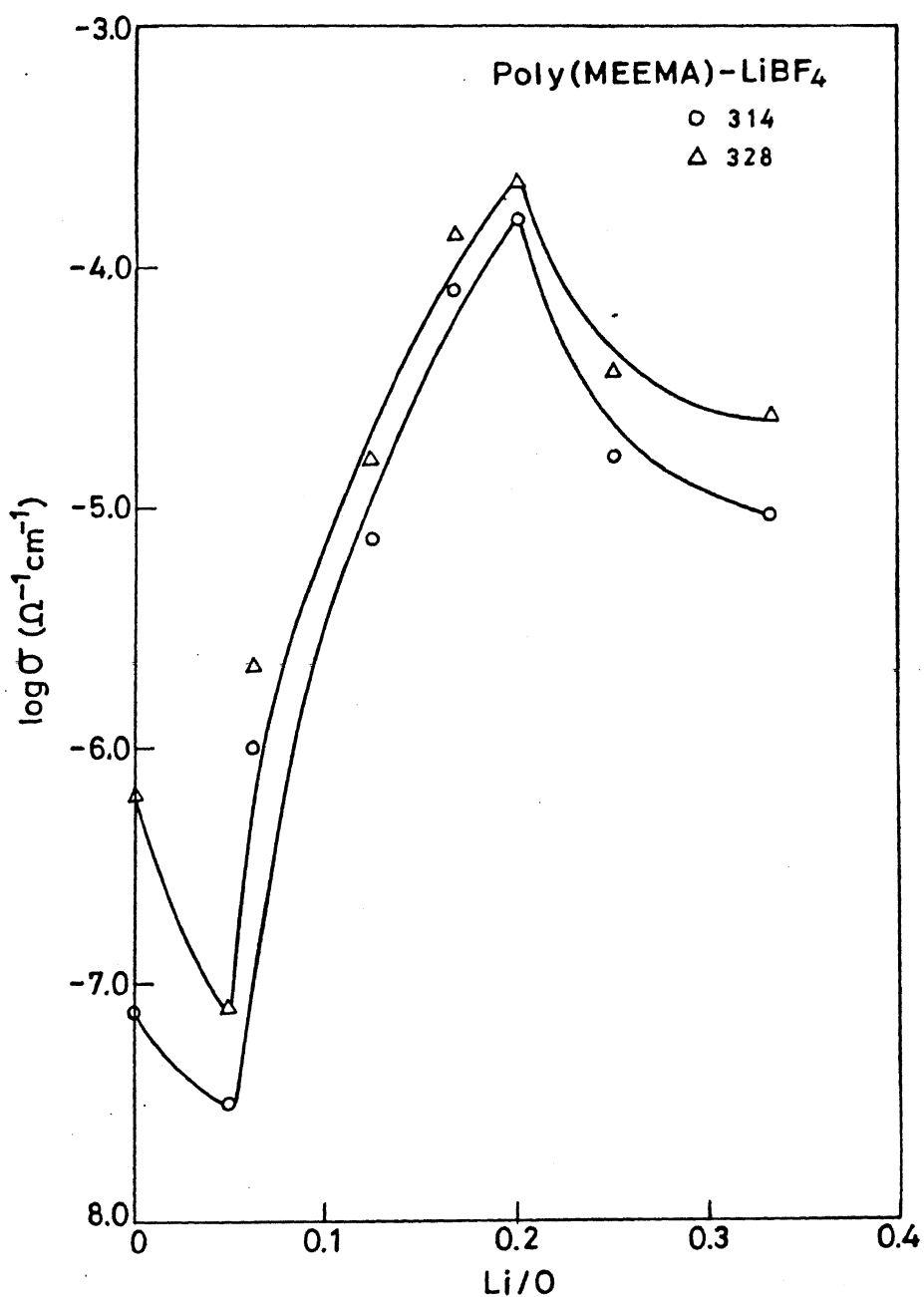


Fig.2.20. Plot of  $\log \sigma$  vs Li/O ratios for Poly(MEEMA)-LiBF<sub>4</sub> complexes

in metal ion concentration in the polymer leads to an increase in ionic conductivity upto an optimum value. After this further addition of metal salt leads to a sharp decrease in conductivity. The plots also show that at very dilute concentrations of  $\text{Li}^+$  in the polymer there is actually a decrease in conductivity. Recent studies by Gray on molar conductance dependence on salt concentration of  $\text{LiClO}_4$  complexes of an amorphous solid polyether,  $[(\text{OCH}_2\text{CH}_2)_x\text{OCH}_2]_y$  and a low molecular weight polyether,  $\text{CH}_3(\text{OCH}_2\text{CH}_2)_4\text{OCH}_3$ , suggest that solid and liquid systems behave similarly: a steep fall in conductivity is seen at low concentration of the salt<sup>15</sup>. This has been attributed to formation of non-conducting ion pairs. Such a behaviour is normal in very low dielectric constant solvents, or other solvating media which in the present instance is the polymer itself.

The ionic conductivity behaviour in Poly(MEEMA)-LiX systems as evident by  $\log \sigma$  Vs  $\frac{10^3}{T}$ , plots follow the pattern observed earlier for other amorphous polymer solid electrolytes such as MEEP. This behaviour is explained by the free volume or excess entropy model (Chapter I). The conductivity of an amorphous polymer can be expressed by Vogel-Tamman-Fulcher (VTF) equation,

$$\sigma = AT^{-1/2} \exp \left[ - \frac{B}{T-T_0} \right]$$

where, the term A is proportional to the number of charge carriers and the  $T_0$  term in the exponential is closely related to the glass transition temperature of the sample. B is the pseudo activation energy.

The data obtained for the present Poly(MEEMA) - LiX systems have been fit into VTF equation. Plots of  $(\ln \sigma \sqrt{T}/A)^{-1}$  vs T for all the three Poly(MEEMA)-LiX systems are shown in Figures 2.21, 2.22 and 2.23. From these plots the  $T_0$ ,  $T_g$  and B values have been computed. These are tabulated in Tables 2.6, 2.7 and 2.8. In general, it can be seen that for the highest conducting compositions the  $T_0$  values are among the lowest. Since the  $T_g$  values of the polymer-metal

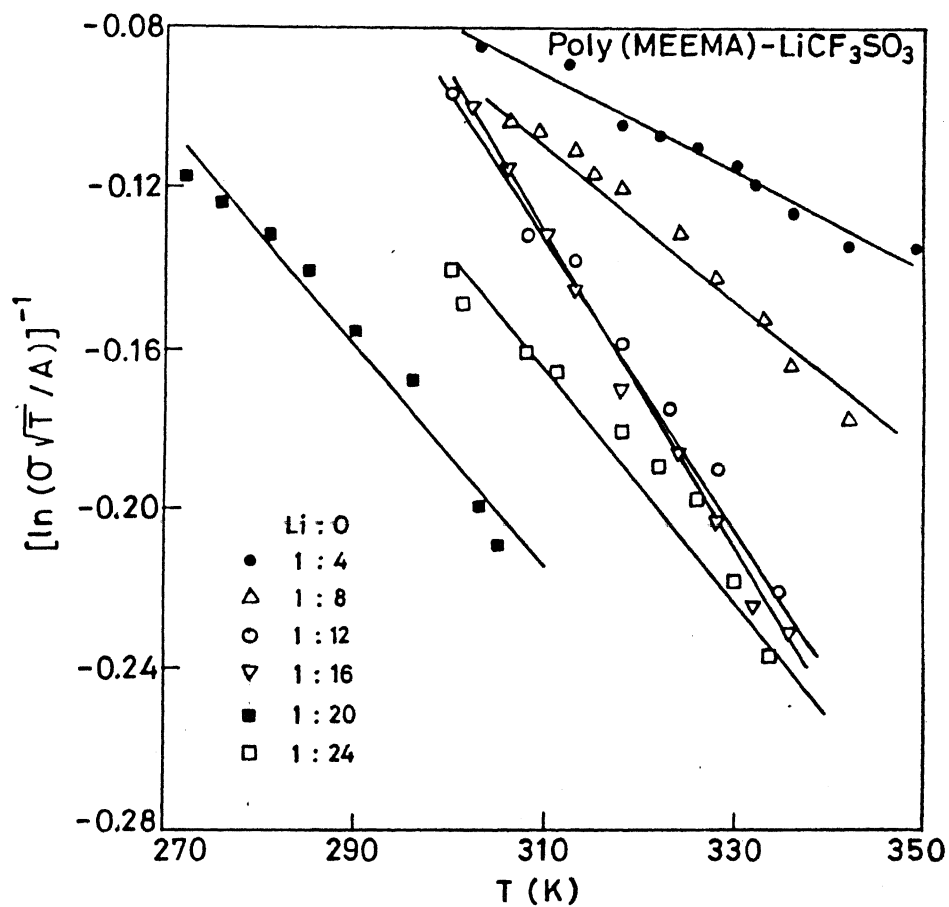


Fig.2.21. Plot of  $(\ln \sigma\sqrt{T}/A)^{-1}$  vs T for Poly(MEEMA)-LiCF<sub>3</sub>SO<sub>3</sub> complexes

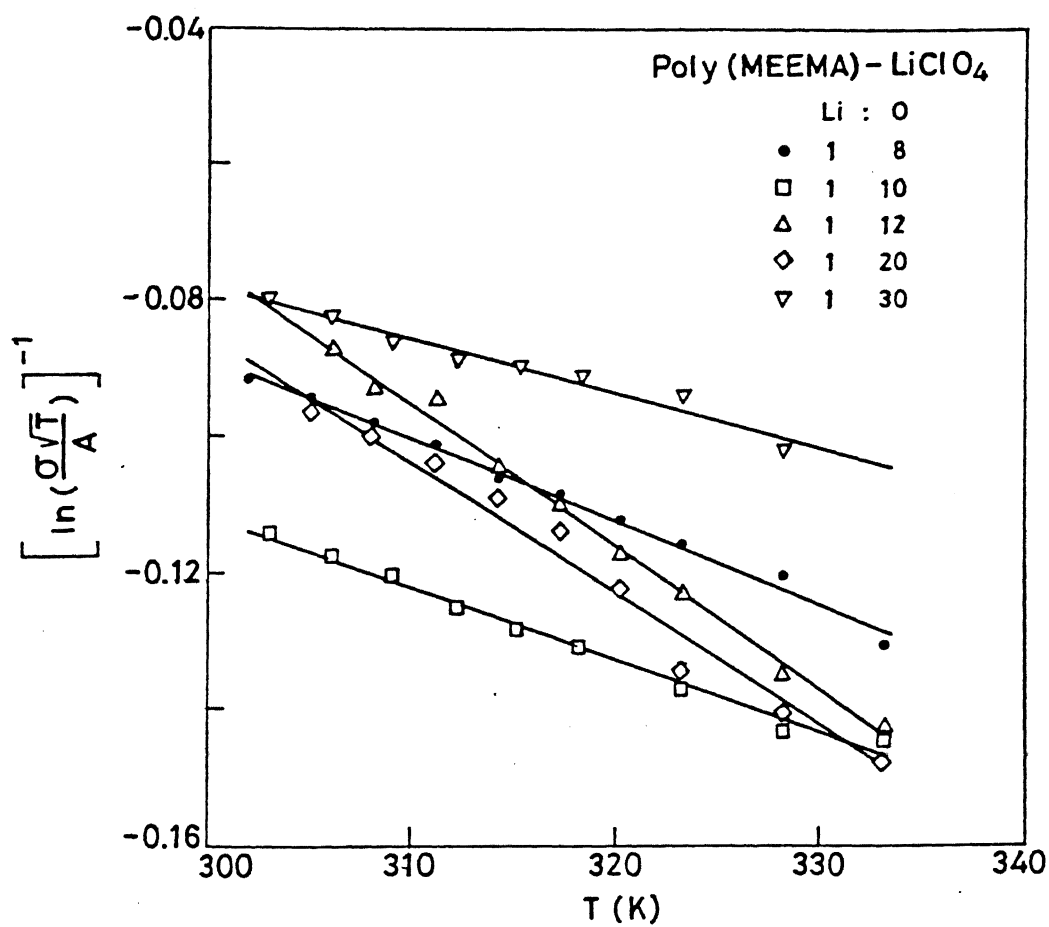


Fig.2.22. Plot of  $(\ln \sigma \sqrt{T}/A)^{-1}$  vs T for Poly(MEEMA)-LiClO<sub>4</sub> complexes

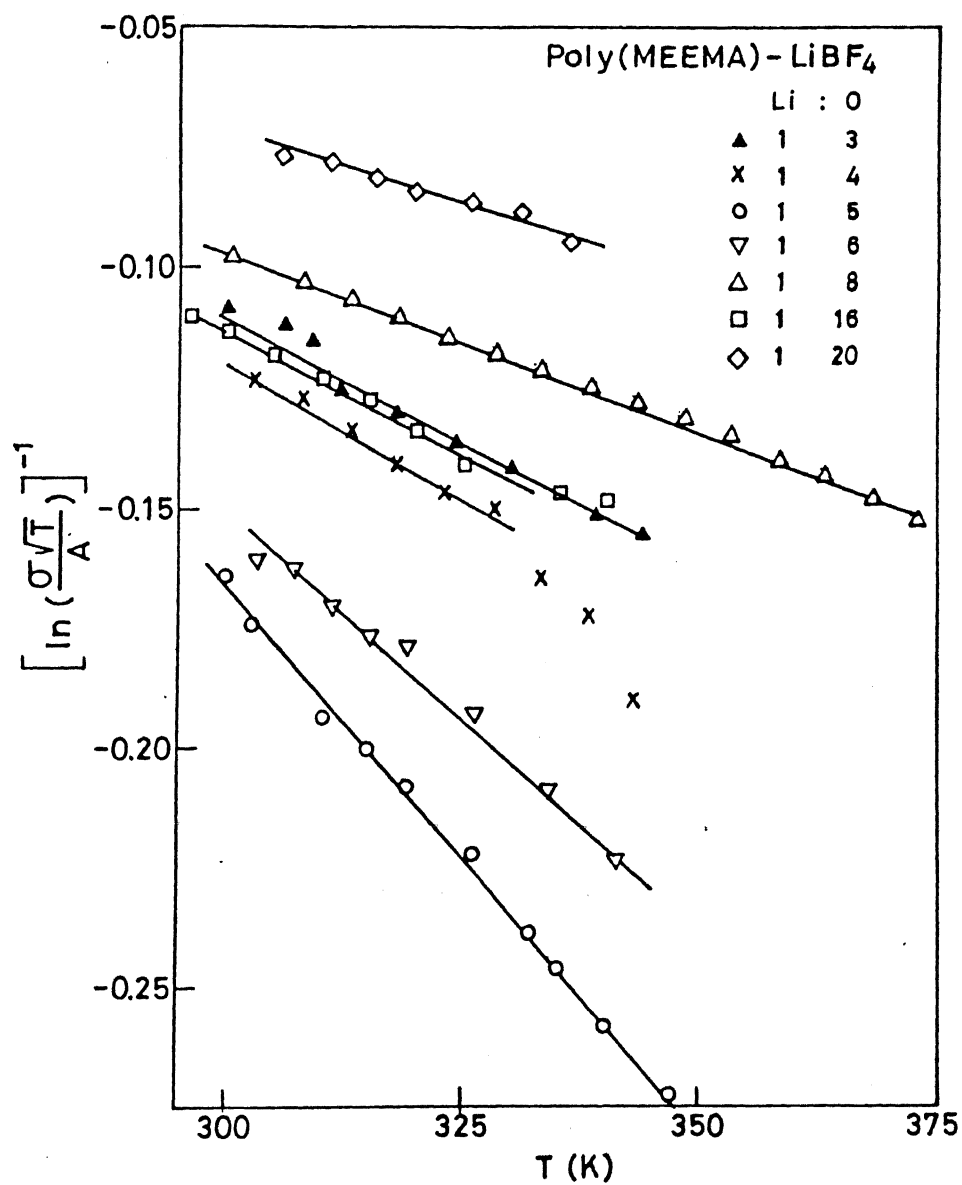


Fig.2.23. Plot of  $(\ln \sigma\sqrt{T}/A)^{-1}$  vs T for Poly(MEEMA)-LiBF<sub>4</sub> complexes



salt complexes are closely related to the calculated  $T_0$  values, it is not unreasonable to conclude that the glass transition temperatures of the highest conducting compositions are among the lowest.

Table 2.6 Poly(MEEMA)-LiCF<sub>3</sub>SO<sub>3</sub>

Composition Li : O	B (eV)	T <sub>0</sub> (K)	T <sub>g</sub> = T <sub>0</sub> + 50 (K)	A
1:4	$7.32 \times 10^{-2}$	232	282	0.500
1:8	$4.58 \times 10^{-2}$	252	302	0.333
1:12	$2.41 \times 10^{-2}$	273	323	0.250
1:16	$2.22 \times 10^{-2}$	276	326	0.200
1:20	$3.13 \times 10^{-2}$	232	282	0.166
1:24	$2.95 \times 10^{-2}$	254	304	0.143

Table 2.7 Poly(MEEMA)-LiClO<sub>4</sub>

Composition Li : O	B (eV)	T <sub>0</sub> (K)	T <sub>g</sub> = T <sub>0</sub> + 50 (K)	A
1:8	$4.24 \times 10^{-2}$	263	313	0.333
1:10	$8.66 \times 10^{-2}$	187	237	0.286
1:12	$4.64 \times 10^{-2}$	254	304	0.250
1:20	$7.38 \times 10^{-2}$	224	274	0.166
1:30	$1.15 \times 10^{-1}$	196	246	0.118

Table 2.8 Poly(MEEMA)-LiBF<sub>4</sub>

Composition Li : O	B (eV)	T <sub>0</sub> (K)	T <sub>g</sub> (K)	A
1:3	$7.69 \times 10^{-2}$	204	254	0.571
1:4	$5.44 \times 10^{-2}$	229	279	0.500
1:5	$4.08 \times 10^{-2}$	220	270	0.444
1:6	$5.19 \times 10^{-2}$	208	258	0.400
1:8	$9.31 \times 10^{-1}$	177	227	0.333
1:16	$6.06 \times 10^{-1}$	252	302	0.200

The conductivity behaviour of Poly(MEEMA)-LiX complexes is analogous to many amorphous polymer-metal salt complexes in general and MEEP-LiX in particular. The conductivity trends observed in the Poly(MEEMA)-LiX system can be rationalized as follows. First, upon addition of metal salts to the native polymer there is an increase in conductivity since the added ion contribute to conductivity. This increase continues with further addition of metal salt as the number of charge carriers also simultaneously increases. However, concomitantly, addition of metal salt to the polymer also increases the glass transition temperature. Extensive research on PEO has clearly established that the conductivity in polymer solid electrolytes is mainly in amorphous phase. Since glass transition temperature increases upon addition of metal salt to the polymer, conductivities decrease. These two counter balancing effects produce an optimum conductivity value at a specific Li/O ratio. Analogous behaviour has been observed for MEEP-metal salt complexes (Table 2.9)

Table 2.9 <sup>(17)</sup>

Salt	Metal : Polymer	T <sub>g</sub> ( °C )
—	0:1	-83.5
AgCF <sub>3</sub> SO <sub>3</sub>	0.080:1	-78.3
	0.125:1	-74.3
	0.167:1	-68.7
	0.250:1	-60.0
	0.500:1	-35.2
	1.000:1	-11.6
	2.000:1	+11.4
LiSO <sub>3</sub> CF <sub>3</sub>	0.125:1	-69.4
	0.167:1	-65.7
	0.250:1	-62.4
	0.500:1	-58.9

### 2.3.4 Comparison of conductivities of Poly(MEEMA)-LiX complexes with other systems

Table 2.10 summarizes conductivities observed for PEO-LiX, ( $X^- = \text{CF}_3\text{SO}_3^-, \text{ClO}_4^-$ ), PPO-LiCF<sub>3</sub>SO<sub>3</sub>, MEEP-LiX ( $X^- = \text{BF}_4^-, \text{CF}_3\text{SO}_3^-$ ) and polyacrylate-LiCF<sub>3</sub>SO<sub>3</sub> and three systems from present work. PEO-LiX systems which have been most widely studied

Table 2.10

Polymer-Salt Complex	O:Li ratio	Conductivity Scm <sup>-1</sup> (K)	Ref
PEO:LiCF <sub>3</sub> SO <sub>3</sub>	12:1	4.0x10 <sup>-6</sup> (312)	18
PEO:LiClO <sub>4</sub>	12:1	5.6x10 <sup>-6</sup> (312)	18
PEO:LiCF <sub>3</sub> SO <sub>3</sub>	9:1	2.2x10 <sup>-5</sup> (312)	18
MEEP:LiCF <sub>3</sub> SO <sub>3</sub>	24:1	1.0x10 <sup>-4</sup> (312)	19
MEEP:LiBF <sub>4</sub>	36:1	5.2x10 <sup>-5</sup> (303)	19
		8.7x10 <sup>-4</sup> (363)	19
Polyacrylate:LiCF <sub>3</sub> SO <sub>3</sub>	--	6.0x10 <sup>-5</sup> (373)	20
Poly(MEEMA):LiCF <sub>3</sub> SO <sub>3</sub>	20:1	2.3x10 <sup>-6</sup> (271)	Present work
		5.6x10 <sup>-5</sup> (303)	
Poly(MEEMA):LiBF <sub>4</sub>	5:1	5.8x10 <sup>-5</sup> (330)	Present work
		3.3x10 <sup>-4</sup> (303)	
Poly(MEEMA):LiClO <sub>4</sub>	10:1	3.3x10 <sup>-6</sup> (305)	Present work
		1.4x10 <sup>-5</sup> (333)	

show a poor conductivity at ambient temperature, only around 310K the conductivity improves to about 10<sup>-6</sup> Scm<sup>-1</sup>. Higher conductivities (10<sup>-4</sup> Scm<sup>-1</sup>) are observed at higher temperature. In contrast the completely amorphous

polymer MEEP, when complexed with metal salts in general and lithium salts in particular shows high conductivities even at ambient temperatures. Thus for example MEEP-LiBF<sub>4</sub> complex even at 303K shows a high conductivity value of  $5.2 \times 10^{-5} \text{ Scm}^{-1}$ . Studies on other comb like polymers such as polyacrylate. LiCF<sub>3</sub>SO<sub>3</sub> reveals, that the conductivities of the order of  $10^{-5} \text{ Scm}^{-1}$  are achieved only at high temperature (373K). Thus, it is interesting to note that the Poly(MEEMA), the polymer being investigated in the current study shows excellent conductivities when complexed with lithium salts such as LiClO<sub>4</sub>, LiCF<sub>3</sub>SO<sub>3</sub>, and LiBF<sub>4</sub> even at ambient temperatures. Thus for example Poly(MEEMA)-LiBF<sub>4</sub> even at 300K shows a conductivity of  $5.8 \times 10^{-5} \text{ Scm}^{-1}$ . At 330 K the conductivity jumps to  $3.3 \times 10^{-4} \text{ Scm}^{-1}$ . This result compares favourably with the one obtained by Inoue and coworkers who had synthesized polystyrene containing cyclotriphosphazene pendant groups. These polymers do not possess a flexible polymer backbone. However, the presence of oligooxy ethylene side groups and the segmental motion arising from them was thought to provide a suitable conducting phase. In an analogous manner Poly(MEEMA) also possesses fairly rigid acrylate backbone. However, the short oligooxy ethylene side chains presumably orient in a favourable geometry to form accessible and continuous conducting phases. The exact mechanism of conduction can only be delineated by a detailed solid state <sup>7</sup>Li NMR study.

## 2.4 Conclusions

The results obtained from this study can be summarized as follows :

- (a) A new polyacrylate, Poly(MEEMA) containing short oligoetheroxy side chain has been synthesized and characterized.
- (b) Poly(MEEMA) forms homogeneous complexes with LiX ( $x^- = \text{CF}_3\text{SO}_3^-, \text{ClO}_4^-, \text{BF}_4^-$ ).  
In contrast to the virgin Poly(MEEMA) which is an insulator, the

polymer-salt complexes show high ionic conductivities. The highest conductivity has been observed for Poly(MEEMA).  $\text{LiBF}_4$  (O : Li, 5:1)  $5.8 \times 10^{-5} \text{ Scm}^{-1}$  (300 K) and  $3.3 \times 10^{-4} \text{ Scm}^{-1}$  (330K).

- (c) The conductivity behaviour of the polymer salt complexes have been analyzed. They do not fit the Arrhenius behaviour. However, the data can be fit into the VTF equation suggesting that either the configuration entropy model or the free volume model is applicable to explain the conductivity behaviour in the present system.
- (d) Comparison of the conductivity of Poly(MEEMA).LiX with other polymers reveals the conductivities observed are among the highest and are comparable to the best conducting polymer electrolyte, MEEP.LiX system.
- (e) In contrast to MEEP, whose synthesis involves complicated synthetic protocol including a lengthy dialysis, Poly(MEEMA) is readily synthesized. Also, in contrast to MEEP, which flows at ambient temperatures, there by making its utilization in a practical device difficult, Poly(MEEMA) is dimensionally more stable. Lastly unlike MEEP, which is hydrophilic, Poly(MEEMA) is hydrophobic. This feature is of considerable advantage since presence of trace amounts of water can lead to severe complications in any practical device.
- (f) Further studies in this direction would be to study the feasibility of using Poly(MEEMA).LiX polymer electrolyte in electrochemical applications such as high energy density batteries. This has to await a detailed study on the compatibility of the electrolyte with Li metal, cyclic voltammetric studies and studies on charge-discharge cycles.

## REFERENCES

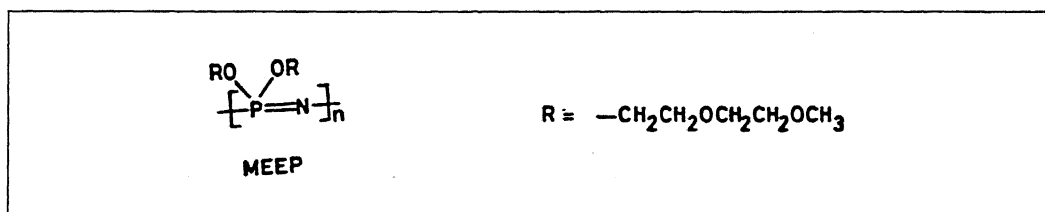
1. Angell, C.A.; Liu, C.; Sanchez, E. *Nature*, 1993, **362**, 137.
2. Shriver, D.F.; Farrington, G.C. *Chem. Eng & News*, 1985.
3. Polymer Electrolyte Reviews-I, Mac Callum, J.R.; Vincent, C.A. Eds. Elsevier Applied Science, New York, 1987.
4. Blonsky, P.M.; Shriver, D.F.; Austin, P.; Allcock, H.R. *J. Am. Chem. Soc.* 1984, **106**, 6854.
5. Inoue, K.; Nishikawa, Y.; Tanigaki, T. *Macromolecules*, 1991, **24**, 3464.
6. Inoue, K.; Nishikawa, Y.; Tanigaki, T. *J. Am. Chem. Soc.*, 1991, **113**, 7609.
7. Inoue, K.; Nishikawa, Y.; Tanigaki, T. *Solid State Ionics*, 1992, **58**, 217.
8. Xia, D.W.; Soltz, D.; Smid, J. *Solid State Ionics*, 1984, **14**, 221.
9. Bannister, D.J.; Davies, G.R.; Ward, I.M.; Mc Intyre, J.E. *Polymer*, 1984, **25**, 1600.
10. Kobayashi, N.; Uchigama, M.; Shigehara, T.; Tsuchida, E. *J. Phys. Chem.*, 1985, **89**, 987.
11. Cowie, J.M.G.; Martin, A.C.S. *Polymer Commun.*, 1985, **25**, 298.
12. Cowie, J.M.G.; Martin, A.C.S. *Polymer*, 1987, **28**, 627.
13. Tsuchida, E.; Ohno, H.; Kobayashi, N.; Zshizaka, H. *Macromolecules*, 1989, **22**, 1771.
14. Furniss, D.S; Hannaford, A.J.; Smith, P.W.G.; Thatchell, A.R. Eds. *Vogel's Text book of Practical Organic Chemistry*, 5<sup>th</sup> Ed. ELBS, UK, 1989.
15. Bhatnagar, S.; Gupta, S.; Shahi, K. *Solid State Ionics*, 1988, **31**, 107.
16. Gray, F.M. *Solid State Ionics*, 1990, **40/41**, 637.
17. Blonsky, P.M. *Ph.D Dissertation*, Northwestern University, Illinois, USA, 1986.
18. Ratner, M.A.; Shriver, D.F. *Chem. Rev.* 1988, **88**, 109.
19. Blonsky, P.M.; Shriver, D.F.; Austin, P.; Allcock, H.R. *Solid State Ionics*, 1986, **18/19**, 258.

## CHAPTER III

SYNTHESIS, CHARACTERIZATION, AND IONIC CONDUCTIVITY STUDIES ON  
POLYPHOSPHAZENES, PP(I) AND PP(II) AND THEIR METAL SALT COMPLEXES

## 3.1 Introduction

There is a lot of interest in polymeric materials as electrolytes for the transport of ions<sup>1</sup>. This aspect has been reviewed in Chapter I. The most widely studied polymeric system has been poly ethylene oxide (PEO)<sup>2</sup>. However, this material has a high degree of crystallinity at ambient temperatures which is detrimental to ionic conductivity. Poly ethylene oxide - metal salt complexes are highly conducting only at higher temperatures beyond the  $T_m$  of PEO (65°C). In 1984 Shriver and Allcock have designed a polyphosphazene containing etheroxy side chains:



This polymer has a very low glass transition temperature ( $T_g = -193\text{K}$ ) and has been shown to be completely amorphous<sup>3</sup>. MEEP-metal salt complexes show excellent ionic conductivities ( $\sim 10^{-5} \text{Scm}^{-1}$ ). However, MEEP suffers from the following disadvantages:

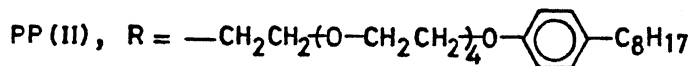
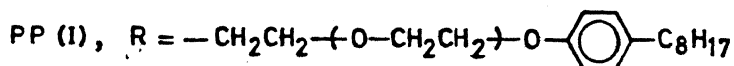
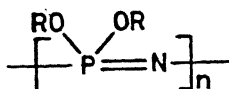
- (a) Synthesis of MEEP involves the reaction of poly(dichlorophosphazene) with methoxy ethoxy ethanol. The by products in this reaction are sodium chloride which has to be separated from the polymer completely, because even traces of residual NaCl can lead to spurious and irreproducible results. Separation of NaCl from the polymer is rendered extremely difficult since MEEP is soluble in water. This entails lengthy and

cumbersome dialysis procedures to remove the residual salt.

- (b) The hydrophobicity of MEEP is a serious disadvantage since it has been shown by various studies that residual water in the polymer leads to non reproducible results.
- (c) The dimensional stability of MEEP is very low and the polymer begins to flow even at ambient temperatures making it difficult to use MEEP in any practical device.

Several methods have been employed to modify MEEP in order to impart greater dimensional stability<sup>4-7</sup>. These include plasticization, cross linking reactions etc. This aspect was discussed in Chapter I (Section 1.3.6).

In this thesis we describe the design and synthesis of two new polyphosphazenes, PP(I) and PP(II), with an attempt to overcome the difficulties associated with MEEP.



This chapter describes the synthesis and conductivity studies on the metal salt complexes of these materials.

## 3.2 Experimental

### 3.2.1 Materials

Hexachlorocyclotriphosphazene (Nippon Soda, Japan) was recrystallised from hexane (m.p. 114°C) prior to use. Sodium hydride (Merck, Germany), Igepal 210<sup>TM</sup> and Igepal 520<sup>TM</sup> (Aldrich, USA) were used as received whereas LiClO<sub>4</sub> and LiBF<sub>4</sub>



(Alfa Products, USA) were dried in an oven at 100°C for 24 hours before use. Sodium metal and  $\text{CaSO}_4 \cdot 5\text{H}_2\text{O}$  (S.D Fine Chemicals, India) were used as received. All the organic solvents were purified and dried by standard literature procedures before use<sup>8</sup>.

### 3.2.2 Measurements

$^1\text{H}$  NMR and  $^{31}\text{P}$  NMR spectra were recorded on a Bruker WM 400 spectrophotometer operating at 400MHz and 136MHz respectively, using  $\text{CDCl}_3$  as solvent. TMS was used as external reference for  $^1\text{H}$  and 85%  $\text{H}_3\text{PO}_4$  was used as external reference for  $^{31}\text{P}$ . The chemical shift values are reported in ppm and upfield shifts are negative. IR spectra were recorded on a Perkin-Elmer FTIR 1600 spectrophotometer. Thermal analysis (TGA, DTA, and DSC) were done on Perkin-Elmer DSC 7 and Dupont 9900 thermal analyzers at a heating rate of 10°C per minute. GPC measurements were carried out on a Maxima 820 instrument using THF as solvent and polystyrene as standard. Dilute solution viscosity measurements were carried out on a Schott-Gerate viscometer in dry benzene at 26°C using Ubbholde viscometer (capillary size 0.46mm). X-ray diffraction patterns of all the samples were recorded on a Rich Seifort (Iso Debye flex 200 2D) counter diffractometer using a  $\text{CuK}_\alpha$  radiation operating at 30 kV. All XRD studies were done at room temperature. The electron micrographs were taken with a Jeol scanning microscope (JSM-840A). Each sample was silver coated using sputtering unit (International Scientific Instruments PS-2 Coating Unit) before loading. The photographs were taken at 10 kV accelerating voltage. The instrument has a provision of 10X to 300000X magnification of the images. The magnification was fixed according to the need.

### 3.2.3 Thin Film Preparation

Appropriate amounts of the polymer and the alkali metal salt were dissolved in dry THF and allowed to form a homogeneous solution of polymer-salt complex by stirring at room temperature for 8 to 20 hours. The concentrated solution was cast on a teflon sheet and the solvent was removed by slow evaporation at room temperature. The samples were dried completely by keeping in a vacuum oven at 40°C with a pressure of  $10^{-1}$  torr for 48 hours. The dried thin films (thickness 0.2mm to 0.8mm) were used to do the conductivity measurements. Fig. 2.2 shows the flow chart of thin film preparation.

### 3.2.4 Electrical Measurements

The conductivity studies were carried out using a HP 4194A impedance / gain phase analyzer with a slow heating rate. A dynamic vacuum of  $\sim 10^{-3}$  torr was maintained throughout the experiment to exclude trace amounts of moisture and solvent that might be present in the sample. The bulk resistance of the complexes at different compositions of the polymer and salt were obtained using the complex impedance at different temperatures. The dc conductivity was derived from the resistance, using the relation given below:

$$\sigma = \frac{g}{R_b}$$

Where,  $\sigma$  is the total ionic conductivity of the polymer-salt complex,  $g$  is the geometric factor which depends on the thickness of the film (sample) and area of the electrodes,  $R_b$  is the bulk resistance obtained from the impedance spectra.

Fig. 2.2 shows the block diagram of the sample holder used to measure the impedance. The impedance of each sample as a function of frequency and temperature was measured with a slow heating rate. The dc conductivity was

determined by complex impedance analysis which was analyzed by a software package<sup>9</sup>.

### 3.2.5 Synthesis of $N_3P_3(OR)_6$ , $R = CH_2CH_2O-(CH_2CH_2O)_4-C_6H_4-C_8H_{17}$

The sodium salt of Igepal 520<sup>TM</sup> was prepared from sodium hydride (85%) (1.0g, 34.5mmol) and Igepal 520<sup>TM</sup> (14.7g, 34.5mmol) in dry THF. To this stirred solution,  $N_3P_3Cl_6$ , hexachlorocyclotriphosphazene, (2.0g, 5.8mmol) was added dropwise over a period of 30 minutes at room temperature. The reaction mixture was allowed to stir for another 48 hours. The solvent THF was removed and the residue was subjected to silica gel column chromatography. Ethyl acetate was used as eluant. Thus, the pure title compound was obtained as yellowish oil (57% yield).

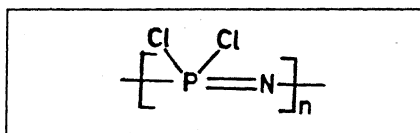
$^1H$  NMR ( $CDCl_3$ ):  $\delta$ , 7.2-6.7 (24H, aromatic, dd); 4.0-3.6 (120H,  $-(CH_2CH_2O)_5-$ , m)  
1.6-0.6 (102H,  $-C_8H_{17}$ , m)

$^{31}P$  NMR ( $CDCl_3$ ):  $\delta$ , 18.3

IR (neat):  $cm^{-1}$ , 3020(vs); 1660(m); 1640(M); 1610(s); 1530(s); 1500(s);  
1242(s); 1110(s); 820(m)

### 3.2.6 Synthesis of Poly[bis {4'-n-octyl-4-phenoxy(oligoethoxy)} phosphazenes]

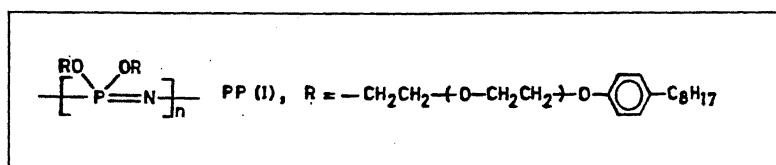
#### 3.2.6.1 Poly(dichlorophosphazene)



Sublimed hexachlorocyclotriphosphazene,  $N_3P_3Cl_6$ , (15.0g, 43.2mmol) was taken in a thickwalled glass ampoule along with  $CaSO_4 \cdot 5H_2O$  (27.0mg) as a catalyst. The tube was evacuated ( $10^{-3}$  torr), to exclude oxygen, for an hour and sealed under

vacuum<sup>10</sup>. Then the tube was kept in an oven at 250°C for 14 hours; the tube was rotated continuously at a slow speed of 5 cycles per minute to ensure complete mixing. The cooled tube was broken into small pieces and taken in a Schlenk vessel. Hexane (200ml) was added to the flask and refluxed under N<sub>2</sub> atmosphere for 30 minutes. After cooling, the unreacted N<sub>3</sub>P<sub>3</sub>Cl<sub>6</sub> dissolved in hexane was transferred to another flask using a Cannula (steel tube). This procedure was repeated three times (3X200ml hexane) to make sure that no trimer is present in the polymer. Then dry THF (100ml) was added to the Schlenk vessel and heated and under reflux for 30 minutes. This THF solution was transferred to another flask using a Cannula. This procedure was also repeated thrice. The THF solution which contained poly(dichlorophosphazene), (5.9g, 39.0%) was used to prepare poly(organophosphazenes). It is important to note that care should be taken at all stages to exclude moisture. Thus, all operations were done in a N<sub>2</sub> atmosphere using either a glove bag or in a Schlenk apparatus.

### 3.2.6.2 Poly [bis(4'-n-octyl-4-phenoxy ethoxy ethoxy)phosphazene], PP(I)



To a stirred solution of sodium hydride (85%) (2.0g, 70.0mmol) in dry THF (50ml), Igepal CA 210<sup>TM</sup> (20.6g, 70.0mmol) in the same solvent (150ml) was added dropwise over a period of 30 minutes in N<sub>2</sub> atmosphere. The resulting mixture was stirred for an hour at 50°C. To this solution, poly(dichlorophosphazene), (4.0g, 34.0mmol) in THF (250ml) was added dropwise over a period of 30 minutes in N<sub>2</sub> atmosphere. The reaction mixture was further stirred for 36 hours at room temperature. After removing most of the solvent, the solution was poured into excess water (2000ml) to remove unreacted sodium salt of Igepal CA 210 and

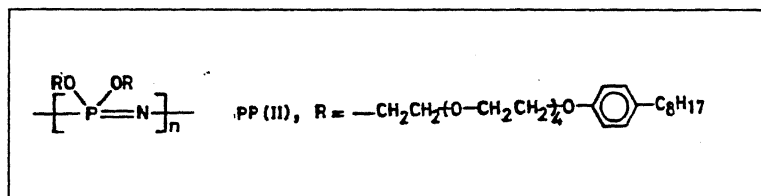
sodium chloride. The insoluble material was extracted from water by using dichloromethane. The dried (anhyd.  $\text{NaSO}_4$ ) dichloromethane solution was concentrated and poured into excess methanol (1000ml). Reprecipitation was done three times using dichloromethane as solvent and methanol as nonsolvent. Finally, the polymer was vacuum dried at  $50^\circ\text{C}$  to give the title polymer, PP(I), (14.1g, 63.6%).

$^1\text{H NMR}(\text{CDCl}_3)$ :  $\delta$ , 7.3-6.5 (4H, aromatic, dd); 4.3-3.5 (8H,  $-(\text{CH}_2\text{CH}_2\text{O})_2$ , m); 1.7-0.5 (17H,  $-\text{C}_{17}\text{H}_{17}$ , m).

$^{31}\text{P NMR}(\text{CDCl}_3)$ :  $\delta$ , -7.42 (singlet)

IR (Neat):  $\text{cm}^{-1}$ , 3020(m); 2960(vs); 1600(vs); 1570(vs); 1500(vs); 1450(vs); 1350(s); 1240(vs); 1180(s); 1120s); 1080(s); 970(s); 910(m); 820(s).

### 3.2.6.3 Poly [bis{4'-n-octyl-4-phenoxy(oligoethoxy)}phosphazene], PP(II)



The same synthetic procedure given in section 3.2.6.2 was adopted here also. Thus, the sodium salt of Igepal 520<sup>TM</sup> was prepared from sodium hydride (85%) (1.6g, 57.4mmol) and Igepal 520<sup>TM</sup> (24.5g, 57.4mmol) in dry THF. To this solution poly(dichlorophosphazene) (3.3g, 28.7mmol) in THF was added dropwise. The reaction mixture was stirred for 48 hours and workedup using the procedure given in section 3.2.6.2 affording the title polymer, PP(II), (12.7g, 49.3%).

$^1\text{H NMR}(\text{CDCl}_3)$ :  $\delta$ , 7.2-6.7 (4H, aromatic, dd); 4.0-3.5 (20H,  $-(\text{CH}_2\text{CH}_2\text{O})_5$ , m); 1.6-0.6 (17H,  $\text{C}_{17}\text{H}_{17}$ , m).

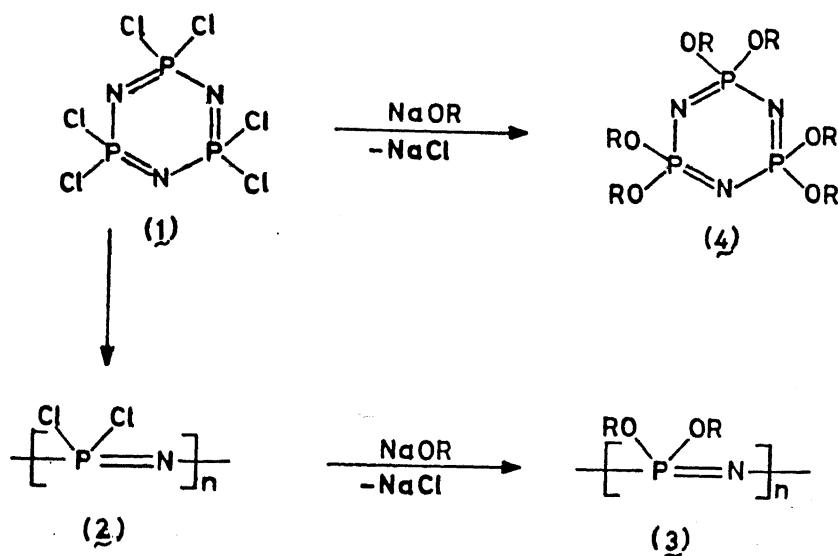
$^{31}\text{P}$  NMR( $\text{CDCl}_3$ ):  $\delta$ , -7.2 ppm (broad)

IR (Neat):  $\text{cm}^{-1}$ , 2929 (vs); 1659(m); 1644(m); 1613(s); 1514(s); 1504(s);  
1246(s); 1110(s); 829.8(m)

### 3.3 Results and Discussion

#### 3.3.1 Synthesis and Characterization of PP(I) and PP(II)

Polyphosphazenes, PP(I), (3a) and PP(II), (3b) and the cyclic model compound (4) were synthesized according to the following scheme.



3(a), PP (I),  $\text{R} = -\text{CH}_2\text{CH}_2-(\text{O}-\text{CH}_2\text{CH}_2)_4-\text{O}-\text{C}_6\text{H}_4-\text{C}_8\text{H}_{17}$

3(b), PP (II),  $\text{R} = -\text{CH}_2\text{CH}_2-(\text{O}-\text{CH}_2\text{CH}_2)_4-\text{O}-\text{C}_6\text{H}_4-\text{C}_8\text{H}_{17}$

Scheme

Poly(dichlorophosphazene), 2, was obtained by ring opening polymerization of hexachlorocyclotriphosphazene, 1<sup>11</sup>. Poly(dichlorophosphazene) is

very reactive and prone to hydrolysis to give decomposed products<sup>12</sup>. The reaction involving substitution of P—Cl bonds in poly(dichlorophosphazene), 2, was done in N<sub>2</sub> atmosphere and in dry condition. The desired end products 3(a) and 3(b) called PP(I) and PP(II) are stable and obtained as solid materials. Both the polymers, PP(I) and PP(II), are soluble in a variety of organic solvents including hydrocarbons such as hexane or heptane. Separation of sodium chloride from the polymers is rendered very easy as polymers PP(I) and PP(II) were completely insoluble in water. This feature was achieved by deliberately choosing the nucleophile which contains (apart from etheroxy units), an aromatic group linked to a long alkyl side chain. Further, the presence of hydrocarbon chain also enables the polymer to be soluble in a variety of organic solvents including hexane, a feature which is a great advantage, particularly when casting films.

The polymers PP(I) and PP(II) are characterized by <sup>1</sup>H NMR, <sup>31</sup>P NMR, IR, GPC, dilute solution viscosity measurements, thermal analysis (TGA, DTA, and DSC), XRD, and SEM techniques. The data obtained are tabulated in Table 3.1.

Table 3.1

Measurement	Model Compound N <sub>3</sub> P <sub>3</sub> (OR) <sub>6</sub>	PP(I)	PP(II)
<sup>31</sup> P NMR	18.3	-7.42	-7.2
M <sub>w</sub>	—	8.7x10 <sup>5</sup>	—
η <sub>intrinsic</sub> (ccg <sup>-1</sup> )	—	94.11	17.62
TGA	—	164.8°C(I) 337.6°C(II) 458.0°C(III)	289.4°C(I) 361.5°C(II) —
DSC	—	-13.28°C	-28.8°C
XRD	—	amorphous	amorphous
SEM	—	amorphous	amorphous

The  $^1\text{H}$  NMR of PP(I) and PP(II) shows the presence of the side chain on the polymer back bone. IR studies clearly show the  $\text{P}=\text{N}$  stretching around  $1240\text{ cm}^{-1}$  indicating the presence of  $\text{P}=\text{N}$  back bone.  $^{31}\text{P}\{^1\text{H}\}$  NMR spectra of PP(I) is given in Fig. 3.1. A single peak for PP(I) observed at  $-7.42\text{ ppm}$  clearly indicates that there is only one kind of phosphorus confirming the complete substitution of the alkoxide group. Similarly the chemical shift of PP(II) is  $-7.2\text{ ppm}$ . The chemical shift values are in good agreement with the chemical shift values of various poly(alkoxy)phosphazenes that are known in the literature<sup>13</sup>. For the cyclic ring phosphazenes the chemical shift values generally are observed in the high frequency region<sup>14</sup>. The model compound,  $\text{N}_3\text{P}_3(\text{OR})_6$ , 4,  $(\text{R} = \text{CH}_2\text{CH}_2(\text{OCH}_2\text{CH}_2)_4\text{O}-\text{C}_6\text{H}_4-\text{C}_8\text{H}_{17})$ , shows (Fig. 3.2) a chemical shift

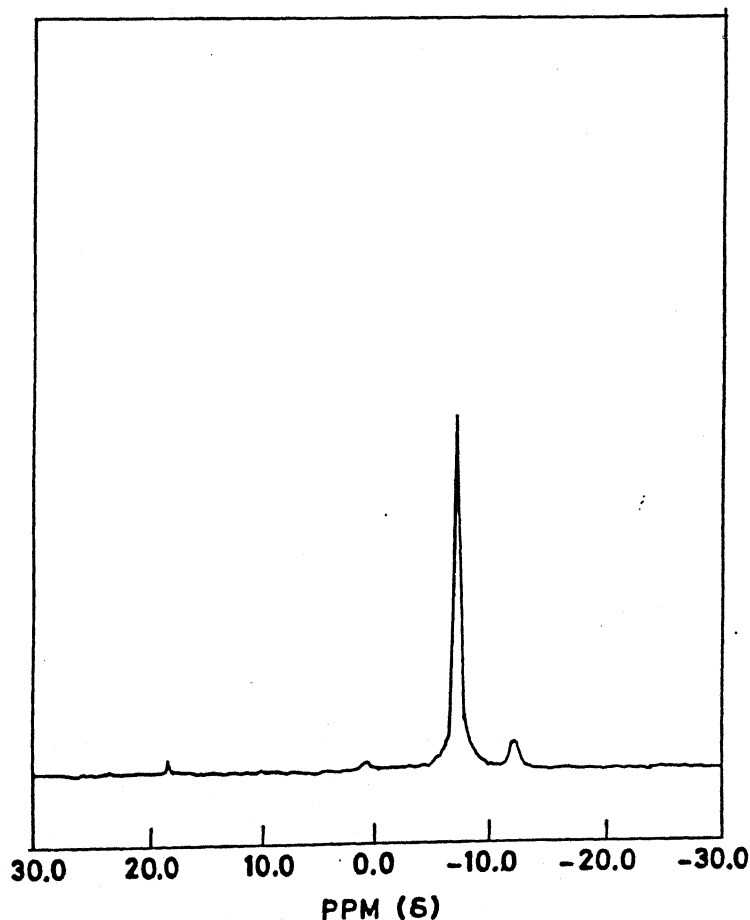


Fig. 3.1  $^{31}\text{P}\{^1\text{H}\}$  NMR spectrum of Polyphosphazene, PP(I).



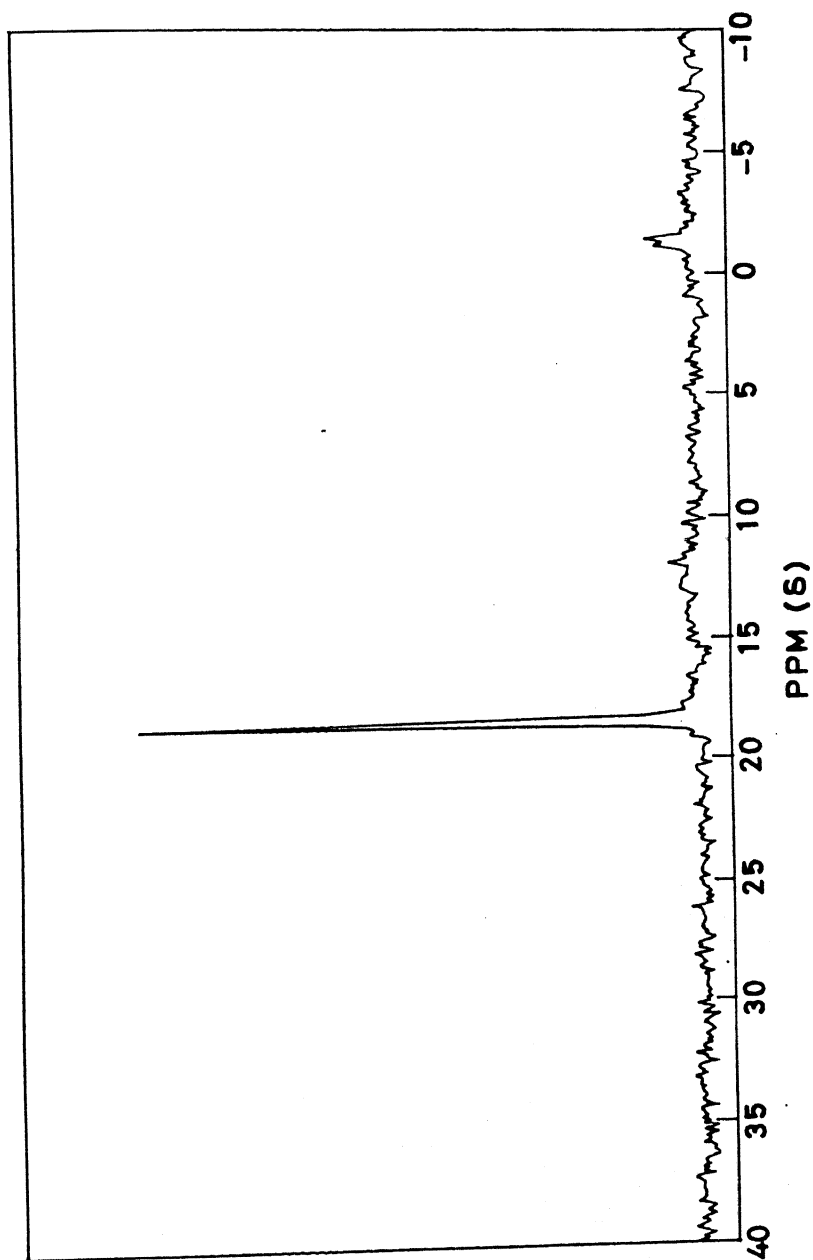


Fig. 3.2  $^{31}\text{P}$   $\{^1\text{H}\}$  NMR spectrum of the model compound,  $\text{N}_3\text{P}(\text{OR})_6$ , (4),  
 (R =  $\text{CH}_2\text{CH}(\text{OCHCH}_2)_4\text{OCHCH}_2$ ).

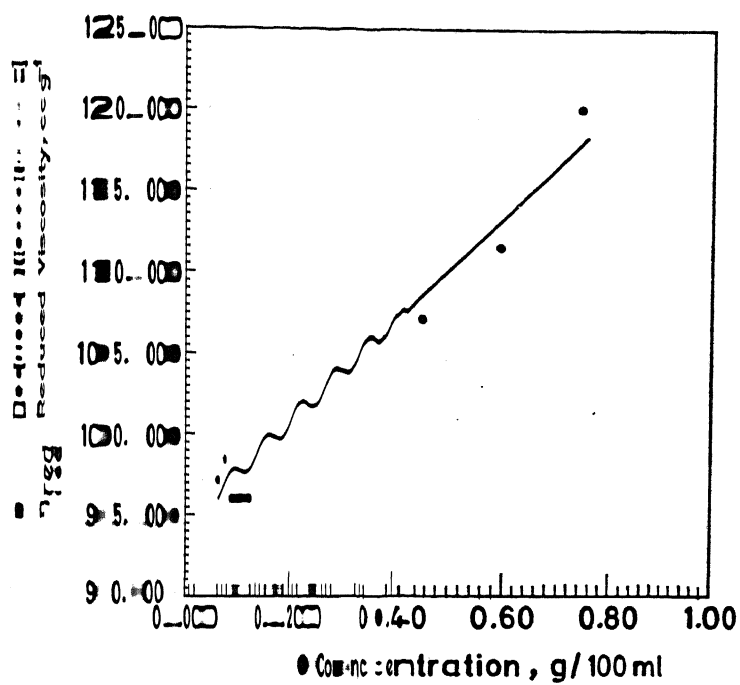


Fig. 1. Reduced Viscosity vs. Concentration plot for PP(I) at 26°C

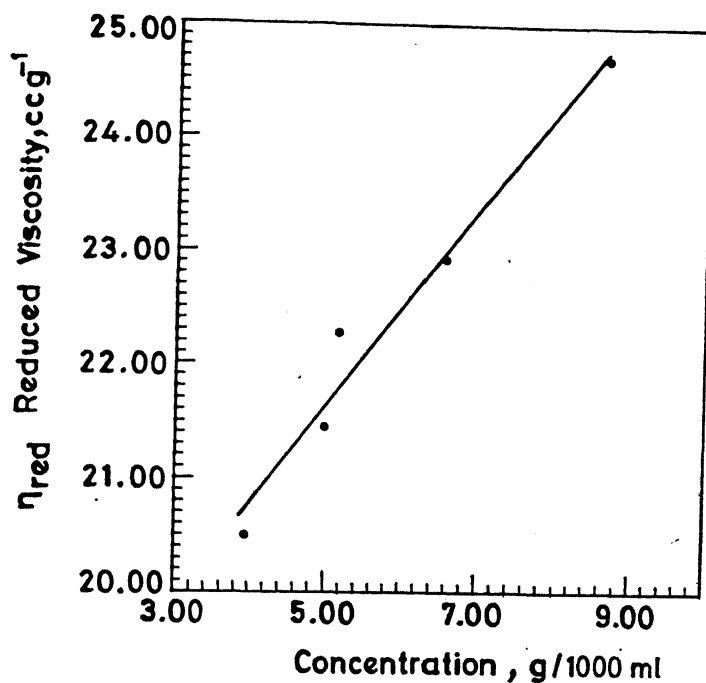


Fig.3.4  $\eta_{\text{reduced}}$  vs Concentration plot for PP(II) at 26°C

Fig. 3.5 shows the thermograms obtained for PP(I) and PP(II). Differential Thermal Analysis (DTA) done from room temperature to higher temperatures on PP(I) and PP(II) reveal that there is no phase transition seen in this region; only decomposition is observed. The glass transition temperature ( $T_g$ ) of PP(I) and PP(II) were obtained from DSC (Differential Scanning Calorimetry) operating from -80°C to +80°C (Fig. 3.6.). These clearly shows that both PP(I), ( $T_g = -13.28^\circ\text{C}$ ) and PP(II), ( $T_g = -28.8^\circ\text{C}$ ) are amorphous polymers containing no crystalline phase at

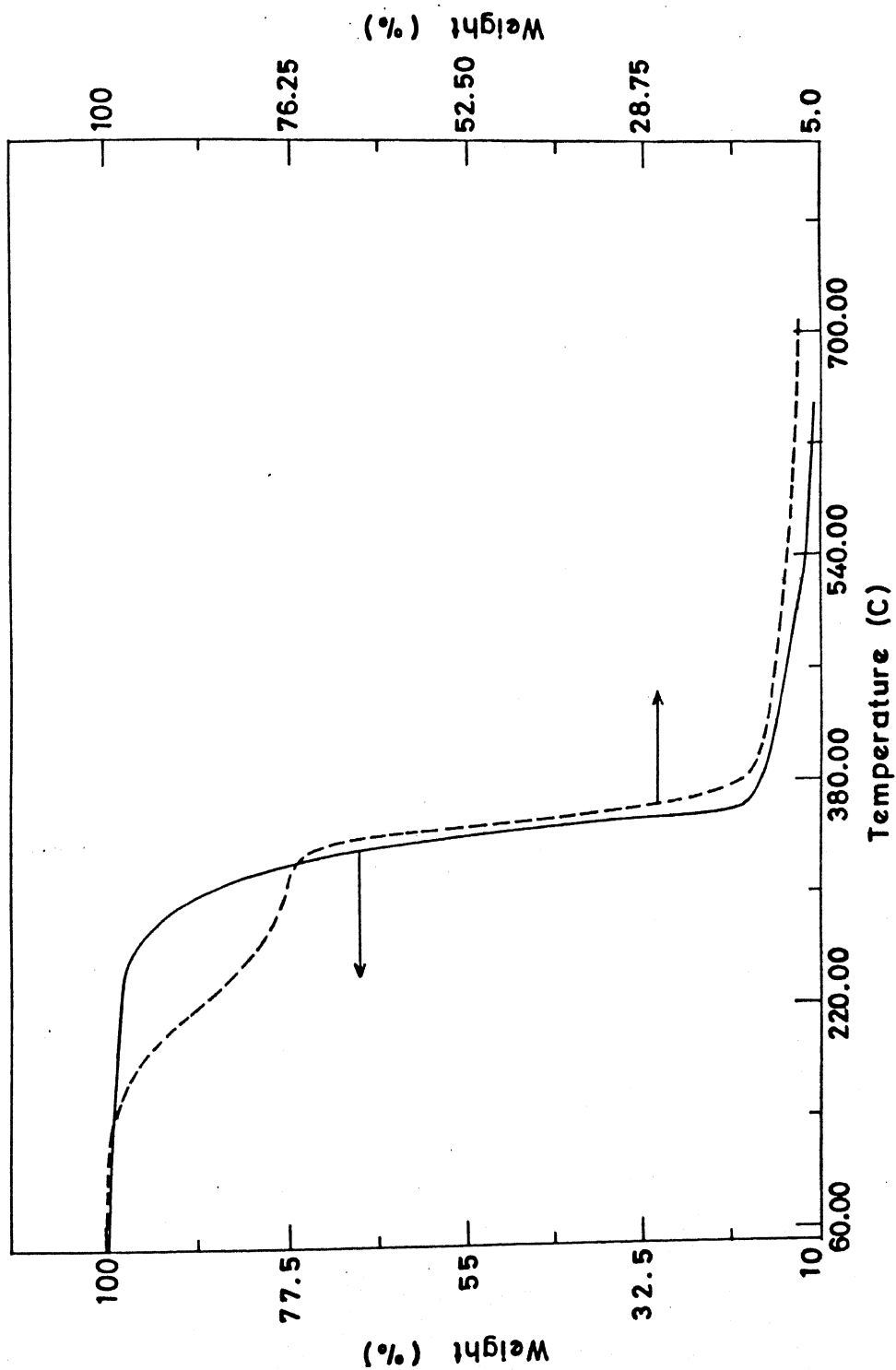


Fig.3.5. Thermograms obtained for (a) — , PP(II) and (b) ---- , PP(I).

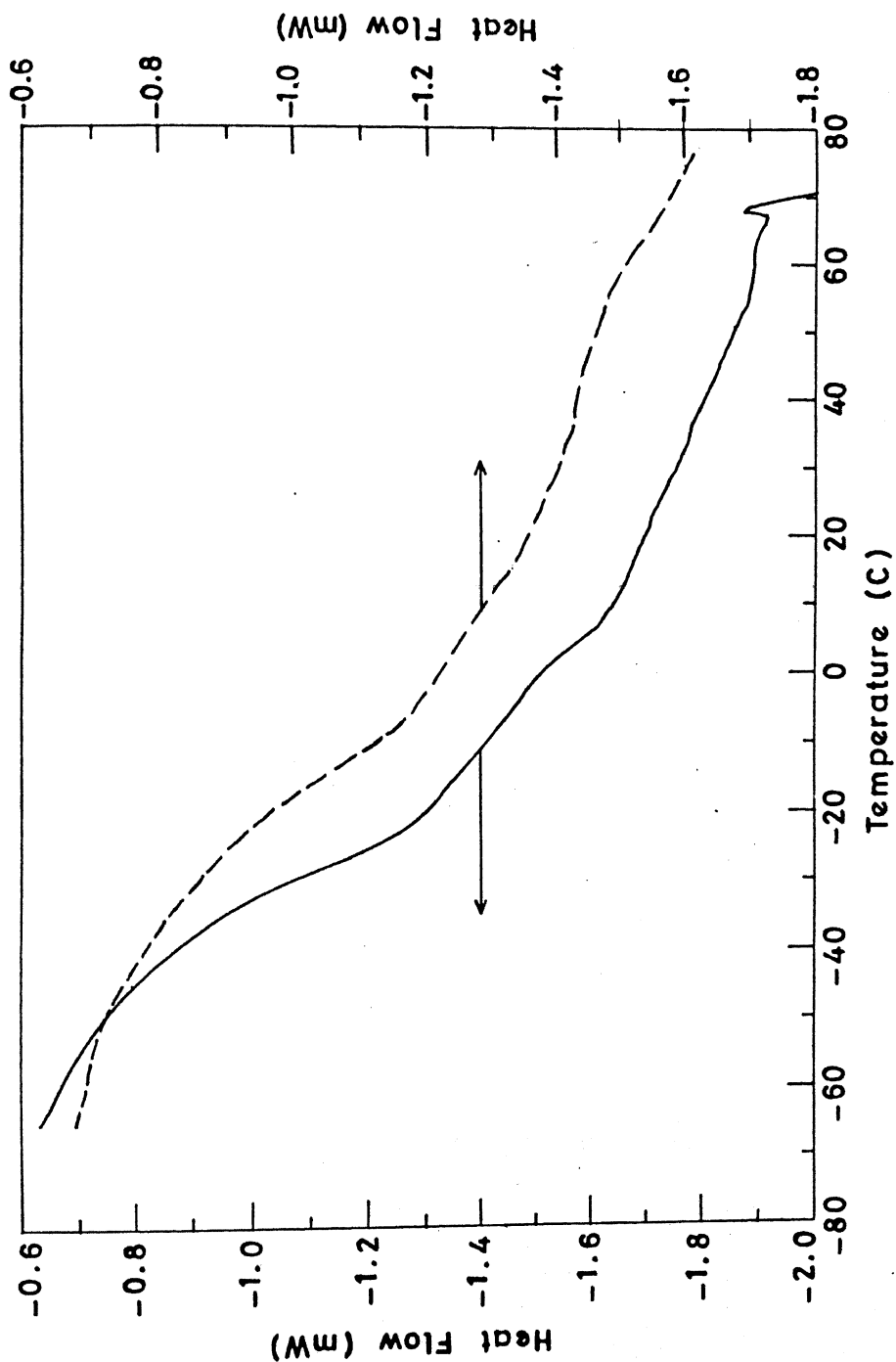
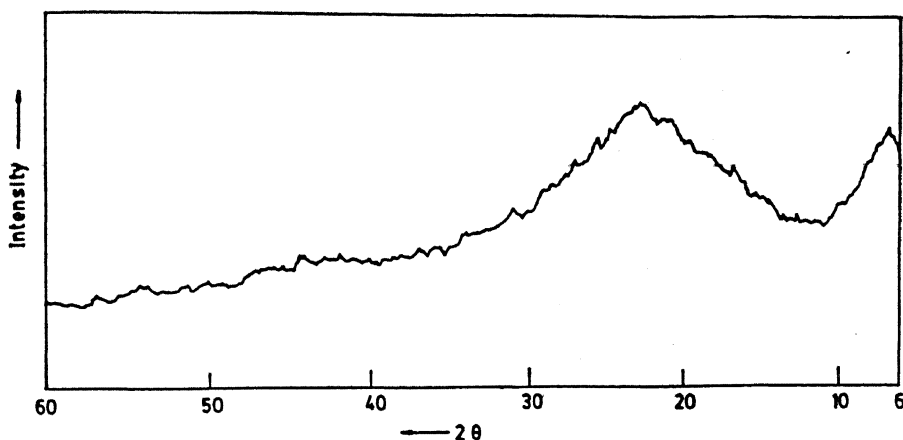


Fig. 3.6. DSC curves obtained for (a) — , PP(I) and (b) ---- , PP(II).

all. This fact is further confirmed by X-ray diffraction (XRD) and Scanning Electron Microscopy (SEM) studies also. No crystalline peaks are detected in XRD (Fig. 3.7 and 3.8). SEM photographs are shown in Fig. 3.9.



*Fig.3.7. XRD plot of PP(I)*

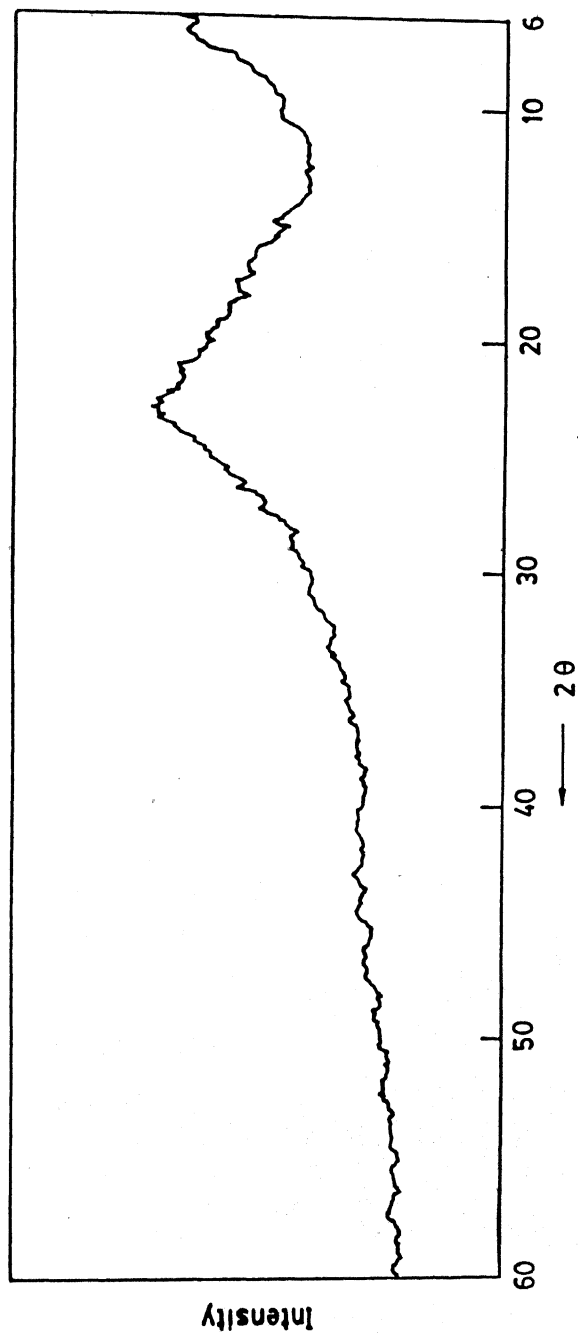
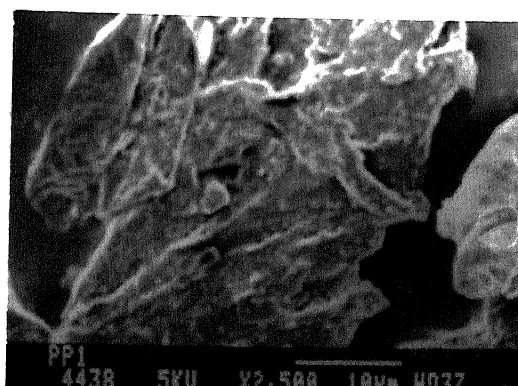
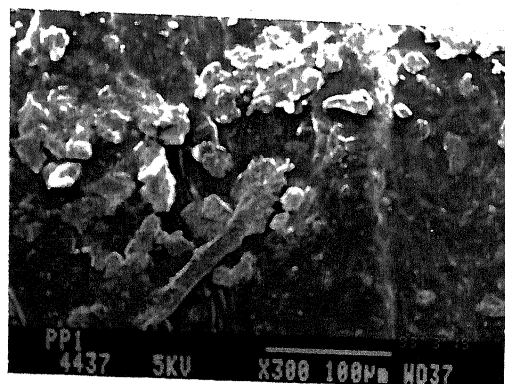


Fig.3.8. XRD plot of PP(II).



*Fig.3.9. SEM photograph of PP(I)*



### 3.3.2 Polymer-Metal Salt Complexes

Both PP(I) and PP(II) form complexes with lithium salts. These have been characterized by IR, XRD, and SEM studies. IR data are tabulated in Table 3.4. From the observation of a very broad C-O-C stretching frequency it is inferred that as in the case of other polymer electrolytes the etheroxy groups must be involved in interaction with the lithium ion<sup>15</sup>. Both XRD and SEM studies on PP(I)-LiClO<sub>4</sub> and PP(II)-LiBF<sub>4</sub> complexes indicate that these are amorphous. Fig.3.10 shows SEM photographs of selected PP(I)-LiClO<sub>4</sub> and PP(II)-LiBF<sub>4</sub> complexes. DTA studies on all the salt complexes from room temperature (~25°C) to 450°C indicate the absence of any phase transition. It was not possible for us to perform low temperature DSC measurements for these samples.

Table 3.4

Complex	O:Li ratio	$\nu_{\text{-C}_6\text{H}_4\text{-}}$	$\nu_{\text{P=N}}$	$\nu_{\text{C-O-C}}$
PP(I)-LiClO <sub>4</sub>	12:1	1611.9(s)	1242.8(s)	1049.4(s)
PP(I)-LiClO <sub>4</sub>	18:1	1612.0(s)	1243.0(s)	1102.0(s)
PP(II)-LiBF <sub>4</sub>	5:1	1611.2(s)	1244.2(b)	1112.0(b)
PP(II)-LiBF <sub>4</sub>	10:1	1612.8(s)	1246.6(s)	1110.5(s)
PP(II)-LiBF <sub>4</sub>	12:1	1613.8(s)	1244.6(b)	1112.4(b)
(s)-Strong; (b)-Broad				

### 3.3.3. Conductivity Studies of Polymer-Salt Complexes

#### 3.3.3.1 General

By using the film casting technique, described in the experimental section, several polymer-alkali metal salt complexes in various compositions were made. The choice of the metal salts has been dictated by the small size of the cation and the large size of the anion. We have used LiClO<sub>4</sub> for the polymer PP(I) and LiBF<sub>4</sub> for the polymer PP(II). Lithium salts were used because it was felt that

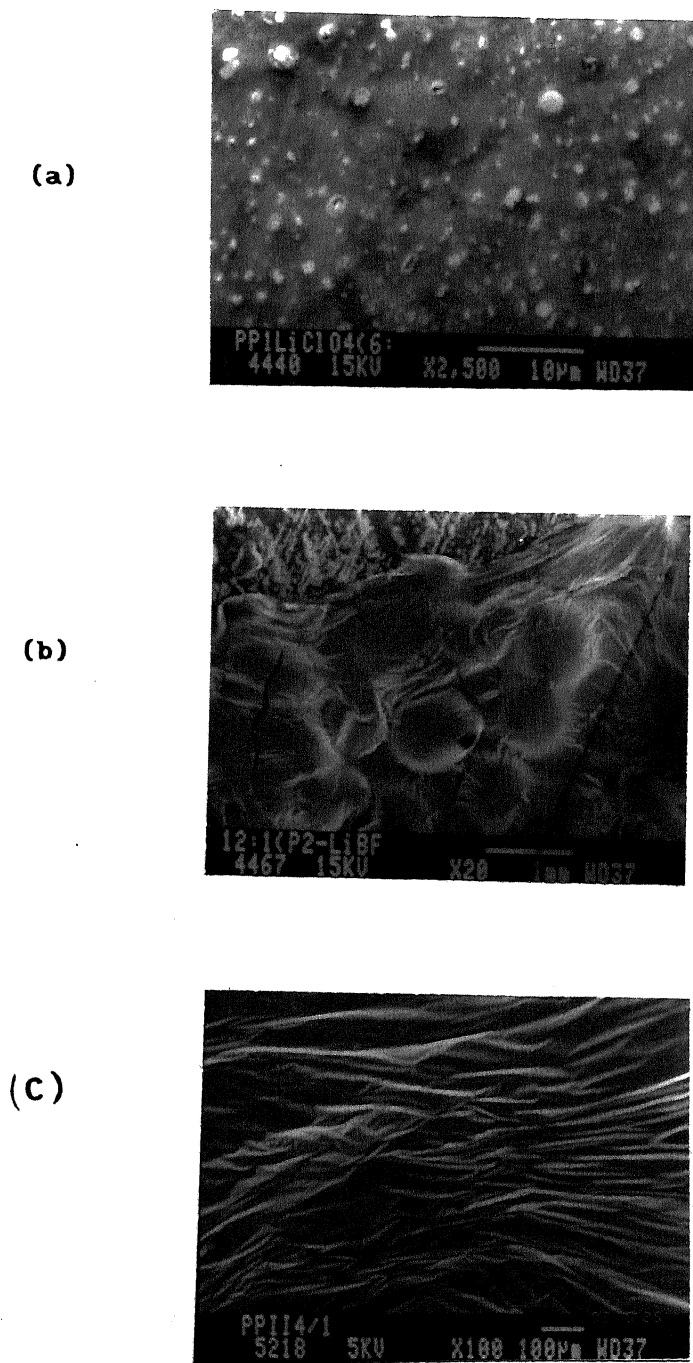


**Fig.3.10 SEM Photographs of selected polymer-metal salt complexes:**

- (a)  $PP(I)-LiClO_4$  (O:Li, 6:1);  $PP(II)-LiBF_4$  (O:Li, 12:1);  
 (c)  $PP(II)-LiBF_4$  (O:Li, 4:1)

the small cation would aid in increased ionic mobility. The larger anions render low ion pairing. Also the lattice energies of these salts are low ( $709 \text{ KJmol}^{-1}$  for  $\text{LiClO}_4$  and  $699 \text{ KJmol}^{-1}$  for  $\text{LiBF}_4$ ) thereby facilitating easier solvation by the polymer matrix<sup>16</sup>.

The various compositions of  $\text{PP(I)-LiClO}_4$  and  $\text{PP(II)-LiBF}_4$  complexes were made by varying the O:Li ratios. All the oxygens in the side chain have been taken into account to calculate the O:Li. The dried polymer-salt complexes were made into thin films and used for conductivity measurements. To avoid cell polarization ac impedance analysis was carried out using stainless steel as ion blocking electrodes. The dc conductivity of each composition at different temperature was measured by complex impedance analysis in view of the strong frequency dependent impedances of the sample. The impedance of all the compositions of  $\text{PP(I)-LiClO}_4$  and  $\text{PP(II)-LiBF}_4$  complexes at different O:Li ratios and temperatures were carried out. Fig. 3.11 and 3.12. show the representative impedance spectra of  $\text{PP(I)-LiClO}_4$  (O:Li, 6:1) and  $\text{PP(II)-LiBF}_4$  (O:Li, 8:1) at three different temperatures respectively.

### 3.3.3.2 Conductivity Studies on $\text{PP(I)-LiClO}_4$ System

The conductivity plot ( $\log \sigma$  vs  $10^3/T$ ) of  $\text{PP(I)-LiClO}_4$  complexes are given in Fig. 3.13. The conductivity values of PP(I) and  $\text{PP(I)-LiClO}_4$  complexes are summarized in Table 3.5. As can be seen clearly, the conductivity of the virgin polymer is very low ( $2.9 \times 10^{-8} \text{ Scm}^{-1}$ ) at 298K. Upon addition of  $\text{LiClO}_4$ , there is a slight increase in conductivity; only at higher temperature for the composition O:Li ratio 6:1 the conductivity is some what significant. At all other compositions and temperatures, there is an insignificant change in the conductivity value for  $\text{PP(I)-LiClO}_4$  complexes in comparison with pure PP(I).

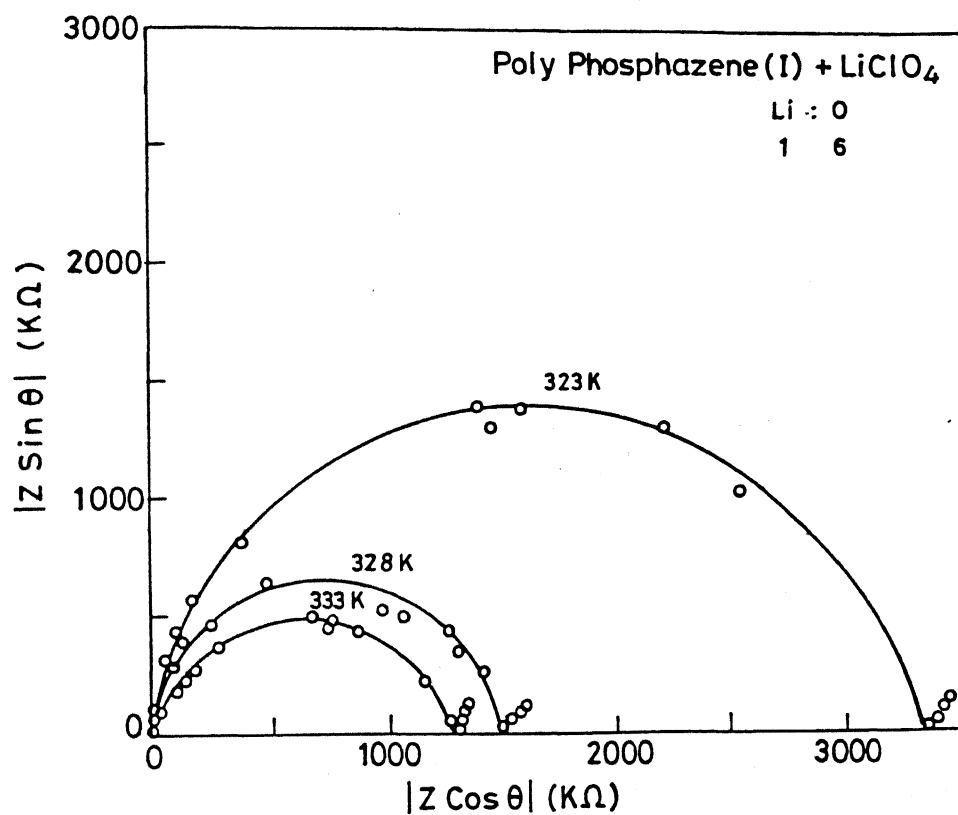


Fig. 3.11.

The representative impedance spectra of  $\text{PP(I)}-\text{LiClO}_4$  (O:Li, 6:1) complex at three different temperatures.

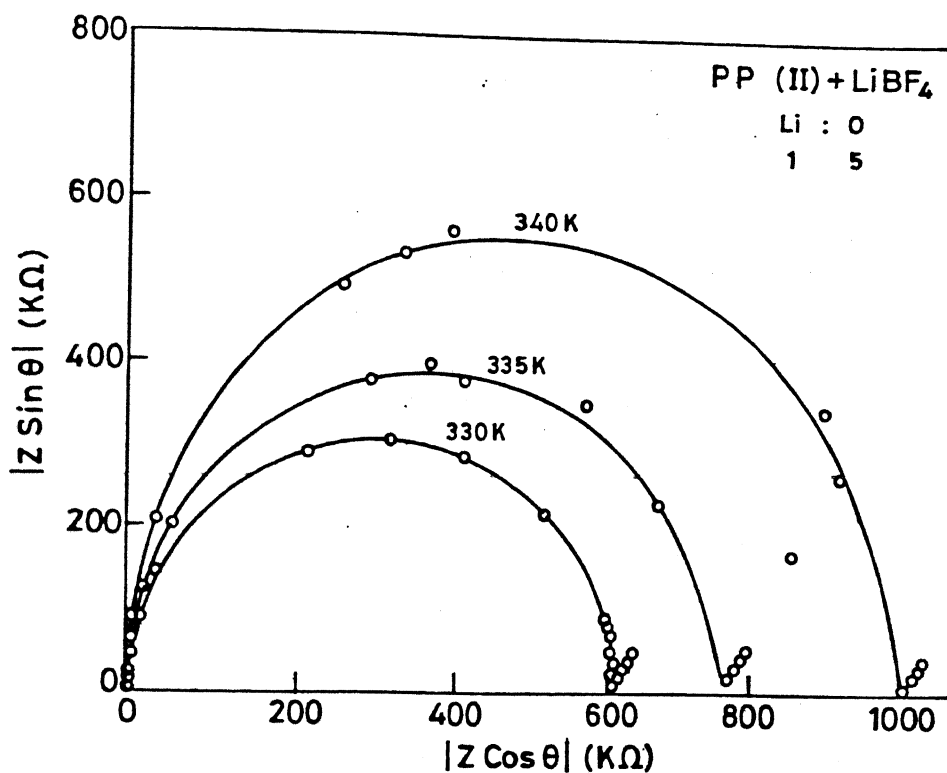


Fig.3.12.

The representative impedance spectra of PP(II)-LiBF<sub>4</sub> (0:Li, 5:1) complex at three different temperatures.

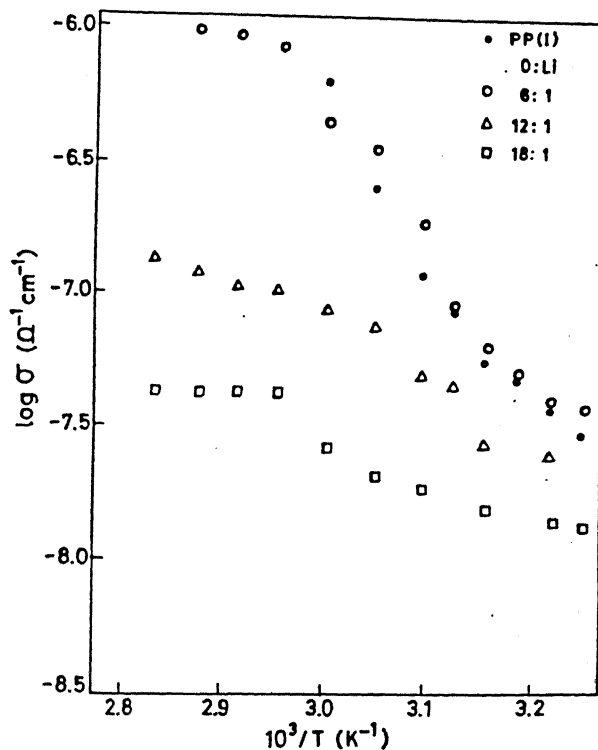


Fig. 3.13  $\log \sigma$  vs  $10^3/T$  plot of PP(I)-LiClO<sub>4</sub> Complexes.

Table 3.5. Conductivity values of PP(I)-LiClO<sub>4</sub> complexes at three different temperatures.

Composition O:Li	$\sigma$ (Scm <sup>-1</sup> ) 310K	$\sigma$ (Scm <sup>-1</sup> ) 333K	$\sigma$ (Scm <sup>-1</sup> ) 348K
6:1	$4.0 \times 10^{-8}$	$4.4 \times 10^{-7}$	$1.0 \times 10^{-6}$
12:1	$2.4 \times 10^{-8}$	$8.7 \times 10^{-8}$	$1.3 \times 10^{-7}$
18:1	$1.9 \times 10^{-8}$	$2.6 \times 10^{-8}$	$4.2 \times 10^{-8}$

### 3.3.3.3 Conductivity Studies on PP(II)-LiBF<sub>4</sub> System

In view of the fact that PP(I)-LiClO<sub>4</sub> complexes showed poor conductivity we have chosen to study the conductivity behaviour of PP(II)-LiBF<sub>4</sub> complexes. It

may be recalled that the highest conductivity observed for Poly(MEEMA)-LiX, ( $X^- = ClO_4^-$ ,  $CF_3SO_3^-$ ,  $BF_4^-$ ) system was in the case of  $X^- = BF_4^-$ <sup>17</sup>. Therefore, it was felt that the best chance for high ionic conductivities can be with  $LiBF_4$  in the present system also. Table 3.6 summarizes the conductivity values of these complexes at different temperatures.

Table 3.6 Conductivity values of PP(II)- $LiBF_4$  Complexes at two different temperatures

Composition O:Li	$\sigma$ (Scm <sup>-1</sup> ) 303K <sup>(a)</sup>	$\sigma$ (Scm <sup>-1</sup> ) 333K
3:1	—	$1.1 \times 10^{-6}$
5:1	$7.6 \times 10^{-7}$	$1.3 \times 10^{-6}$
6:1	$1.3 \times 10^{-8}$	$2.8 \times 10^{-6}$
8:1	$2.3 \times 10^{-7}$	$5.8 \times 10^{-6}$
12:1	$6.9 \times 10^{-8}$	$2.5 \times 10^{-6}$
15:1	$8.3 \times 10^{-8}$	$6.3 \times 10^{-7}$

(a) Measurement was taken at this temperature

The conductivity plot ( $\log \sigma$  vs  $10^3/T$ ) of PP(II)- $LiBF_4$  complexes at different compositions and temperatures is given in Fig. 3.14.

The dc conductivity of PP(II) is  $\sim 1 \times 10^{-9}$  Scm<sup>-1</sup> at 303K. The conductivity increases steadily with the increase of lithium salts, reaches an optimum value and starts to decrease again. The highest conductivity value observed for PP(II)- $LiBF_4$  system is for an O:Li ratio of 8:1, which shows a conductivity of  $5.8 \times 10^{-6}$  Scm<sup>-1</sup> (333K) and  $2.3 \times 10^{-7}$  Scm<sup>-1</sup> (303K). These values are atleast 3 orders of magnitude higher than the virgin polymer. The low conductivity of PP(II)- $LiBF_4$  complexes can be explained based on the studies of Gray, on the molar conductance dependance of amorphous solid poly ether,  $[(CH_2CH_2O)_xOCH_2]_y$  and low molecular weight poly ether,  $CH_3(OCH_2CH_2)_4-OCH_3$  complex of the  $LiClO_4$  upon salt concentration<sup>18</sup>. In these systems also the low conductivities at low

concentration of the salt is seen and has been confirmed as due to formation of

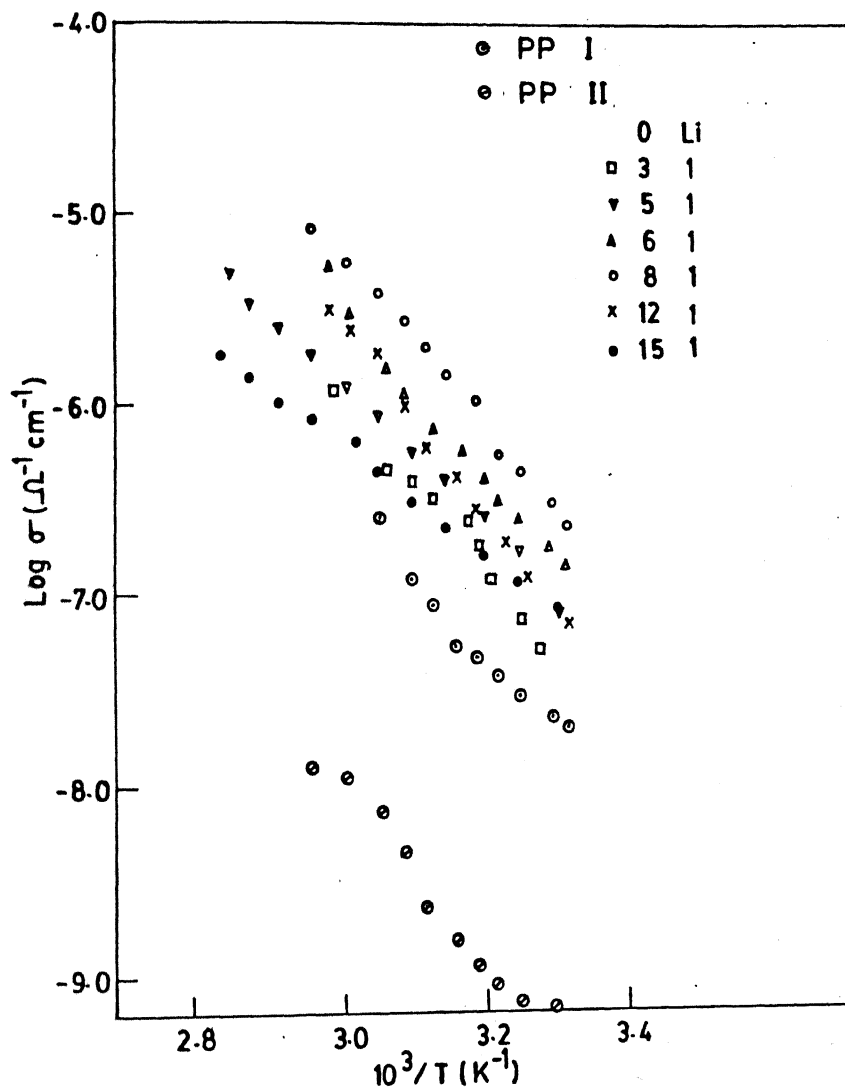


Fig.3.14.  $\log \sigma$  vs  $10^3/T$  plot of PP(II)- $\text{LiBF}_4$  Complexes.

non conducting ion pairs. The author has concluded that at low salt concentrations the tendency to form ion pairs is much larger. This feature



explains the relatively low conductivity values at lower salt concentrations in the PP(II)-LiBF<sub>4</sub> systems.

As can be seen from Fig. 3.14 the conductivity behaviour is explained by Arrhenius equation,

$$\sigma = A \exp( -E_a / kT )$$

Thus, a straight line is expected in the plots of  $\log \sigma$  vs  $10^3/T$ . The nearly straight line behaviour seen for PP(II)-LiBF<sub>4</sub> complexes suggests that the conductivity is better explained by Arrhenius model in contrast to either free volume or configurational entropy model. It might be noted that the conductivity behaviour of MEEP-alkali metal salt complexes fits into both Arrhenius and VTF equations. The activation energy values obtained are tabulated in Table 3.7.

Table 3.7 Activation Energies obtained for PP(II)-LiBF<sub>4</sub> Complexes

O:Li	Activation Energy (eV)	A
3:1	0.47	0.800
5:1	0.65	0.674
6:1	0.84	0.666
8:1	0.69	0.600
12:1	0.63	0.500
15:1	0.49	0.444

#### 3.3.3.4 Comparison of the Present System with Other Known Systems

The ionic conductivity behaviour in PP(I)-LiClO<sub>4</sub> and PP(II)-LiBF<sub>4</sub> systems follow the pattern observed earlier for other amorphous polymer solid electrolytes including MEEP. Both PP(I) and PP(II), show a conductivity value which is comparable with MEEP indicating that they are electrical insulators. Between the two systems studied PP(II)-LiBF<sub>4</sub> system shows a better

conductivity. The highest conductivity observed is for the O:Li ratio 8:1 ( $5.8 \times 10^{-6} \text{ Scm}^{-1}$  at 333K) which is atleast 3 orders of magnitude greater than that the virgin polymer, PP(II). Presumably since PP(II) has a  $T_g$  of  $-28.8^\circ\text{C}$  compared to PP(I) which has a  $T_g$  of  $-13.28^\circ\text{C}$ , the conductivities observed in the lithium electrolytes of the former are greater than that in the latter. It is interesting to compare the conductivity values observed for PP(II)- $\text{LiBF}_4$  complexes with other polymer electrolytes. Analogous to MEEP as well as Poly(MEEMA) the  $\text{LiBF}_4$  complexes of PP(II) show a high conductivity. However, the conductivity values are clearly lower than either MEEP or POLY(MEEMA) and closer to the values obtained in PEO system. It is possible that the high glass transition temperature,  $T_g$ , of PP(II) ( $-28.2^\circ\text{C}$ ) coupled with the presence of long alkyl group in the side chain prevent effective ion transport. Clearly, the latter feature may be a dominant factor in determining the exact magnitude of conductivities observed. Thus Poly(MEEMA) which has a  $T_g$  of  $-26.5^\circ\text{C}$  but without the presence of the long alkyl side chain is quite effective as a polymer electrolyte. It is possible that the long alkyl side chains present in PP(I) and PP(II) form separate domains and inhibit free mobility of ions. Between PP(I) and PP(II), the conductivity values are higher for lithium electrolytes derived from PP(II) since the  $T_g$  of the latter is lower. However, inspite of the relatively lower conductivities observed for PP(I) and PP(II) electrolytes, these polymers possess definitely better dimensional stability compared to MEEP. Also they are both hydrophobic. Table 3.8 summarizes the ionic conductivity of various polymer-salt complexes along with PP(I)- $\text{LiClO}_4$  and PP(II)- $\text{LiBF}_4$  systems.

Table 3.8 Ionic conductivity values of some polymer-salt complexes

Polymer-Salt Complex	O:Li	Conductivity S <sub>cm</sub> <sup>-1</sup>	Ref.
MEEP:LiCF <sub>3</sub> SO <sub>3</sub>	24:1	1.0x10 <sup>-4</sup> (312)	19
MEEP:LiBF <sub>4</sub>	36:1	5.2x10 <sup>-5</sup> (303)	19
Poly(MEEMA):LiBF <sub>4</sub>	5:1	5.8x10 <sup>-5</sup> (300)	17
		3.3x10 <sup>-4</sup> (333)	
Poly(MEEMA):LiCF <sub>3</sub> SO <sub>3</sub>	20:1	2.3x10 <sup>-6</sup> (271)	17,20
		5.6x10 <sup>-5</sup> (303)	
Poly(MEEMA):LiClO <sub>4</sub>	10:1	3.3x10 <sup>-6</sup> (305)	17,21
		1.4x10 <sup>-5</sup> (333)	
PP(I):LiClO <sub>4</sub>	6:1	1.0x10 <sup>-6</sup> (348)	Present work
PP(II):LiBF <sub>4</sub>	8:1	5.8x10 <sup>-6</sup> (333)	Present work

### 3.4 Conclusions

The results obtained from the present study can be summarized as follows:

- # New polyphosphazenes, PP(I) and PP(II), containing oligo oxy ethylene side chains with long alkyl chain substituted phenyl group have been synthesized. These novel polyphosphazenes are water insoluble and readily soluble in a wide range of organic solvents including hexane. Thus, separation of sodium chloride is readily achieved. Secondly, the hydrophobicity of the polymers is a major advantage. Thirdly, the ready solubility of these polymers renders easy film formation.
- # PP(I) and PP(II) readily form homogeneous complexes with alkali metal salts. While the virgin polymers, PP(I) and PP(II) are electrical insulators, the lithium electrolytes derived from these polymers are

conducting. The highest conductivity observed for PP(II)-LiBF<sub>4</sub> complex (O:Li, 8:1) is  $5.6 \times 10^{-6} \text{ Scm}^{-1}$  at 333K.

- # Comparison of the conductivity of PP(II)-LiBF<sub>4</sub> complexes with other polymer electrolytes show that the conductivities observed for the present system are comparable to the conductivity of PEO-alkali metal salt complexes at ambient temperatures and an order of magnitude less than that of the best known polymer electrolytes like MEEP or Poly(MEEMA) systems.
- # Thus, we were able to synthesize new polyphosphazenes one of which atleast in its lithium complexes show good conductivities along with attributes such as water insolubility and dimensional stability.
- # Further improvements in this system can be made by either plasticization or modification of side groups such as removal of the alkyl side chains from the aromatic group.

## REFERENCES

1. (a) Angell, C.A; Liu, S.; Sanchez, E. *Nature*, 1993, **362**, 137.  
(b) Ratner, M.A.; Shriver, D.F. *Chem. Rev.* 1988, **88**, 109.
2. (a) "Polymer Electrolytes Review - I", Vincent, C. A.; Mac Callum, J.R. Eds. Elsevier Applied Science, New York, 1989.  
(b) "Polymer Electrolytes Review - II", Vincent, C. A.; Mac Callum, J.R. Eds. Elsevier Applied Science, New York, 1989.
3. Blonsky, P.M.; Shriver, D.F.; Austin, P; Allcock, H.R. *J. Am. Chem. Soc.* 1984, **106**, 6854.
4. Tonge, J.S; Blonsky, P.M; Shriver, D.F.; Allcock, H.R.; Austin, P.; Neenan, T.X.; Sisko, J.T. *Proc. Symp. on Lithium Batteries*, 1987, **87-1**, 533.
5. Tonge, J.S.; Shriver, D.F. *J. Electrochem. Soc.* 1987, **134**, 269.
6. Abraham, K.M.; Alamgir, M.; Perrotti, S.J. *J. Electrochem. Soc.* 1988, **105**, 535.
7. Nazri, G.A.; Meibuhr, S.G. *J. Electrochem. Soc.* 1989, **136**, 2460.
8. "Vogel's Text Book of Practical Organic Chemistry", Furniss, D.S.; Hannaford, A.J.; Smith, P.W.G.; Thatchell, A.R. Eds. 5<sup>th</sup> Ed. ELBS, UK, 1989.
9. Bhatnagar, S.; Gupta, S.; Shahi, K. *Solid State Ionics*, 1988, **31**, 107.
10. Ganapathiappan, S.; Dhathathreyan, K.S.; Krishnamoorthy, S.S. *Macromolecules*, 1987, **20**, 1501.
11. (a) Allcock, H.R.; Kugel, R.L. *J. Am. Chem. Soc.* 1965, **87**, 4216.  
(b) Allcock, H.R.; Kugel, R.L. *Inorg. Chem.* 1966, **5**, 1709.
12. Allcock, H.R. "Phosphorus-Nitrogen Compounds", Academic Press, New York, 1972.
13. Allcock, H.R.; Connolly, M.S.; Sisko, J.T.; Al-Shali, S. *Macromolecules*, 1988, **21**, 323.
14. Chandrasekhar, V.; Thomas, K.R.J. *Structure and Bonding* , 1993, **81**, 41.
15. (a) Dupon, R.; Papke, B.L.; Ratner, M.A.; Whitmore, D.H.; Shriver, D.F.; *J. Am. chem. Soc.* 1982, **104**, 6247.  
(b) Manoravi, P.; Selvaraj, I.I.; Chandrasekhar, V.; Shahi, K. *Polymer*, 1993, **34**, 1339 (and references cited therein).
16. "CRC Hand Book of Chemistry and Physics", Weast, R.C.; Astle, M.J.; Beyer, W.H. Eds. 67<sup>th</sup> Edn. CRC Press, Florida, 1987.
17. Chapter II, this Thesis.
18. Gray, F.M. *Solid State Ionics*, 1990, **40/41**, 637.

19. Blonsky, P.M.; Shriver, D.F.; Austin, P.; Allcock, H.R. *Solid State Ionics*, 1986, 28/29, 256.
20. Selvaraj, I.I.; Manoravi, P.; Chandrasekhar, V. *Solid State Ionics, Materials and Applications*, Chowdari, B.V.; Chandra, S.; Singh, S.; Srivastava, P.C. Eds. World Scientific, Singapore, 1992, 591.
21. Selvaraj, I.I.; Chaklanobis, S.; Chandrasekhar, V. *J. Polym. Sci. Polym. Chem. Ed.* 1993, 31, 2643.

*PART B*

STUDIES ON ORGANIC POLYMERS CONTAINING CYCLOPHOSPHAZENE  
PENDANT GROUPS

## CHAPTER IV

COPOLYMERIZATION OF 2-(4'-VINYL-4-BIPHENYLYLOXY)PENTACHLORO  
CYCLOTRIPHOSPHAZENE WITH METHYLACRYLATE, ETHYLACRYLATE,  
METHYLMETHACRYLATE, AND STYRENE

## 4.1 Introduction

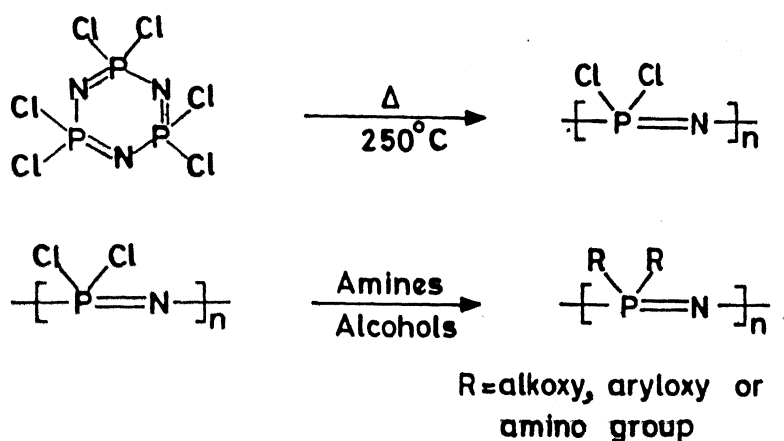
Most polymers that are known have been built based on a carbon backbone making use of the well known and rich functional group chemistry of organic molecules.<sup>1</sup> The traditional applications of polymers have been centered on the nature of the polymer synthesized viz., elastomeric, thermoplastic or thermosets etc. Attempts to achieve new properties in polymers such as high temperature resistivity, low temperature flexibility electronic and ionic conductivity etc., have focused attention on new types of polymers based on new synthetic approaches including use of non-carbon backbones or hybrid organic-inorganic polymers.<sup>2</sup> Several polymers based on inorganic elements such as P, N, B, Si etc., are now known.<sup>3</sup> Similarly, polymers containing organometallic moieties have also been synthesized.<sup>4</sup> In the following account a brief review on the P-N polymers, polyphosphazenes, and the hybrid organic-inorganic polymers containing cyclophosphazenes as pendant group is presented.

## 4.1.1 Polyphosphazenes

Polyphosphazenes are polymers containing alternate phosphorus and nitrogen atoms in the backbone. The basic poly (dichlorophosphazene) is synthesized by a ring opening polymerization of the six-membered heterocycle, hexachlorocyclo triphosphazene.<sup>5</sup> Several methods of ring opening  $\text{N}_3\text{P}_3\text{Cl}_6$  are now known



including solid state and solution polymerization methods. The mechanism of ring opening is believed to proceed via an initial heterolysis of the P-Cl bond.<sup>6</sup> The poly(dichlorophosphazene) is extremely reactive making the native polymer unsuitable as such for any application. However, this reactivity enables reactions to be performed on the polymer by a replacement of P-Cl



bonds by a variety of nucleophiles such as primary and secondary amines, alcohols, phenols etc.<sup>7</sup> The property of the polymer is strongly dependent on the nature of the nucleophile. Over 250 such polymers have been synthesized.<sup>8</sup> Table 4.1 summarizes some of the polymers and their properties.

Polyphosphazenes containing alkyl or aryl substituents on phosphorus cannot be synthesized by the above approach since the reaction of alkyl and aryl lithium or Grignard reagents with poly(dichlorophosphazenes) leads to degraded products.<sup>9</sup>

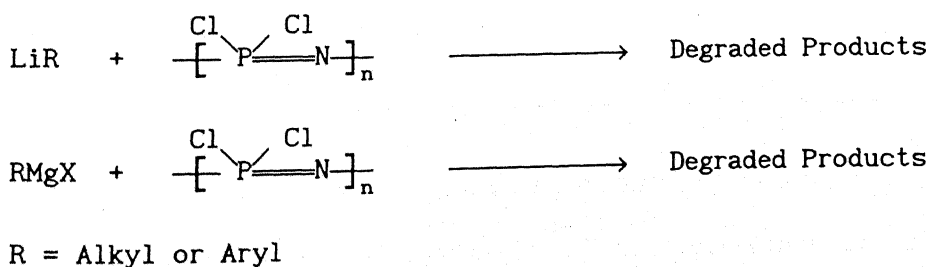


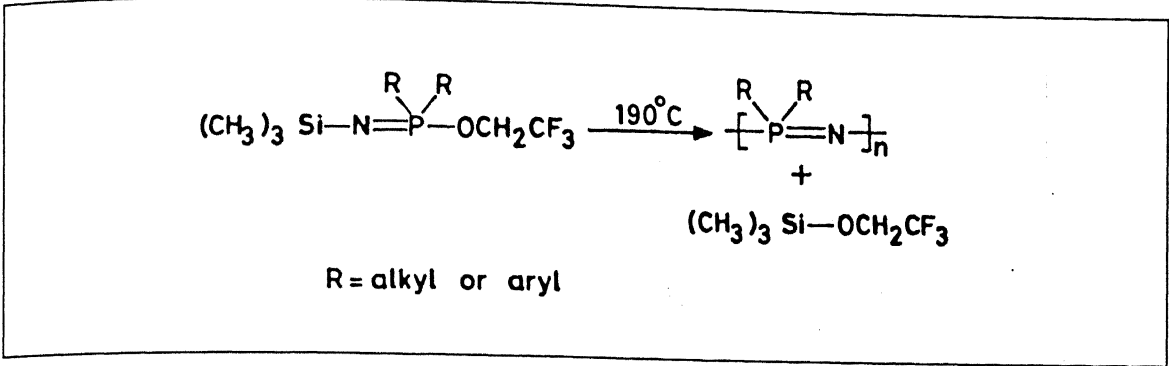
Table 4.1

## Properties of Polyphosphazenes

Formula	T <sub>g</sub> , °C	T <sub>m</sub> , °C	Properties
[NP(OC <sub>3</sub> H <sub>7</sub> ) <sub>2</sub> ] <sub>n</sub>	-100	-68, -40	elastomer
[NPF <sub>2</sub> ] <sub>n</sub>	- 96		hydrolytically unstable elastomer
[NP(OC <sub>2</sub> H <sub>5</sub> ) <sub>2</sub> ] <sub>n</sub>	- 84		elastomer
[NP(OCH <sub>2</sub> CH <sub>2</sub> OCH <sub>2</sub> CH <sub>2</sub> OCH <sub>3</sub> ) <sub>2</sub> ] <sub>n</sub>	- 84		Water-soluble elastomer
[NP(OCH <sub>3</sub> ) <sub>2</sub> ] <sub>n</sub>	- 76		elastomer
[NPCl <sub>2</sub> ] <sub>n</sub>	- 66	-7.2(+39) <sup>a</sup>	hydrolytically unstable elastomer
[NP(OCH <sub>2</sub> CF <sub>3</sub> ) <sub>2</sub> ] <sub>n</sub>	- 66	+242	microcrystalline film-forming polymer
[NP(OCH <sub>2</sub> CF <sub>3</sub> (OCH <sub>2</sub> (CF <sub>2</sub> ) <sub>x</sub> CF <sub>2</sub> H))] <sub>n</sub>	- 60 <sup>b</sup>		elastomer
[NP(OC <sub>9</sub> H <sub>19</sub> ) <sub>2</sub> ] <sub>n</sub>	- 56		elastomer
[NPBr <sub>2</sub> ] <sub>n</sub>	- 15		hydrolytically unstable leathery material
[NP(OC <sub>6</sub> H <sub>5</sub> )OC <sub>6</sub> H <sub>4</sub> C <sub>2</sub> H <sub>5</sub> )] <sub>n</sub>	- 10 <sup>c</sup>	<sup>d</sup>	elastomer
[NP(OC <sub>6</sub> H <sub>5</sub> ) <sub>2</sub> ] <sub>n</sub>	-8	+390	microcrystalline, film-forming polymer
[NP(OC <sub>6</sub> H <sub>4</sub> CH <sub>3</sub> )(OC <sub>6</sub> H <sub>4</sub> CHO)] <sub>n</sub>	+ 11		thermoplastic
[NP(NHCH <sub>3</sub> ) <sub>2</sub> ] <sub>n</sub>	+ 14		Water-soluble glass and film former
[NP(NHC <sub>6</sub> H <sub>5</sub> ) <sub>2</sub> ] <sub>n</sub>	+ 91		glassy thermoplastic
[NP(OC <sub>6</sub> H <sub>4</sub> C <sub>6</sub> H <sub>5</sub> -p) <sub>2</sub> ] <sub>n</sub>	+ 93		microcrystalline thermoplastic

<sup>a</sup>For the stretched polymer,<sup>b</sup>Value varies with values of x and ratio of side groups.<sup>c</sup>Varies with ratio of side groups.<sup>d</sup>Complex melting phenomena.

Neilson and coworkers have developed an alternative method of synthesis.<sup>10</sup> Neilson's method consists of the synthesis of an appropriate monophosphazene containing a silylated 'N'. Heating the silylphosphinimine affords the linear



polymer by the expulsion of the silyl ether. This topic has been reviewed recently.<sup>11</sup>

#### 4.1.2 Cyclophosphazene Pendant Polymers

#### 4.1.2.1 Homopolymerization of Cyclophosphazene Containing Organic Monomers

The polymers discussed so far are inorganic backbone polymers with organic side groups on phosphorus atom. In contrast to these kind of polymers, there has also been interest to develop hybrid polymers containing an organic backbone and a cyclophosphazene ring as a pendant (side) group. The synthetic route to develop such polymers is to introduce a polymerizable organic substituent on the phosphorus atom of the cyclophosphazene ring, and subsequently polymerizing such a derivative.

Allen and coworkers have synthesized cyclophosphazenes with exocyclic vinyl groups such as 2-(2-propenyl) pentafluorocyclotriphosphazene (1)<sup>12</sup>, 2-( $\alpha$ -Ethoxyvinyl) pentafluorocyclotriphosphazene (2)<sup>13</sup>, and [( $\alpha$ -methylethenyl) phenyl]pentafluorocyclotriphosphazene (3)<sup>14</sup> (Fig. 4.1). All of these have been synthesized by making use of the well developed substitution chemistry of halogenocyclophosphazenes. Since reactions of chlorocyclophosphazenes with alkyl or aryl lithium reagents leads to ring degraded products, fluoro cyclophosphazenes were the preferred starting materials for the synthesis of (1), (2) and (3). However, Allen and coworkers have observed that the

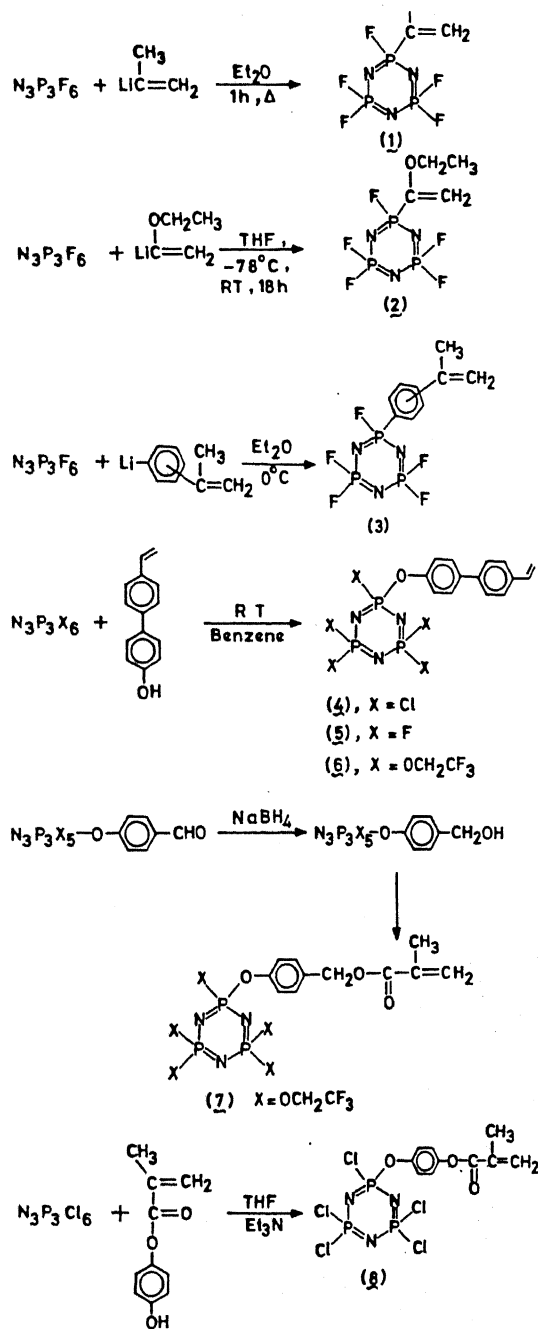


Fig.4.1. Synthesis and structure of cyclophosphazene monomers.

cyclophosphazene containing monomers (1), (2), and (3) could not be homopolymerized by free radical initiators at moderate temperatures. It was suggested by the authors that the  $\sigma$  - electron withdrawing effect of the cyclotriphosphazene ring depletes the electron density on the olefinic functionality and prevents the homopolymerization. It is possible that since the monomers (1), (2), and (3) are  $\alpha, \alpha'$ -disubstituted olefins a steric factor might also be operating in preventing homopolymerization. However, these cyclotriphosphazenes could be copolymerized with certain organic monomers such as styrene or methylmethacrylate (vide infra).<sup>12-14</sup> We have reasoned that since the cyclophosphazene functions as a  $\sigma$ -electron withdrawing group, this effect could be minimized on the polymerizable moiety by the incorporation of a suitable insulating spacer group between the cyclophosphazene unit and the polymerizable functional unit. While our work was in progress, Inoue and coworkers have reported the synthesis and homopolymerization of [2-(4'-vinyl-4-biphenyloxy) pentachlorocyclotriphosphazene (4)]<sup>15</sup> (Fig. 4.1). In this monomer the vinyl group is separated from the cyclophosphazene by means of a biphenyleneoxy unit. Inoue and coworkers have also reported the fluoro analogue (5)<sup>16</sup> and trifluoroethoxy derivatives (6)<sup>16</sup>, 2-(p-methacryloxymethyl-phenoxy)pentakis(trifluoroethoxy) cyclotriphosphazene (7)<sup>17</sup>, and 2-(4-methacryloxyphenoxy)pentachlorophosphazene(8)<sup>18</sup>, which also undergo homopolymerization. In an extension of their earlier work, Inoue and coworkers have recently reported the polymerization studies on the styrene derivatives containing multiarmed oligooxy ethylene cyclotriphosphazenes. These polymers have been shown to function as polymer solid electrolytes when complexed with lithium salts in the solid state.<sup>19</sup>

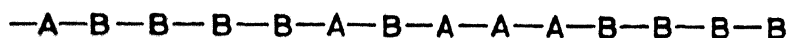
#### 4.1.2.2 Copolymers of Cyclophosphazene Substituted Derivatives with Other Organic Monomers

Before describing the copolymers involving cyclophosphazenes, a brief discussion on some general aspects of copolymerizations are given below :

##### 4.1.2.2.1 Copolymers

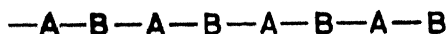
A polymer made from two or more different monomers is called a 'copolymer'. If A and B are the two monomers involved in copolymerization the following types of copolymers can be formed.

- (1) 'Random copolymer' is a copolymer where no definite sequence of monomer units exist.eg.



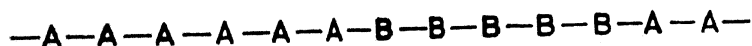
Free radical polymerization of two monomers generally affords random copolymers.

- (ii) 'Regular or Alternating copolymer' consists of a regular alternating sequence of two monomer units, represented as



Polymerization of two monomers involving ionic mechanism affords this kind of copolymers.

- (iii) 'Block copolymer' is a copolymer which contain a block of one monomer to a block of another monomer in a sequence i.e.,



These type of polymers are also synthesized by ionic polymerization methods.

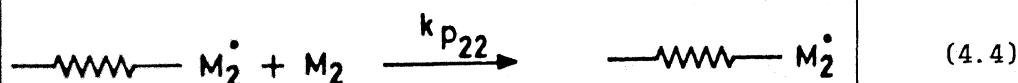
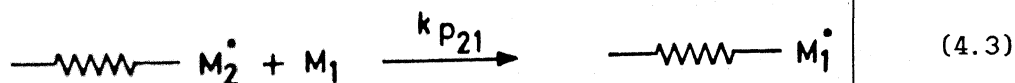
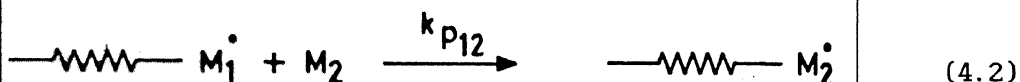
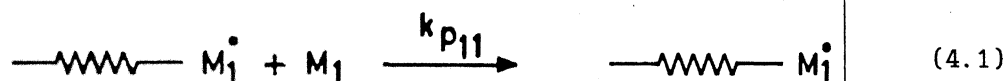
- (iv) 'Graft copolymer' is not derived by the preparative methods described

above. To a preformed homopolymer derived from one monomer, oligomers or polymers from a different monomer are grafted. They can be prepared by irradiation of gamma-rays or X-rays or even by mechanical blending of the two homopolymers.

The properties of random and alternating copolymers are different from the respective homopolymers whereas both block and graft copolymers retain most of the properties of the native homopolymers.

#### 4.1.2.2.2 Copolymerization Equation

Suppose two monomers are present in the reaction mixture and both are susceptible to free radical polymerization, according to terminal model, there are four types of propagation reactions that can exist, as shown in equations



The copolymer composition is given by the following expression<sup>20</sup>:

$$\frac{-d[m_1]/dt}{-d[m_2]/dt} = \frac{1 + r_1([m_1]/[m_2])}{1 + r_2([m_2]/[m_1])} \quad (4.5)$$

where  $r_1$  and  $r_2$  are the reactivity ratios of the monomer 1 and monomer 2 respectively, which are defined as follows :

$$r_1 = \frac{k_{p_{11}}}{k_{p_{12}}} \text{ and } r_2 = \frac{k_{p_{22}}}{k_{p_{21}}}$$

The monomer reactivity ratios  $r_1$  and  $r_2$  are the ratios of rate constant for a given radical adding to its own monomer to the rate constant for its adding to the other monomer.

Therefore,  $r_1 > 1$  means that the radical  $m^\circ$ , prefers to add  $M_1$  rather than to  $M_2$  and the reverse i.e.  $r_1 < 1$  means that it prefers adding to  $M_2$  than  $M_1$ .

The composition of the copolymer is independent of the overall reaction rate and initiator concentration. The reactivity ratios are unaffected by the presence of inhibitors, chain transfer agents or solvents, but are dependent on the temperature.

#### 4.1.2.2.3 Evaluation of Monomer Reactivity Ratios

Experimental determination of  $r_1$  and  $r_2$  involves polymerization to low conversion for a variety of feed compositions of the monomers involved in copolymerization. The composition of the polymer is measured after isolating the polymer. Several methods of analysis are known, out of which there are atleast three methods that are commonly used to find out  $r_1$  and  $r_2$ .

The first method was developed by Mayo and Lewis in 1944<sup>21</sup>, in which  $r_1$  is plotted against  $r_2$ . The copolymer equation which is solved for one of the reactivity ratios, is given by equation (4.6).



$$r_2 = \frac{[M_1]}{[M_2]} \left[ \frac{d [M_2]}{d [M_1]} \left( 1 + \frac{[M_1]}{[M_2]} r_1 \right) - 1 \right] \quad (4.6)$$

Each experiment with a given feed ratio gives a straight line, the intersection of several of these lines allow the evaluation of  $r_1$  and  $r_2$ . To use this method the conversion need not to be less than 10% as is required by other methods (vide infra). This method gives only a qualitative estimate of  $r_1$  and  $r_2$ . Moreover, this method involves large uncertainties in the slopes and consequently in the  $r_1$  and  $r_2$  values, particularly where the slopes are steep. The obtained estimate of  $r_1$  and  $r_2$  values are not reliable when experimental data at very low and very high concentration ratios are not available.

The second method, linearization method, was developed by Finemann and Ross in 1950.<sup>22</sup> The copolymer composition equation may be written as in equation (4.7).

$$\frac{m_1}{m_2} = \left( \frac{M_1}{M_2} \right) \left( \frac{r_1 M_1 + M_2}{r_2 M_2 + M_1} \right) \quad (4.7)$$

where  $M_1$  and  $M_2$  are the monomer composition of monomer 1 and monomer 2 respectively. Similarly  $m_1$  and  $m_2$  are the polymer compositions.

Equation 4.7 can be rearranged to give equation 4.8.

$$\frac{F}{f} (f-1) = r_1 \frac{F^2}{f} - r_2 \quad (4.8)$$

where,  $f = m_1/m_2$  and  $F = M_1/M_2$

A plot of  $(F/f)(f-1)$  as ordinate and  $\left(\frac{F^2}{f}\right)$  as abscissa gives a straight line, whose slope is  $r_1$  and intercepts is  $-r_2$ .

To use Finemann-Ross method the conversion should be less than 10%, because eqn-7 holds good for low conversions only. This method also provides only a qualitative measure of the estimate of  $r_1$  and  $r_2$ .

The third method, a non linear least square fit method, developed by Mortimer and Tidwell in 1965,<sup>23</sup> is generally accepted as one of the more accurate methods. In this method, given initial estimates of  $r_1$  and  $r_2$ , a set of computations are performed which, on repetition, rapidly leads to a pair of values of the reactivity ratios which yields the minimum value of the sum of the differences between the observed and computed polymer composition.

All the three methods mentioned above are non statistical methods. Kelen and Tudos reported a method for evaluating  $r_1$  and  $r_2$ , in 1975,<sup>24</sup> which is statistically invalid, still give good initial reactivity ratios to derive more accurate  $r_1$  and  $r_2$ . Recently, error-in-variables model (EVM)<sup>25</sup> is used to estimate  $r_1$  and  $r_2$ , which is held to be statistically valid.

#### 4.1.2.2.3 Q-e Scheme

Reactivity in radical copolymerization is determined by a combination of steric, resonance and polar factors. Although a number of theoretical and empirical treatments of reactivity are available in literature, it is the Q and e scheme which is universally accepted and most widely used.

Alfrey and Price<sup>26</sup> expressed the rate,  $k_{12}$ , for copolymerization in the form given in equation 4.9.

$$k_{12} = P_1 Q_2 \exp (-e_1 e_2) \quad (4.9)$$

where  $P_1$  is the general reactivity, characteristic of the radical  $M_1^\cdot$ ,  $Q_2$  is the reactivity of the monomer  $M_2$ ,  $e_1$  and  $e_2$  are measures of the polarity of the monomer and radical respectively, with the assumption that the same polarity parameter  $e$  is used for monomer and for the radical derived from it. From the terminal model, which assumes that the terminal radical of a chain decides the state of propagation, to find out the copolymer composition, equation 4.5,

the definitions of the monomer reactivity ratios may be written as follows :

$$r_1 = \frac{Q_1}{Q_2} \exp \left[ -e_1(e_1 - e_2) \right]$$

$$r_2 = \frac{Q_2}{Q_1} \exp \left[ -e_2(e_2 - e_1) \right]$$

Thus,  $r_1 r_2 = \exp [-(e_1 - e_2)^2]$ .

The utility of the Q-e scheme is that one can predict reactivity ratios for any pair of monomers for which Q and e are known. Q-e scales are based on styrene as the reference monomer which has been arbitrarily assigned the values  $Q = 1.00$  and  $e = -0.80$ . An extensive tabulation of values of Q and e can be found in literature.<sup>27</sup>

The parameter Q is considered a rough measure of the ability of the substituents attached to the double bond to stabilize the monomer and the radical derived from it. Large Q values are associated with an effective conjugative stabilization. Thus for example, styrene has a Q of 1.00 and 1-3-butadiene has a Q of 2.39 whereas the Q values for ethylene and vinylchloride are 0.015 and 0.044 respectively. Attempts to correlate the e values with some molecular property have been somewhat controversial. Negative e values are associated with substituents generally regarded as electron donating, ( $e = -1.17$  for ethylvinyl ether) and positive e values with electron withdrawing groups ( $e = 1.20$  for acrylonitrile). Copolymerizations of monomers with large e values of opposite sign are characterized by small values of  $r_1$  and  $r_2$  which shows a strong tendency toward alternation. Also the monomers of very different Q values do not copolymerize readily, i.e., reactivity ratios for such systems are greatly different from 1, for example,

in the copolymerization of styrene ( $Q = 1.00$ ) with vinylacetate ( $Q = 0.026$ ) cross propagation from the styryl terminated macroradical to vinyl acetate is so slow that copolymerization is essentially inhibited, particularly, at low feed concentrations of styrene.

#### 4.1.2.2.4 Copolymers Containing Cyclophosphazene Pendant Groups

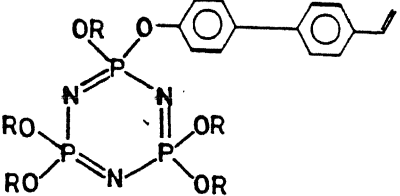
As discussed earlier (4.1.2.1), attempts to prepare cyclophosphazene containing organic monomers have focussed on substitution reactions of halogeno cyclophosphazenes in general and fluorocyclotriphosphazenes in particular with organo lithium reagents. Allen and coworkers have synthesized certain, organic monomers containing pendant cyclophosphazenes viz., 2(2-propenyl) pentafluorophosphazene (1), 2-( $\alpha$ -ethoxy-vinyl) pentafluorotriphosphazene (2), [ $\alpha$ -methyl (ethenyl)phenyl] pentachlorophosphazene (3)<sup>12-14</sup> (Fig. 4.1). These monomers were found to be inert to homopolymerization. However, they could be copolymerized with other organic monomers. These studies are quite limited and the known examples are summarized in Table 4.2.

In monomers (1) and (2) the vinyl functionality is directly attached to the phosphorus atom of the cyclophosphazene while in (3) a phenyl group separates the olefinic moiety from the cyclophosphazene. All the three monomers can be considered as  $\alpha, \alpha'$  disubstituted olefins and all of these were found to be resistant to homopolymerization.

Certain general trends emerged from the copolymerization studies, particularly with styrene.

1. When the olefin is directly attached to the cyclophosphazene as in (1) and (2) the reactivity ratios for these monomers are generally smaller (1.35 and 0.30 respectively) than that observed for styrene (2.20 and 3.40 respectively). This suggests that in the copolymerization styrene prefers

Table 4.2 Cyclophosphazene monomers known in literature

Cyclophosphazene monomer	Comonomers	Reference
2-(2-propenyl)pentafluorotriphosphazene (1)	Styrene and vinyl benzyl chloride	12
2-( $\alpha$ -Ethoxyvinyl)pentafluorotriphosphazene, (2)	Styrene and MMA	13
[( $\alpha$ -methylene)phenyl]pentachlorotriphosphazene, (3)	Styrene and MMA	14
2-[4-methacryloyloxyphenoxy]-pentachlorotriphosphazene, (8)	Styrene and MMA	18
2-(4'-vinyl-4-biphenyloxy)penta-(oligoxyethylene)triphosphazene.		
		
(9) $R - OCH_2CH_2OCH_3$	Styrene	28
(10) $R - O(CH_2CH_2O)_2CH_3$		

- to attach itself to another styryl moiety. Surprisingly monomers (1) and (2) which do not undergo homo polymerization show significant values of  $r_1$ .
- When the olefin is insulated from the cyclophosphazene by a phenyl group the  $r_1$  for monomer (3) is (0.28) as compared to the styrene (0.41). This indicates the tendency to form an alternate copolymer.
  - A computation of the Q and e values reveal that in monomer (2) the olefinic centre is highly polar ( $e = 0.18$ ) as opposed to styrene ( $e =$

is separated from the cyclophosphazene by means of the spacer group, the polarity increases ( $e = 0.72$ ). Indeed this value is even larger than that observed for p-nitrostyrene ( $e = 0.39$ )

4. An analysis of the Q values shows that while in monomer (1) and (2) there is virtually no conjugative mesomeric interaction of the cyclophosphazene ring with the vinyl group (Q for 1 = 0.21, Q for 2 = 0.18, Q for styrene = 1.00), in (3) the insulating phenyl group does interact mesomerically but the cyclophosphazene ring does not appear to be participating in conjugation (Q = 0.72).

An analysis of the results suggests that in monomer (1) and (2) due to a combination of steric and electronic reasons there is no tendency to form homopolymers and copolymers with large blocks of styrene are preferred. The vinyl moieties are highly polar and have a significant mesomeric interaction. Monomer (3) prefers to cross propagate with styrene presumably due to the electrostatic attraction between the aryl ring and styryl moiety. Also sterically it would be favourable for (3) to attack a styrene moiety than itself.

More recently Inoue and coworkers have reported the copolymerization of (8)<sup>18</sup> and (9, 10)<sup>28</sup> with styrene and MMA. The reactivity ratios of (8) with styrene [ $r_1 = 0.26$ ,  $r_2(\text{styrene}) = 0.33$ ] suggest that the tendency to cross propagate perhaps due to analogous reasons as for (3). Similarly, the Q and e for (8) [Q = 0.87,  $e = 0.76$ ] shows that monomer (8) is very similar to (3).

The copolymerization of (9) with styrene shows that the reactivity ratios are solvent dependent. [ $r_1(9) = 0.71$ ;  $r_2 = 0.63$  in 1,2-dichloroethane,  $r_1 = 1.04$ ;  $r_2 = 0.40$  in ethanol]. The reactivity ratios were obtained by Mayo-Lewis method which is not entirely reliable (vide supra). Further, the authors argue that penultimate effects in propagation step rather than

terminal effects might be operating making an interpretation of the observed reactivity ratios more difficult.

#### 4.1.2.3 Properties of the Cyclophosphazene Containing Copolymers

All the copolymers synthesized by Allen and Inoue discussed so far are flame retardant and thermally quite stable. The thermal stability increases with the increased cyclophosphazene content in the copolymer.

Although precise structure-property relationships are not known, Allen and coworkers relate the presence of phosphazene group in the copolymer to the increased thermal stability. Increased thermal stabilities are seen for copolymers derived from the monomers (8), (9) and (10). Thus a copolymer of styrene with (8) shows a char yield of 47% at 700°C whereas analogous copolymers derived from (1), (2) or 3 decompose completely by 500°C.

#### 4.1.2.4 Statement of the Problem Undertaken in this Thesis

As discussed in the preceding pages copolymerization studies of cyclophosphazene substituted organic monomers are limited to only five examples of which only three have been studied in some detail. Even these studies are limited to styrene as the comonomer. We thought it would be rewarding to explore this subject further and have chosen a cyclophosphazene monomer where the vinyl group is (a) sterically unencumbered in contrast to all the previous examples that have been studied and (b) separated from the cyclophosphazene by an effective spacer group in the form of a biphenyleneoxy unit.

We have chosen to study the copolymerization of (4) with styrene as well as acrylate monomers methylacrylate, ethylacrylate and methylmethacrylate. Further the nature of the homopolymer derived from (4) indicates that it is extremely stable to heat (at 800°C char yield is > 70%). In view of this, the

thermal properties of the copolymers would be expected to be interesting. Small amounts of (4) in copolymers are expected to incorporate large thermal stabilities and flame retardancy.

## 4.2 Experimental

### 4.2.1 Materials

Hexachlorocyclotriphosphazene, (Nippon soda, Japan) was recrystallized from hexane (mp 114°C) prior to use. 4-hydroxybiphenyl (Aldrich, USA and LOBA Chemicals, India), aluminium chloride, sodium borohydride, Zinc chloride (anhydrous). (S.D. Fine Chemicals, India), Trichloro acetic acid (Qualigens, India) were used without any further purification. Acetyl chloride (Qualigens, India) was distilled before use. The organic monomers, methylacrylate, methyl-methylacrylate, styrene (Fluka, Switzerland), Ethylacrylate (BDH, England) were washed twice with dil. NaOH solution followed by distilled water to remove the tert-Butyl Catechol inhibitor. The dried monomers were then distilled at reduced pressure and stored in the refrigerator. The monomers were added in drops to excess methanol or hexane to detect the presence of any polymer prior to use.<sup>29</sup> The organic solvents were distilled and dried with appropriate drying agents according to standard literature procedures.<sup>30</sup> The initiator AIBN, was recrystallized from methanol and vacuum dried before use.

### 4.2.2 Measurements

<sup>1</sup>H NMR spectra were obtained on Bruker WP80 and Bruker WM400 spectrophotometers operating at 80 MHz and 400 MHz respectively, using CDCl<sub>3</sub> as solvent and TMS as internal reference. <sup>31</sup>P NMR spectra were recorded on a Bruker WM400 spectrophotometer functioning at 135 MHz using CDCl<sub>3</sub> as solvent and 85% H<sub>3</sub>PO<sub>4</sub> as external reference. Infrared spectra were obtained on a



Perkin-Elmer FTIR 1600 series spectrophotometer using KBr pellets. Thermogravimetric analysis was obtained on a Shimadzu Thermal analyzer and a Cahn 2000 thermal analyzer in  $N_2$  atmosphere at a heating rate of  $10^\circ\text{C}/\text{min}$ . Gel permeation chromatography was carried out with a maxima 800 instrument using THF as solvent and polystyrene was used as the standard. The dilute solution viscosity studies were done with a Schott-Gerate viscometer using Ubbholde viscometer with a capillary pore size of 0.645 mm. The experiment was carried out at  $26^\circ\text{C}$  in dry benzene. The elemental analyses were done using Carl Erba 1108 elemental analyzer.

#### 4.2.3 Synthesis of 2-(4'-vinyl-4-biphenyloxy) Pentachlorocyclo triphosphazene (CPHVB)

##### 4.2.3.1 4-Acetoxy-4'-acetylbiphenyl (AAB)

4-hydroxybiphenyl (80.0 g, 0.47 mole) was added as solid in portions (5.0 g each) to an ice cold solution of acetyl chloride (110.0 g, 1.40 mol) and  $\text{AlCl}_3$  (160.0 g, 1.20 mol) in 500 ml of dichloromethane with stirring over a period of 30 minutes. The reaction mixture was further stirred for 3 hours at room temperature and then poured into ice cold water. The dichloromethane solution was separated, washed with water and dried over anhydrous sodium sulphate. After removing the dichloromethane, the solid residue obtained was recrystallized from methanol to give AAB (110.0 g, 96.7 %) mp  $124^\circ\text{C}$  (lit.  $124.5\text{--}126^\circ\text{C}$ )<sup>31</sup>.

$^1\text{H NMR}(\text{CDCl}_3)$  :  $\delta$ , 2.25 (3H,s, -  $\text{OCOCH}_3$ ); 2.55 (3H,s,  $\text{COCH}_3$ ); 6.9 - 7.8 (8H,m,aromatic)

##### 4.2.3.2 4-Hydroxy-4'-hydroxyethylbiphenyl (HEB)

To the stirred solution of AAB (20.0 g, 0.08 mol) in methanol (300 ml), sodium borohydride, (3.0 g, 0.08 mol) in the same solvent (100 ml) was added over a period of 20 minutes. The resulting mixture was stirred for another two hours

at room temperature. Most of the methanol was stripped off from the solution to yield an oil to which ethylacetate (300 ml) was added. This solution was washed with dil. hydrochloric acid (3x300ml) followed by water (3x300ml). After drying (anhyd.  $\text{Na}_2\text{SO}_4$ ) ethylacetate was removed *in vacuo* to give a solid mass. Recrystallization of this material from ethylacetate afforded pure HEB (16.0 g, 98%) m.p.  $145^\circ\text{C}$  (lit.  $145\text{--}146^\circ\text{C}$ )<sup>31</sup>.

$^1\text{H}$  NMR( $\text{CDCl}_3$ ) :  $\delta$ , 1.5 (3H, d,  $-\text{CH}_3$ ); 4.9 (1H, q,  $-\text{CH}$ ); 6.8 - 7.6 (8H, m, aromatic)

#### 4.2.3.3 4-Hydroxy-4'-vinyl biphenyl (HVB)

In a three necked RB flask, 150 ml of DMSO containing 20.0 g (0.09 mol) of HEB and 4.0 g (0.09 mol) of zinc chloride was heated to  $180^\circ\text{C}$  with stirring for 20 minutes. To this solution, 4.0 g (0.09 mol) of trichloro acetic acid was added in portions of 2.0 g and kept at the same temperature for an additional 3 minutes. After allowing the reaction mixture to come to room temperature it was poured into a large amount of water (~2 litres). A solid mass was obtained. It was allowed to settle and filtered. The precipitate was washed repeatedly with water and was dried at room temperature. It was then dissolved in dry acetone (200 ml) and extracted with hexane. Removal of hexane *in vacuo* from the extract afforded HVB as a semicrystalline solid. HVB was purified by recrystallizing from benzene at room temperature (12.0 g, 60%) m.p.  $192^\circ\text{C}$  (lit.  $191.5^\circ\text{C}$ )<sup>31</sup>

$^1\text{H}$  NMR ( $\text{CDCl}_3$ ,  $\text{DMSO}-d_6$ ) :  $\delta$ , 5.1 - 6.6 (3H,  $-\text{CH}=\text{CH}_2$ ) 6.8-7.5 (8H, aromatic)

#### 4.2.3.4 2-(4'-vinyl-4-biphenyloxy)pentachlorocyclotriphosphazene (CPHVB)

To a stirred solution of hexachlorocyclotriphosphazene,  $\text{N}_3\text{P}_3\text{Cl}_6$ , (10.6 g, 0.03 mol) in 100 ml of dry benzene a solution of HVB (6.0 g, 0.036 mol) and 4.0 ml

of triethylamine (0.04 mol) in dry benzene (100 ml), was added dropwise over a period of 30 minutes at room temperature. The resulting solution was stirred for an additional 4 hours. The amine hydrochloride formed in the reaction was removed by filtration. The solvent benzene was stripped off from the filtrate under reduced pressure to give an oil. The oil was subjected to column chromatography (silica gel 60-120 mesh) using hexane as the eluant. After collecting the unreacted  $N_3P_3Cl_6$  as the first fraction, the product CPHVB was collected and recrystallized from hexane to give pure CPHVB (m.p  $112^{\circ}C$ ) yield 40% (lit. 45%)<sup>15</sup>

IR ( $cm^{-1}$ ) : 1600.1 (m); 1521.5(m); 1492.0(s); 618.6(s); 590.8(vs);  
 (KBr pellet) 1212.0 (vs); 1017.6(s); 969.6(s); 528.5(vs); 464.78(s);  
 916.0(s); 891.9(s); 871.0(s); 826.0(s); 781.7(s); 746.1(s);  
 663.6(s); 644.1(s)

$^1H$  NMR( $CDCl_3$ ) :  $\delta$ , 5.28 (dd, =  $CH_2$ ), 5.75 (dd, =  $CH_2$ ) 6.78 (dd, -  $CH$  = ),  
 7.2-7.68 (m, aromatic)

$^{31}P$  NMR( $CDCl_3$ ) :  $\delta$ , 20.8 ( d,  $\equiv P \begin{smallmatrix} Cl \\ OR \end{smallmatrix}$  ); 10.62 ( t,  $\equiv P \begin{smallmatrix} Cl \\ Cl \end{smallmatrix}$  )

Mass spectrum (electron impact) : 507 ( $m^+/e$ )

#### 4.2.3.5 Copolymerization of CPHVB with Methylacrylate

The monomers CPHVB (1.0 g, 1.97 mmol) and methylacrylate (0.2 g, 2.30 mmol) in 20 ml of the solvent dichloromethane were placed in a polymerization tube along with 2% AIBN. The tube was fitted with a reflux condenser and nitrogen was bubbled through the solution for 45 minutes. Then the tube was kept in an oil bath which was maintained at  $70^{\circ} \pm 0.1^{\circ}C$  for 3 hours. The polymerization tube was kept under a positive pressure of  $N_2$  throughout. After cooling to room

temperature the reaction mixture was poured into an excess of hexane (1000 ml). The precipitated residue was filtered and reprecipitated twice using dichloromethane as solvent and hexane as non solvent. Finally, the solid material was dried in vacuum to afford 0.12 g (10.1%) of the copolymer, (CPHVB-MA-1).

Different initial feeds of the two monomers were used to get different copolymers. The data are tabulated (Table 4.3). Using a similar procedure as above, the copolymers of CPHVB with ethylacrylate, methyl methacrylate and styrene have been synthesized. The detailed experimental conditions are given in Tables 4.4, 4.5 and 4.6 respectively.

---

**Table 4.3 Experimental details of the copolymerization of CPHVB with methylacrylate.**

Copolymer Code	CPHVB (g)	MA (g)	Amount of Polymer (g)	wt % conversion
CPHVB-MA-(1)	0.9979	0.2010	0.1214	10.13
CPHVB-MA-(2)	0.9920	0.5385	0.3723	24.33
CPHVB-MA-(3)	1.5304	0.2233	0.2362	13.47
CPHVB-MA-(4)	1.1571	0.0805	0.0428	3.46
CPHVB-MA-(5)	1.0240	0.4986	0.2972	16.99
CPHVB-MA-(6)	0.9988	1.3193	0.8338	35.97
CPHVB-MA-(7)	1.1192	0.2033	0.1507	11.31
CPHVB-MA-(8)	1.1087	1.4601	0.2073	8.07
CPHVB-MA-(9)	1.0289	0.5659	0.0722	4.54
CPHVB-MA-(10)	1.5852	0.2708	0.1259	6.78

**Table 4.4 Experimental details of the copolymerization of CPHVB with Ethylacrylate**

Copolymer Code	CPHVB (g)	EA (g)	Amount of Polymer (g)	wt % conversion
CPHVB-EA-(1)	1.0104	0.2048	0.0106	0.87
CPHVB-EA-(2)	1.012	0.4151	0.0306	2.14
CPHVB-EA-(3)	1.0010	0.7929	0.6313	36.31
CPHVB-EA-(4)	1.0027	0.1012	0.1024	9.28
CPHVB-EA-(5)	0.8896	0.7268	0.3574	22.11
CPHVB-EA-(6)	0.9401	0.0447	0.1148	11.66
CPHVB-EA-(7)	0.8234	0.4115	0.0121	0.98
CPHVB-EA-(8)	0.8352	0.3704	0.0840	6.97
CPHVB-EA-(9)	0.5933	0.2202	0.0714	8.78
CPHVB-EA-(10)	0.5524	0.4066	0.0766	7.99

**Table 4.5 Experimental details of the copolymerization of CPHVB with Methylmethacrylate**

Copolymer Code	CPHVB (g)	MA (g)	Amount of Polymer (g)	wt % conversion
CPHVB-MMA(1)	1.0140	0.2148	0.2223	18.09
CPHVB-MMA(2)	1.0213	0.1161	0.0402	3.53
CPHVB-MMA(3)	1.5188	0.1069	0.0882	5.43
CPHVB-MMA(4)	0.5054	0.3040	0.0692	8.55
CPHVB-MMA(5)	0.5092	0.5035	0.3185	31.45
CPHVB-MMA(6)	0.5084	0.2321	0.0366	4.94
CPHVB-MMA(7)	0.5001	0.5081	0.1275	12.65
CPHVB-MMA(8)	0.5149	0.1166	0.1823	28.87
CPHVB-MMA(10)	0.7974	0.2818	0.0723	6.70
CPHVB-MMA(11)	0.8176	0.1535	0.0924	9.52
CPHVB-MMA(12)	0.8215	0.3115	0.0852	7.51

**Table 4.6 Experimental details of the copolymerization of CPHVB with Styrene**

Copolymer Code	CPHVB (g)	MA (g)	Amount of Polymer (g)	wt % conversion
CPHVB-STY(1)	1.0157	0.2408	0.0416	3.31
CPHVB-STY(2)	1.010	0.1125	0.0866	3.72
CPHVB-STY(3)	0.5206	0.4000	0.1917	20.82
CPHVB-STY(4)	0.5064	0.3208	0.0219	2.65
CPHVB-STY(5)	1.0417	0.0878	0.5438	48.15
CPHVB-STY(6)	0.7933	0.5015	0.2795	21.59
CPHVB-STY(7)	1.0100	0.0698	0.2537	23.50
CPHVB-STY(8)	0.4972	0.5685	0.0956	8.97
CPHVB-STY(9)	0.8478	0.1963	0.0143	2.53
CPHVB-STY(10)	0.8139	0.3120	0.0131	3.24

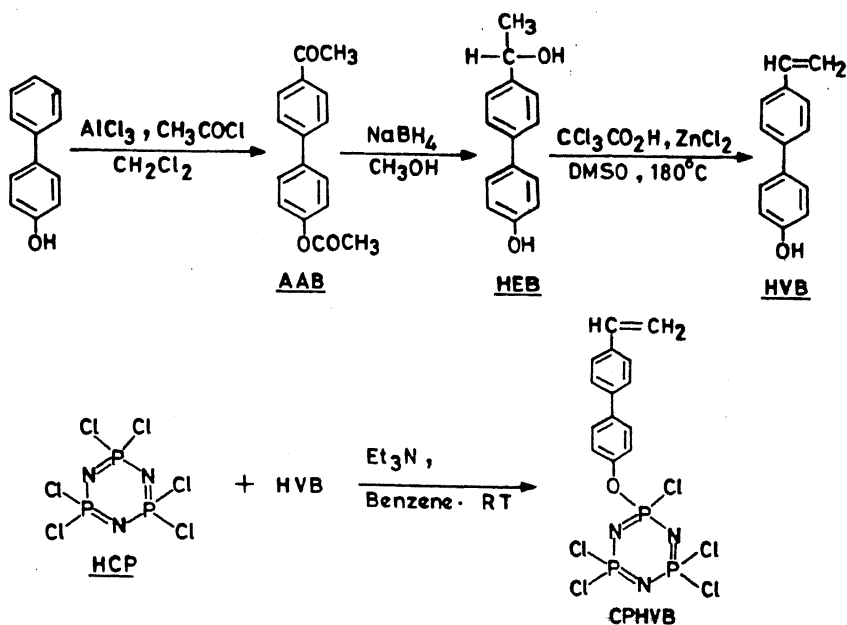
### 4.3 Results and Discussion

#### 4.3.1 Synthesis of $N_3P_3Cl_5$ ( ), CPHVB (4)

The synthesis of monomer, CPHVB, has been carried out according to the scheme shown below.

The first two steps leading to the formation of AAB and HEB are straightforward and quantitative yields are obtained. However, the conversion of HEB to HVB is tricky, and requires stringent experimental conditions. We have found that the purity of the reagents involved viz., zinc chloride, trichloroacetic acid, and DMSO is extremely crucial and has a bearing on the final yields. Particularly care was taken to free these reagents of last traces of moisture. Unlike p-hydroxy styrene which polymerizes even at room temperature, pure HVB is resistant to autopolymerization.

CPHVB was prepared by a stoichiometric reaction of  $N_3P_3Cl_6$  with HVB in presence of triethyl amine which acts as a hydrogen chloride acceptor. Since



$N_3P_3Cl_6$  contains six replaceable chlorines, often mixtures of products are obtained in this reaction necessitating the use of column chromatography to separate pure CPHVB, (Expt. 4.2.3.4). It was observed that long residence times on the column have to be prevented to avoid polymerization of the cyclophosphazene monomers on the silica gel column. Once separated and purified (recrystallization), CPHVB is very stable and can be stored indefinitely in an atmosphere of  $N_2$ . CPHVB is soluble in almost all organic solvents varying from hexane to DMSO.

The  $^{31}P \{^1H\}$  NMR of CPHVB is of the  $AB_2$  type indicating the presence of two different types of phosphorus nuclei. The doublet at 20.8 ppm is assigned to  $\equiv PCl_2$  and the triplet at 10.62 ppm to  $\equiv PCl(OR)$ , (Fig. 4.2). These chemical shift assignments are consistent with literature reports<sup>31</sup>. Further, both

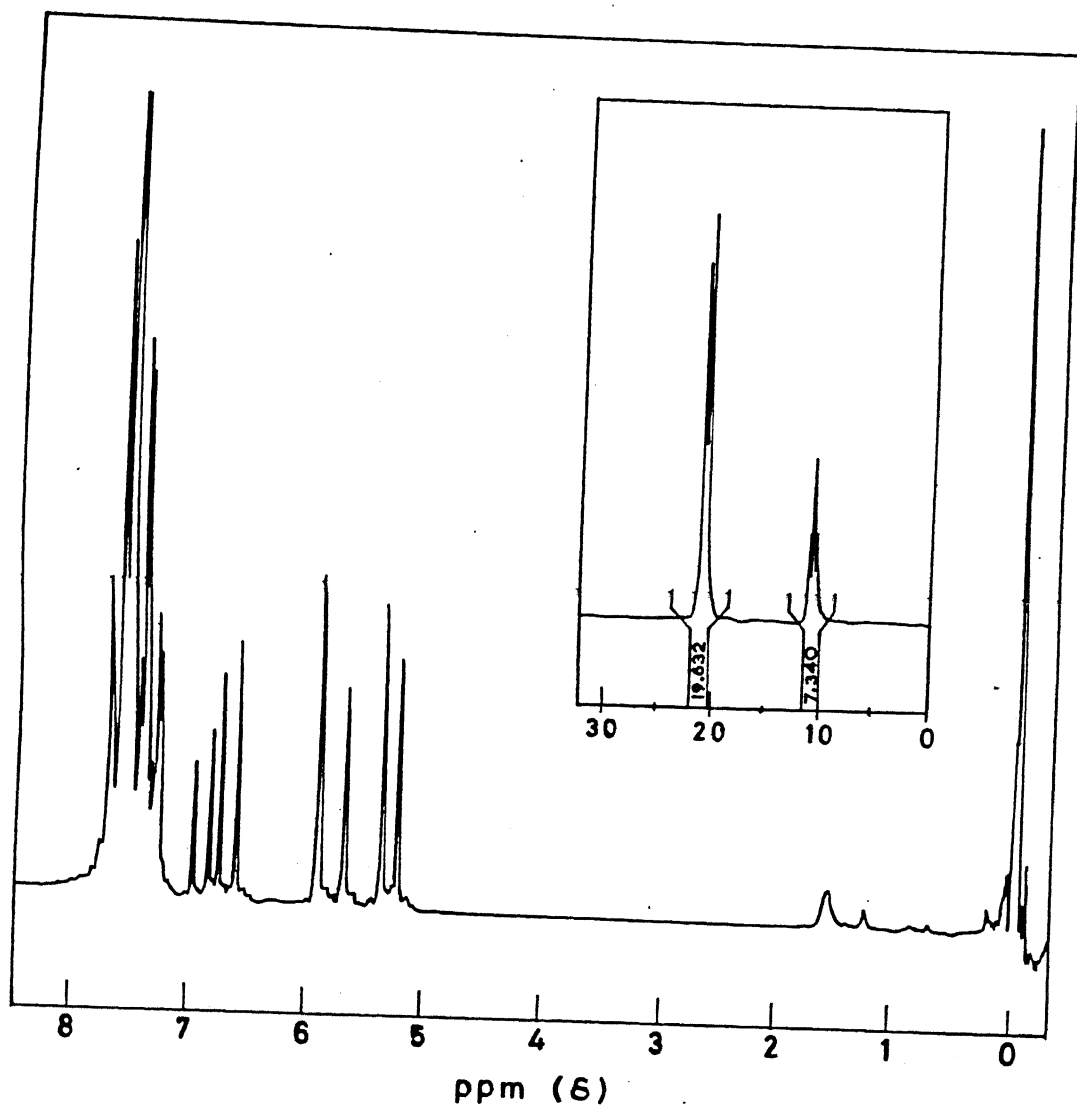


Fig.4.2.  $^1\text{H}$  NMR (400 MHz) spectrum of the monomer, CPHVB.

(Inset)  $^{31}\text{P}$   $\{^1\text{H}\}$  NMR (137 MHz) spectrum of CPHVB.



chemical analysis and mass spectral data confirm the molecular formula of CPHVB (4). The  $^1\text{H}$  NMR of CPHVB clearly shows an ABX type of multiplet for the vinyl protons (Fig. 4.2).

#### 4.3.2 Synthesis of Copolymers

CPHVB could be copolymerized readily with acrylates such as methylacrylate; ethylacrylate, methylmethacrylate and styrene at  $70^\circ\text{C}$  in dichloroethane in  $\text{N}_2$  atmosphere (Fig 4.3). Tables 4.3, 4.4, 4.5, 4.6 summarize the details of the

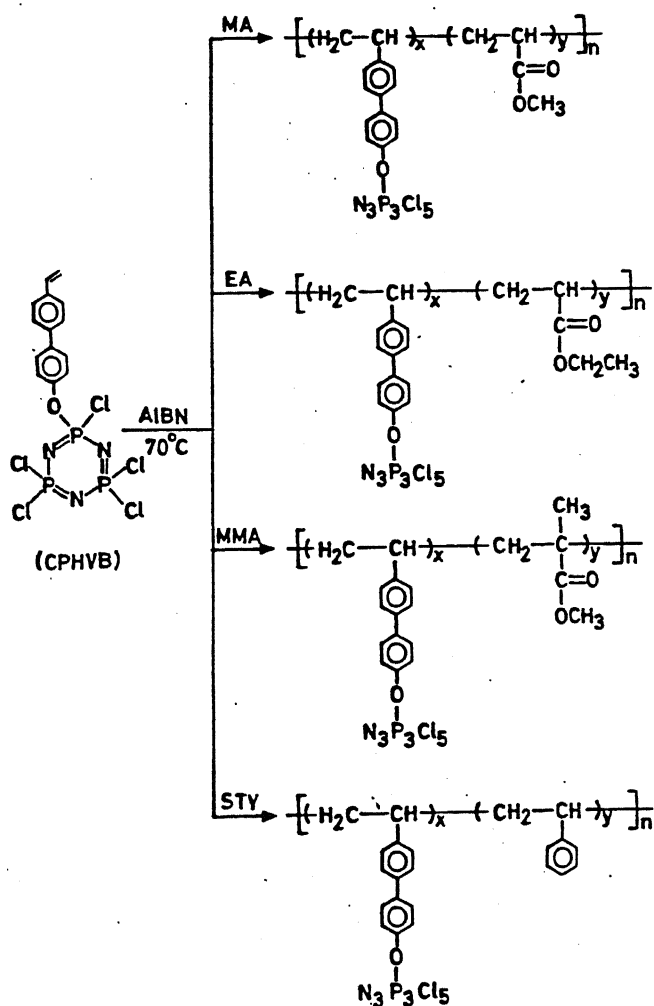


Fig. 4.3.

Copolymerization of CPHVB with methylacrylate, ethylacrylate, methylmethacrylate, and styrene.

experimental conditions and Tables 4.7, 4.8, 4.9, 4.10 give the composition and conversion data.  $^1\text{H}$  NMR is used to find out the percent incorporation of the monomer CPHVB in the copolymers. No cross linked products were obtained in any experiments. The maximum incorporation of CPHVB in the copolymer is 93%. This is the maximum incorporation of any cyclophosphazene monomer in the copolymer known in the literature. Attempts were made such that low copolymer conversions were obtained so that the data could be used in the evaluation of reactivity ratios. All the copolymers obtained were isolated as white powders and were found to be soluble in a variety of organic solvents such as benzene, dichloromethane, THF etc., but were found to be insoluble in solvents like hexane, water and methanol. The copolymers are quite stable to moisture and have long shelf lives.

---

**Table 4.7 Composition and conversion data for CPHVB-MA copolymers  
used for reactivity ratio calculations**

Copolymer code	CPHVB (mol %)		Conversion (wt%)
	Feed	Polymer	
CPHVB-MA (1)	45.72	70.80	10.13
CPHVB-MA (2)	23.80	55.56	24.33
CPHVB-MA (3)	53.76	78.48	13.47
CPHVB-MA (4)	70.92	82.53	3.47
CPHVB-MA (5)	25.84	57.00	16.99
CPHVB-MA (6)	11.38	32.85	35.97
CPHVB-MA (7)	48.29	79.83	11.31
CPHVB-MA (8)	11.41	39.78	8.07
CPHVB-MA (9)	23.57	40.24	4.53
CPHVB-MA (10)	49.83	78.95	6.78

**Table 4.8 Composition and conversion data for CPHVB-EA copolymers used for reactivity ratio calculations**

Copolymer code	CPHVB (mol %)		Conversion (wt%)
	Feed	Polymer	
CPHVB-EA (1)	49.33	70.09	0.87
CPHVB-EA (2)	32.48	64.52	2.14
CPHVB-EA (3)	19.94	50.17	36.31
CPHVB-EA (4)	66.16	81.18	9.28
CPHVB-EA (5)	19.45	51.56	22.11
CPHVB-EA (6)	80.58	88.89	11.66
CPHVB-EA (7)	41.80	49.56	0.98
CPHVB-EA (8)	28.30	55.93	6.97
CPHVB-EA (9)	34.71	38.84	8.78
CPHVB-EA (10)	21.14	56.41	7.99

**Table 4.9 Composition and conversion data for CPHVB-MMA copolymers used for reactivity ratio calculations**

Copolymer code	CPHVB (mol %)		Conversion (wt%)
	Feed	Polymer	
CPHVB-MMA(1)	48.22	74.82	18.09
CPHVB-MMA(2)	63.44	88.13	3.53
CPHVB-MMA(4)	24.70	55.52	8.55
CPHVB-MMA(6)	30.17	59.97	4.94
CPHVB-MMA(7)	16.26	42.06	12.65
CPHVB-MMA(8)	46.56	93.16	28.87
CPHVB-MMA(9)	44.42	69.62	22.78
CPHVB-MMA(10)	35.82	72.46	6.70
CPHVB-MMA(11)	51.24	84.16	9.52
CPHVB-MMA(12)	34.22	70.91	7.51

**Table 4.10 Composition and conversion data for CPHVB-STY copolymers used for reactivity ratio calculations**

Copolymer code	CPHVB (mol %)		Conversion (wt%)
	Feed	Polymer	
CPHVB-STY(1)	46.40	50.70	3.31
CPHVB-STY(2)	64.82	37.81	7.72
CPHVB-STY(3)	21.08	29.66	20.82
CPHVB-STY(4)	24.47	28.65	2.65
CPHVB-STY(5)	70.89	90.42	48.15
CPHVB-STY(6)	24.51	31.93	21.59
CPHVB-STY(7)	74.81	87.44	23.50
CPHVB-STY(9)	46.99	60.50	2.53
CPHVB-STY(10)	34.87	44.65	3.24

### 4.3.3 Characterization of CPHVB Copolymers

Table 4.11 summarizes the IR spectral data for representative copolymers of CPHVB along with CPHVB. Representative IR spectrum of one copolymer from each system is given in Fig. 4.4. Two features merit attention.

- (i) In CPHVB as well as in the copolymers the (P=N) stretching frequency is retained and is found within a narrow range (1185 - 1213  $\text{cm}^{-1}$ ) indicating that the cyclophosphazene ring is probably intact and is retained in the copolymers. This fact has been confirmed by  $^{31}\text{P}$  NMR studies on the copolymers (vide infra).
- (ii) In the acrylate copolymers strong peaks due to C = O stretch are seen (Table 4.11).

The comparison of  $^1\text{H}$  NMR of CPHVB and the copolymers (Fig. 4.5) clearly reveals the disappearance of the olefinic multiplet in the copolymers and the appearance of the new signals due to alkyl groups. The  $^{31}\text{P}$  NMR spectral data of selected copolymers are listed in Table 4.12 and the spectra are given in Fig. 4.6. The chemical shift values observed for the copolymers clearly and unambiguously prove that the original cyclophosphazene moiety is retained in the copolymers without any modification. It is to be noted that linear polyphosphazenes containing the  $\text{--P--N--}$  back bone generally show chemical shift values which are upfield to 85%  $\text{H}_3\text{PO}_4$ . Secondly, in all the cases the  $^{31}\text{P}$  NMR spectrum is of  $\text{AB}_2$  type indicating that cyclophosphazene ring suffers no change in the copolymers.

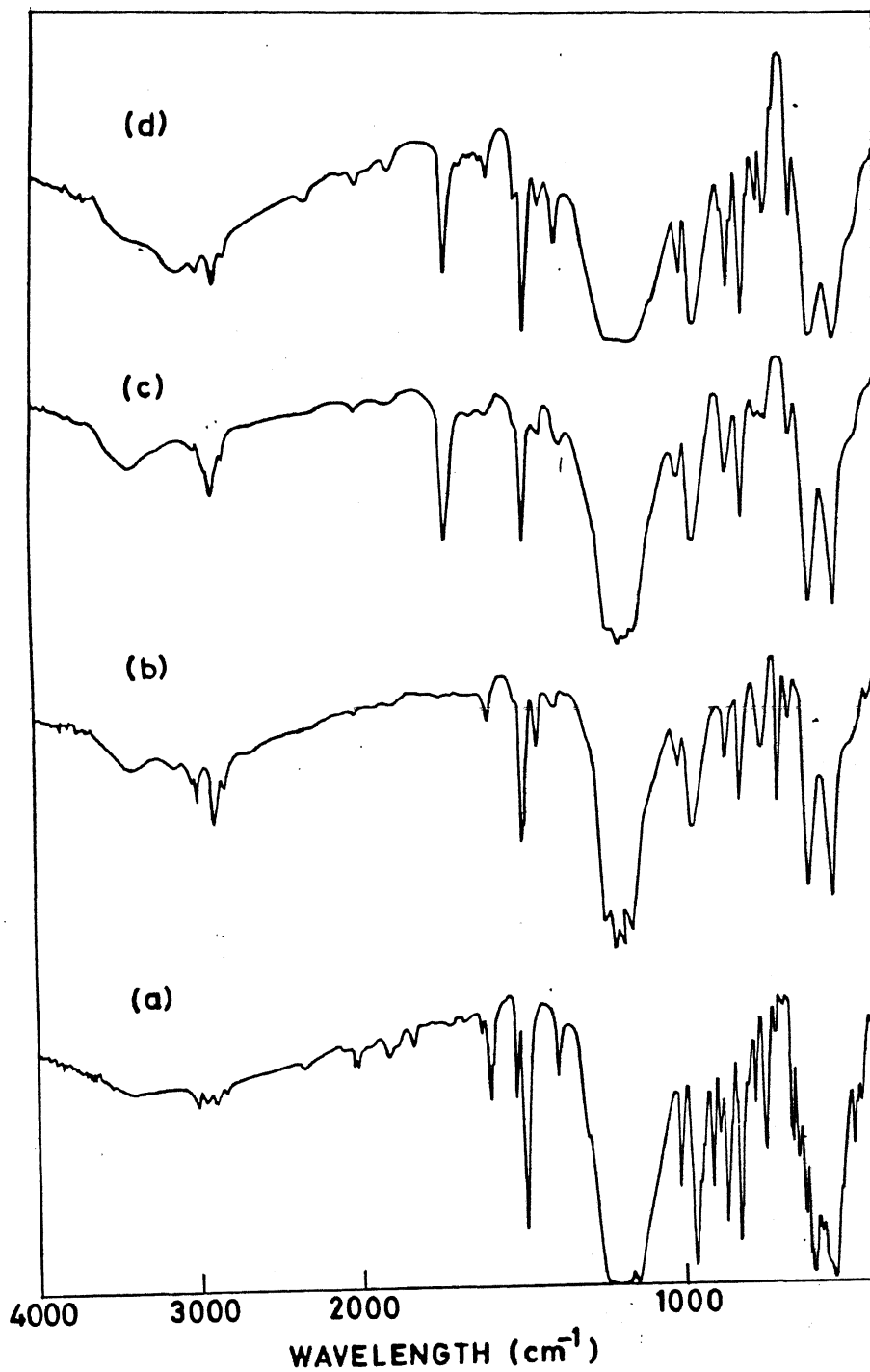
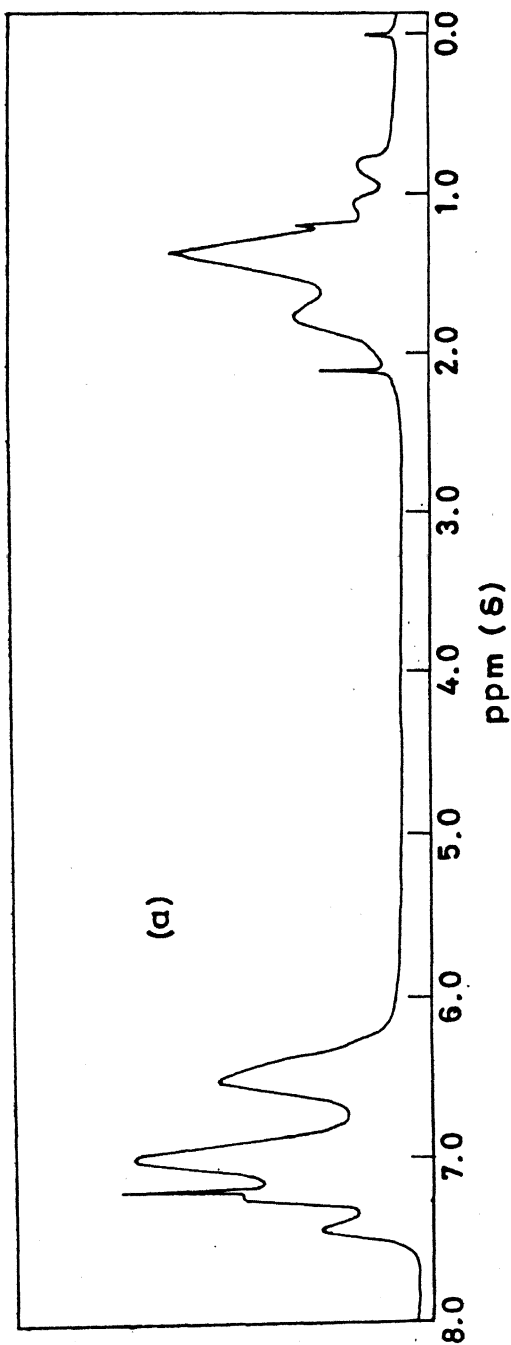
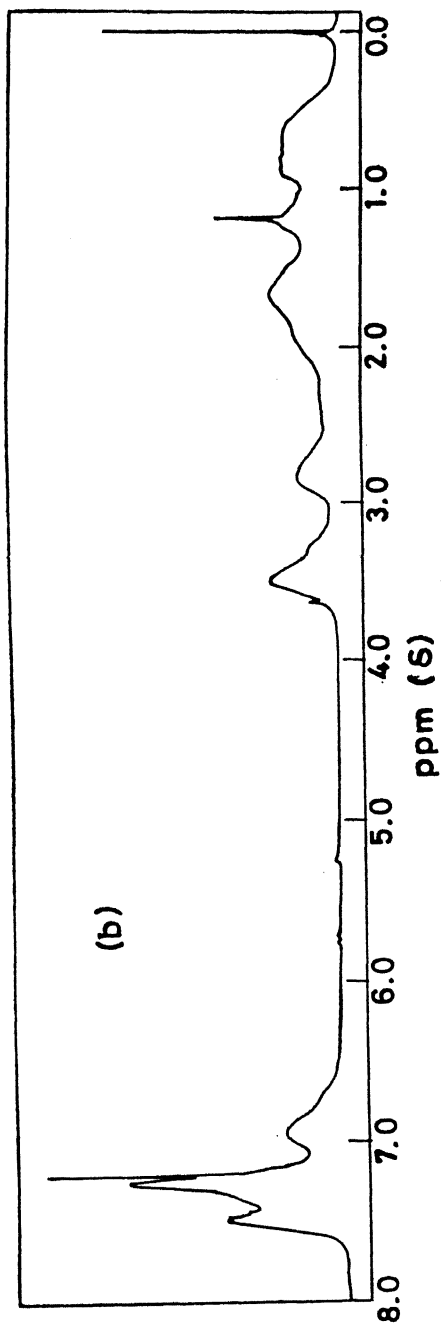


Fig.4.4.

IR spectra of selected copolymers: (a) CPHVB monomer; (b) CPHVB-STY-6;  
(c) CPHVB-EA-8; (d) CPHVB-MA-6.



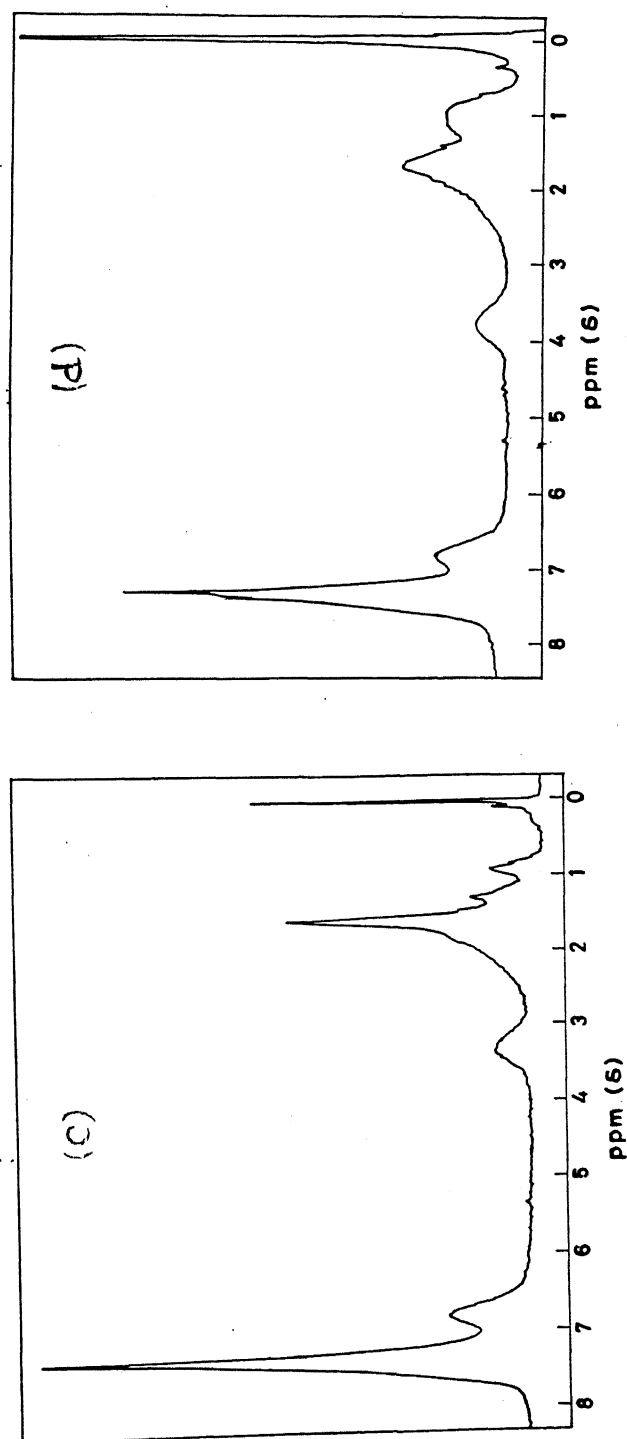


Fig. 4.5.  $^1\text{H}$  NMR (400 MHz) spectra of selected copolymers: (a) CPHVB-STY-3; (b) CPHVB-MMA-6; (c) CPHVB-MA-1; (d) CPHVB-EA-2.

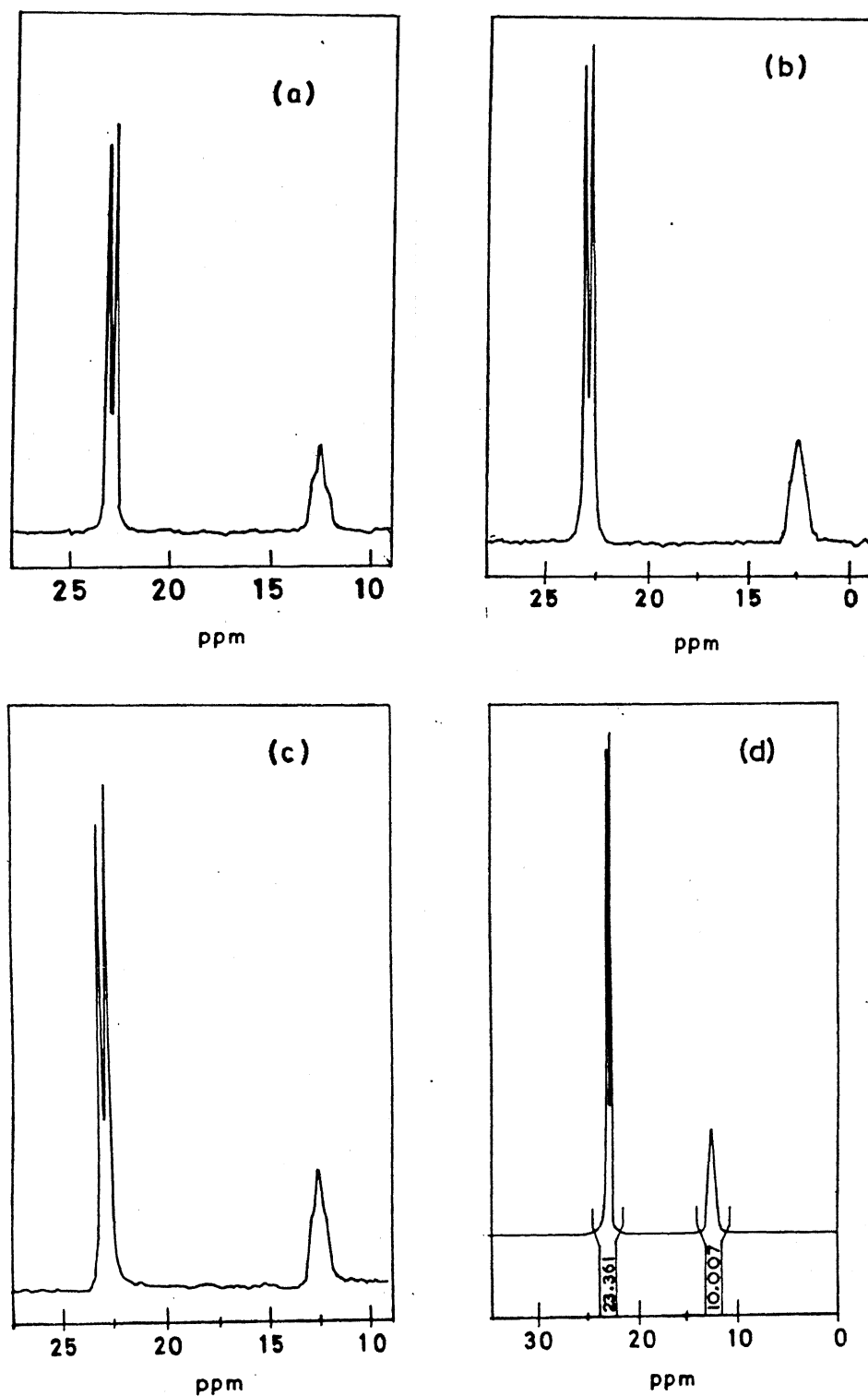


Fig.4.6.

$^{31}\text{P}$  NMR ( $^1\text{H}$ ) NMR (137 MHz) spectra of selected copolymers: (a) CPHVB-MA-1; (b) CPHVB-MMA-6; (c) CPHVB-STY-7; (d) CPHVB-EA-4.



Table 4.11

Copolymer	$\nu_{\text{P}=\text{N}}$ ( $\text{cm}^{-1}$ )	$\nu_{\text{C}=\text{O}}$ ( $\text{cm}^{-1}$ )
CPHVB	1212.7 (vs)	---
CPHVB-MA(7)	1184.8 (vs)	1732.4 (s)
CPHVB-EA(8)	1209.2 (vs)	1729.0 (s)
CPHVB-STY(6)	1211.7 (vs)	---
CPHVB-MMA(8)	1210.7 (vs)	1728.1 (m)

Table 4.12

Copolymer	Chemical shift values $\text{AB}_2$ type, (ppm)
CPHVB	20.8(d), 10.62(t)
CPHVB-MA(1)	22.8(d), 12.46(t)
CPHVB-EA(4)	22.8(d), 12.47(t)
CPHVB-MMA(8)	22.9(d), 12.54(t)
CPHVB-STY(7)	22.8(d), 12.43(t)

#### 4.3.4 Thermal Analysis

Thermogravimetric analysis of the copolymers reveal that CPHVB containing polymers are extremely stable. Table 4.13 summarizes the thermal data of selected copolymers. Figure 4.7 gives the thermal analysis curves for selected samples. The main features of the TGA studies can be summarized as follows :

(a) In comparison with the homopolymer derived from CPHVB, CPHVB containing copolymers are less stable thermally; the former has a char yield of 67% at  $800^{\circ}\text{C}$  whereas the latter in various compositions show a char yield of atleast 54-68% at  $600^{\circ}\text{C}$  (Table 4.13)

(b) The CPHVB containing copolymers (CPHVB-MA, CPHVB-EA, CPHVB-MMA and CPHVB-STY) are more stable than any previous organic polymers containing cyclophosphazene pendant groups. Thus for example styrene copolymers containing  $\text{N}_3\text{P}_3\text{F}_5$  ( $\text{C}^{\text{OEt}}=\text{CH}_2$ ) and  $\text{N}_3\text{P}_3\text{F}_5$  ( $\text{O}-\text{C}_6\text{H}_4-\text{C}^{\text{Me}}=\text{CH}_2$ ) are much less stable (char yields, < 10% at around  $450^{\circ}\text{C}$ ).

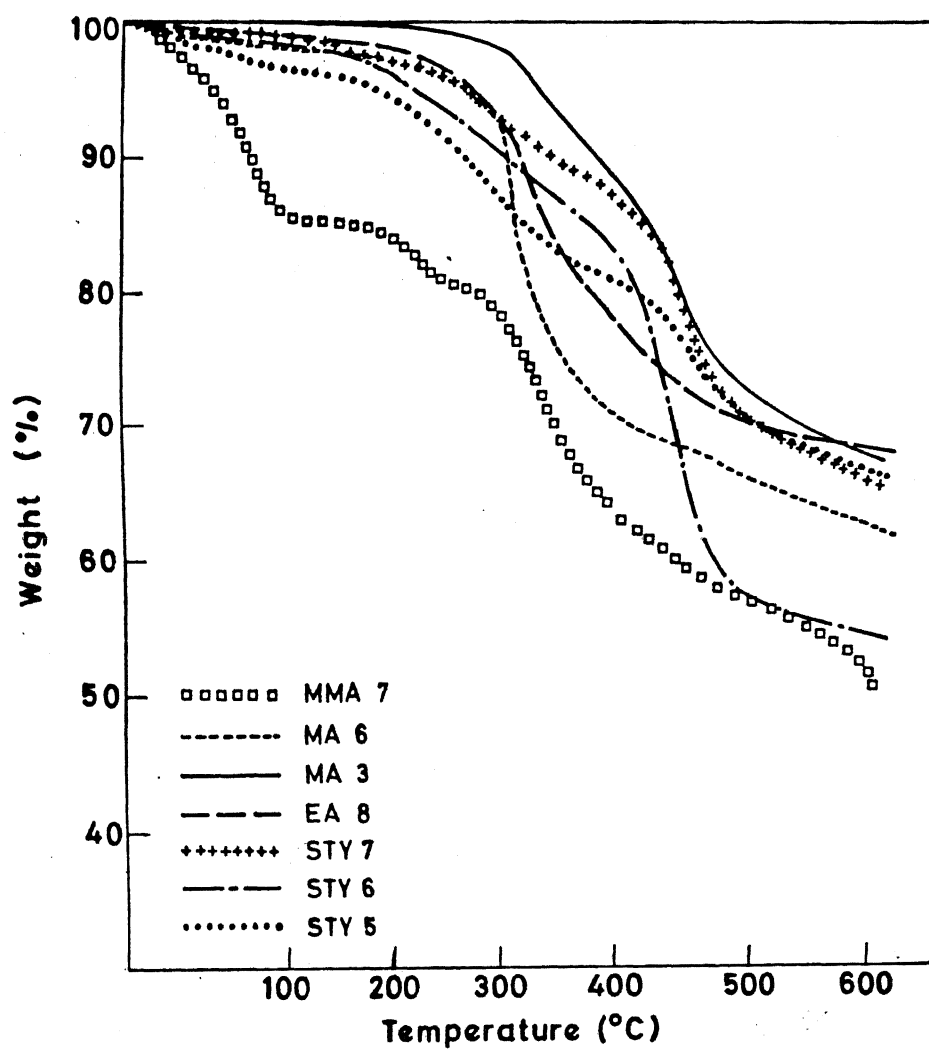


Fig.4.7. Thermograms obtained for selected copolymers.

- (c) Only small amounts of CPHVB incorporation in the organic polymers can lead to dramatic thermal stabilities. Thus CPHVB-MA, (6) which has only 32.85% of CPHVB has a char residue of 62% at 600°C. However, there is no linear relationship between the thermal stability imparted and the extent of CPHVB incorporation.
- (d) All the thermal decompositions of the CPHVB copolymers reveal that in general there is no change or decomposition upto 300°C and beyond that they show a single or two step decompositions (Fig. 4.7).

Infrared spectra of chars obtained from CPHVB-MA, CPHVB-EA, CPHVB-MMA, and CPHVB-STY show the complete absence of  $C = O$  along with  $P = N$  stretching frequencies (Fig. 4.8).

In addition to TGA studies simple flame tests were conducted on all the copolymers containing CPHVB. All of these are flame retardant. When soaked in a flammable solvent such as petroleum ether and burned against a spirit lamp blue flame the copolymers act as self extinguishers.

It is clear that the incorporation of the hydroxy vinylbiphenyl on the cyclophosphazene moiety imparts excellent thermal stabilities to the resulting polymers. It is to be noted that the homopolymer derived from hydroxy vinyl phenyl (HVB) itself or copolymers of HVB are not that thermally stable (Table 4.13). Evidently, the char contains highly stable aromatic rings containing P and N. The nature of the materials (insolubility in common organic solvents) precluded any attempts at their characterizations.

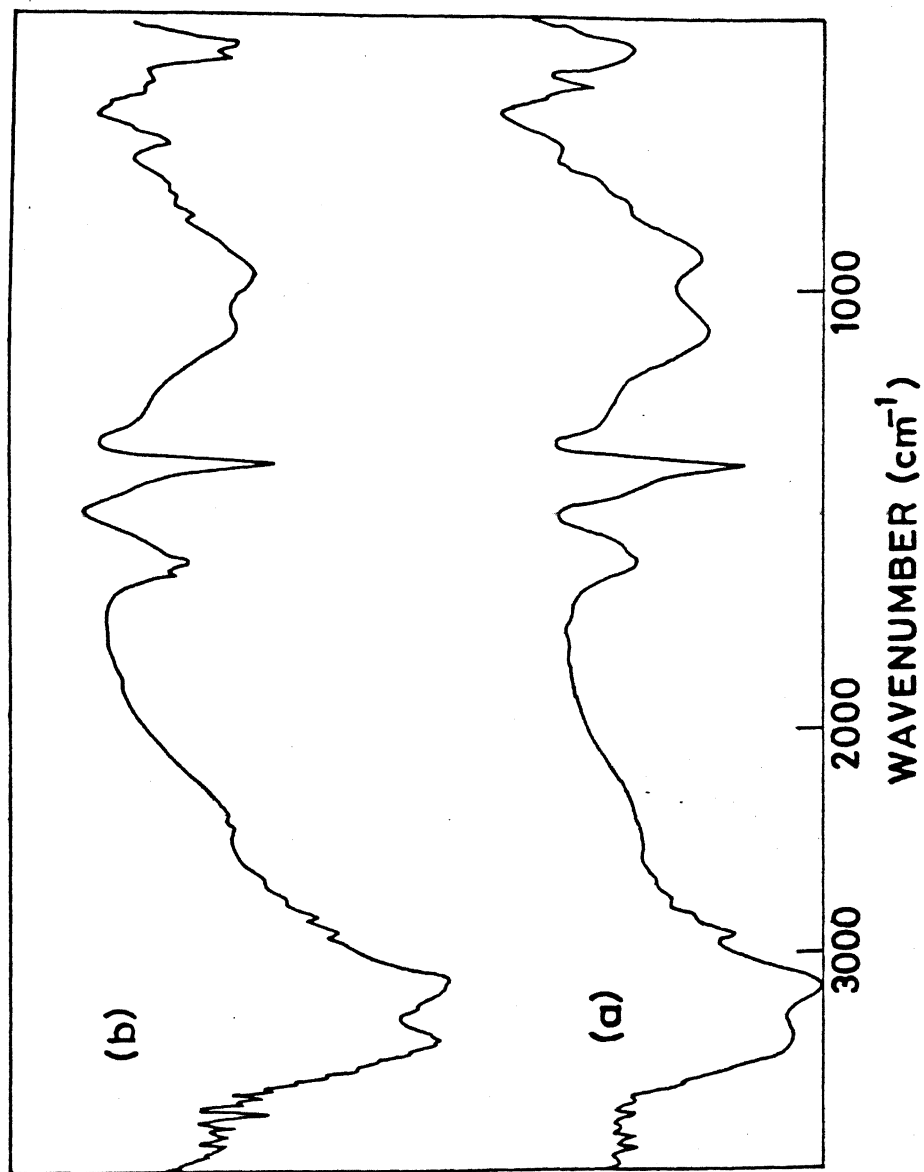


Fig.4.8. IR spectra of chars obtained from thermogravimetric analysis of samples: (a) CPHVB-EA-4 and (b) CPHVB-MMA-8.

Table 4.13

Copolymer	Cyclophosphazene content in Copolymer (wt%)	PDT*	Char Yield% (600°C)	T <sub>g</sub> * (°C)	Ref.
CPHVB-MA(3)	78.5		67	91.3	Present work
CPHVB-MA(5)	57.0		69	92.4	- do -
CPHVB-MA-6	32.9		62	86.0	- do -
CPHVB-EA-8	35.9		68	103.5	- do -
CPHVB-EA-B1	76.7		70	----	- do -
CPHVB-MMA-7	61.5		65	85.2	- do -
CPHVB-MMA-8	87.8		67	----	- do -
CPHVB-STY-3	29.7		56	----	- do -
CPHVB-STY-5	90.4		67	119.8	- do -
CPHVB-STY-6	31.9		54	114.7	- do -
CPHVB-STY-7	87.4		66	----	- do -
CPHVB (homopolymer)	100	300	65	----	16
2-STY	42.5	200	50 <sup>(a)</sup>	----	13
3-STY	31.9	295	50 <sup>(b)</sup>	93.0	14
8-STY	44.0	230	47 <sup>(c)</sup>	----	18
a = at 350°C      b = at 410°C      c = at 700°C * — pre decomposition temperature, # DTA reported for selected samples					

#### 4.3.5 Molecular Weight Measurements

##### 4.3.5.1 Dilute Solution Viscosity

Due to lack of instrumental facility we did not attempt obtaining absolute molecular weights by methods such as light scattering or vapour pressure osmometry, instead dilute solution viscosity measurements were carried out on all the copolymer samples and the viscosity obtained give an indication of the relative molecular weights involved.

The copolymer solutions (1%) were prepared using dry benzene as solvent and introduced into an Ubbelohde viscometer. The flow time from the viscometer

was measured for the initial charge of polymer solution. The charge was then diluted and the flow time remeasured. In this way, the flow times were obtained at four or five concentration levels for each copolymer containing varied cyclophosphazene content. The relative viscosity, may be given in terms of  $\eta$ , the viscosity of the solution and  $\eta_0$ , the viscosity of the solvent; and hence in terms of the viscometer flow times,  $t$  and  $t_0$ .

$$\eta_r = \frac{\eta}{\eta_0} = \frac{t}{t_0}$$

Here,  $t$  and  $t_0$  are the flow time of solution and solvent respectively at a particular concentration. The relative viscosity is always greater than unity because the presence of the polymeric solute always increases the viscosity.

The specific viscosity,  $\eta_{sp}$ , is defined as the fractional increase in viscosity caused by the presence of dissolved polymer in the solvent, given by

$$\eta_{sp} = \frac{\eta - \eta_0}{\eta_0} = \eta_r - 1$$

The specific viscosity and the relative viscosity depend on the concentration of the polymer in solution. They increase with increasing concentration.

The reduced viscosity is a measure of the specific capacity of the polymer to increase the relative viscosity which can be expressed as follows :

$$\eta_{red} = \frac{\eta_{sp}}{c} \text{ cm}^3 \text{ g}^{-1}$$

Finally from a set  $\eta_{red}$  values for a particular polymer the intrinsic viscosity is calculated defined as the limit of the reduced viscosity as the concentration approaches zero and is given by

$$[\eta] = \lim_{C \rightarrow 0} \left[ \frac{\eta_{sp}}{C} \right]$$

$\eta_{red}$  and  $[\eta]$  have the dimensions of a specific volume i.e.,  $\text{cm}^3 \text{ g}^{-1}$ .

Table 4.14 summarizes all the viscosity values of CPHVB copolymers. Fig 4.9, 4.10, 4.11 and 4.12 show the plots of reduced viscosity vs concentration for CPHVB copolymers, CPHVB-MA, CPHVB-EA, CPHVB-MMA, CPHVB-Styrene respectively. Table 4.15 summarizes the intrinsic viscosity values of selected copolymers.

Table 4.14

Copolymer	$\eta_r$	$\eta_{sp}$	$\eta_{red}$ (g/cc)	concentration (g/100ml)
CPHVB-MA-B3	1.0437	0.0437	5.42	0.8058
	1.0247	0.0247	3.74	0.6608
	1.0173	0.0173	3.37	0.5154
	1.0404	0.0404	3.95	1.0236
	1.0120	0.0120	2.83	0.4256
CPHVB-EA-3	1.0826	0.0826	8.03	1.0040
	1.0570	0.0570	7.10	0.8032
	1.0350	0.0350	5.32	0.6586
	1.0237	0.0237	4.52	0.5242
	1.0168	0.0168	4.12	0.4089
CPHVB-MA-B-3	1.0745	0.0745	8.03	0.9278
	1.0608	0.0608	8.19	0.7422
	1.0469	0.0469	7.80	0.6012
	1.0359	0.0359	7.47	0.4810
	1.0263	0.0263	7.40	0.3559
CPHVB-MA-B4	1.0798	0.0798	7.33	1.0892
	1.0514	0.0514	5.76	0.8931
	1.0413	0.0413	6.00	0.6877
	1.0296	0.0296	6.09	0.4855
	1.0187	0.0187	5.00	0.3738
CPHVB-EA-B-1	1.0859	0.0859	8.58	1.0012
	1.0727	0.0727	8.67	0.8390
	1.0512	0.0512	8.35	0.6125
	1.0389	0.0389	8.13	0.4777
CPHVB-EA-B-2	1.1267	0.1267	10.42	1.2164
	1.0987	0.0987	10.15	0.9731
	1.0891	0.0891	9.91	9.0000
	1.0586	0.0586	9.30	0.6321

Table 4.14 (continued...)

Copolymer	$\eta_r$	$\eta_{sp}$	$\eta_{red}$	concentration (g/100ml)
CPHVB-MMA-B1	1.0833	0.0833	7.38	1.1288
	1.0564	0.0564	6.94	0.8127
	1.0484	0.0484	7.18	0.6746
	1.0408	0.0408	7.08	0.5789
	1.0315	0.0315	6.80	0.4630
CPHVB-MMA-B2	1.0662	0.0662	6.12	1.0821
	1.0525	0.0525	5.82	0.9012
	1.0339	0.0339	5.44	0.6236
	1.0365	0.0365	5.85	0.7541
	1.0253	0.0253	5.44	0.5652
CPHVB-MMA-B3	1.0643	0.0643	6.19	1.0024
	1.0507	0.0507	5.54	0.9155
	1.0437	0.0437	5.62	0.7784
	1.0403	0.0403	5.80	0.6952
	1.0265	0.0265	4.95	0.5351
CPHVB-STY-B1	1.0889	0.0889	8.68	1.0246
	1.0701	0.0701	8.24	0.8502
	1.0569	0.0569	7.65	0.7440
	1.0423	0.0423	7.29	0.5796
	1.0320	0.0320	6.84	0.4676
CPHVB-STY-B2	1.0840	0.0840	6.92	1.2134
	1.0745	0.0745	7.09	1.0512
	1.0546	0.0546	5.84	0.9355
	1.0411	0.0411	5.27	0.7794
	1.0349	0.0349	5.26	0.6627

#### 4.3.5.2 Gel Permeation Chromatography (GPC)

It was possible for us to obtain GPC data for a few samples. The molecular weights obtained along with the polydispersity values are given in Table 4.16. From this data it is suggested therefore that the molecular weights involved are in the order of  $10^4$ . However, the molecular weights obtained from GPC measurements are not entirely accurate. According to the reports of Allen and coworkers, the molecular weight data obtained using absolute methods like membrane osmometry and vapour-phase osmometry are significantly higher than the



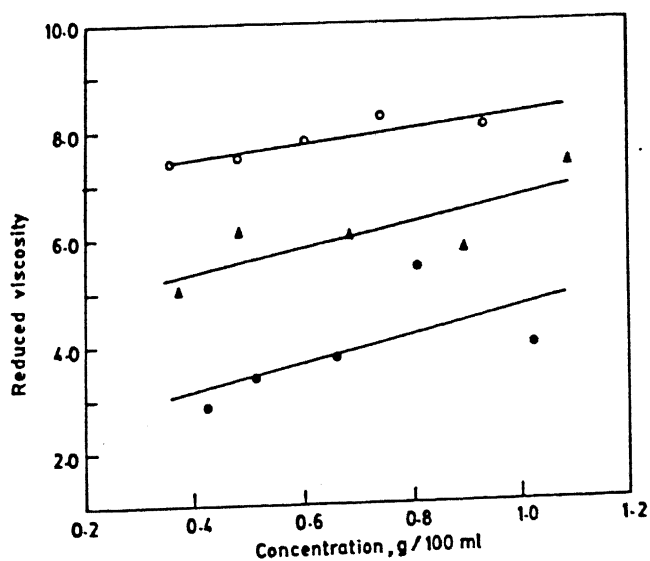


Fig. 4.9.

Reduced viscosity vs concentration plots: ○ CPHVB-MA-B1; △ CPHVB-BA-B4 ● CPHVB-MA-B3

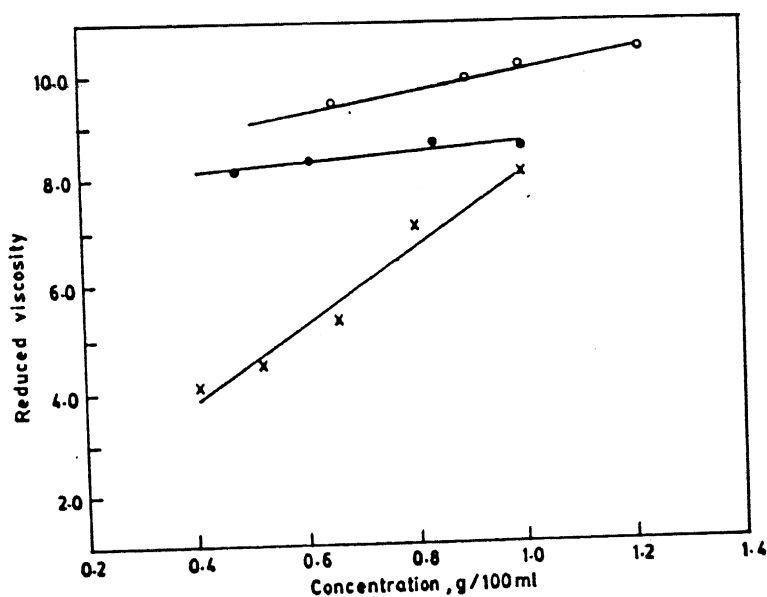


Fig. 4.10.

Reduced viscosity vs concentration plots: ● CPHVB-EA-B2 × CPHVB-EA-3 ○ CPHVB-EA-B1

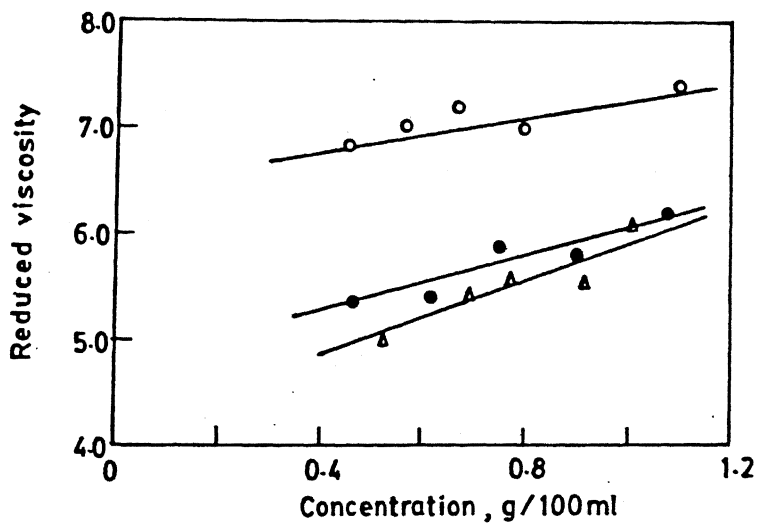


Fig.4.11.

Reduced viscosity vs concentration plots: ○ CPHVB-MMA-B1; ● CPHVB-MMA-B2; ▲ CPHVB-MMA-B3.

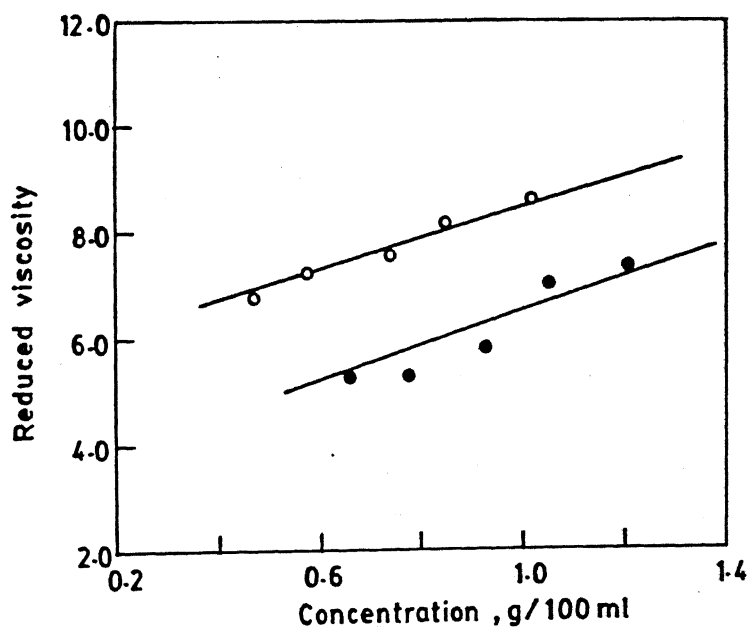


Fig.4.12.

Reduced viscosity vs concentration plots: ○ CPHVB-STY-B1; ● CPHVB-STY-B2.

GPC data. This is due to the fact that polystyrene may not be a good GPC calibrant for poly phosphazenes. The true values are closer to those obtained from the absolute methods. The reason for the low GPC values is probably due to the electrostatic attraction between the phosphazene and phenyl rings, resulting in size of the copolymer over the expected average dimensions of an unperturbed chain. From an inspection of the Table 4.15 , it can be clearly seen the intrinsic viscosities of the copolymers increase with increased cyclophosphazene content. This is in keeping with the high reactivity ratios

Table 4.15

Copolymer	Intrinsic viscosity ( $\frac{g}{cc}$ )	CPHVB in copolymer (%)
CPHVB-MA-B1	6.93	76.84
CPHVB-MA-B4	4.43	68.18
CPHVB-MA-B3	2.12	66.50
CPHVB-EA-B-3	1.20	50.17
CPHVB-EA-B-1	7.75	76.74
CPHVB-EA-B-2	8.45	79.43
CPHVB-MMA-B-1	6.45	72.42
CPHVB-MMA-B-2	4.80	66.27
CPHVB-MMA-B-3	4.15	55.68
CPHVB-STY-B-1	5.58	52.78
CPHVB-STY-B-2	3.34	40.34

Table 4.16

Copolymer	$M_w^{(a)}$	Poly dispersity	CPHVB in copolymer (%)
CPHVB-MA-6	11995	1.88	32.85
CPHVB-EA-8	10450	1.61	55.93
CPHVB-MMA-7	3406	6.28	42.06

( $r_2$ ) obtained for CPHVB in its copolymerization with MA, EA, MMA and styrene (vide infra). Previously, Allen and coworkers have studied the copolymerization of styrene with cyclophosphazene monomers,  $\text{N}_3\text{P}_3\text{F}_5\text{-C}(\text{CH}_3)=\text{CH}_2$ , (1),  $\text{N}_3\text{P}_3\text{F}_5\text{-C}(\text{OEt})=\text{CH}_2$ , (2),  $\text{N}_3\text{P}_3\text{F}_5\text{-C}_6\text{H}_4\text{C}(\text{CH}_3)=\text{CH}_2$ , (3) and have found that increased amounts of cyclophosphazene in the copolymers leads to a decrease in molecular weights. It was proposed that high reactivity of the cyclophosphazene radical and the low homopropagation rate leads to increased occurrence of termination steps in the copolymerization. Since in our systems we find that CPHVB has a high propensity to add on to itself it is not surprising to see increased molecular weights in the copolymers with increased cyclophosphazene content. Similar observations have been made by Inoue and coworkers, in the copolymerization studies of 8 and 9 with styrene.

#### 4.3.6 Reactivity Ratios

In order to understand the reactivity of CPHVB and to compare its reactivity to other cyclophosphazene monomers known in the literature, we have calculated the reactivity ratios for all the four copolymerization systems, viz., CPHVB-MA, CPHVB-EA, CPHVB-MMA, CPHVB-STY. These data were calculated by 2 different methods and are summarized in Table 4.17. It is to be noted that the input values for the more reliable Mortimer Tidwell calculation were derived from Finemann-Ross method. In all the cases one can observe that  $r_2$  (CPHVB) is much greater than one, indicating the large propensity for CPHVB to add to itself. The product  $r_1 r_2 < 1$  except for CPHVB-STY system.

A comparison of the reactivity ratios of the CPHVB systems with that of other cyclophosphazene monomer studied by Allen and coworkers earlier is quite appropriate. In two of Allen's monomers,  $\text{N}_3\text{P}_3\text{F}_5\text{-C}(\text{CH}_3)=\text{CH}_2$  (1),  $\text{N}_3\text{P}_3\text{F}_5\text{-C}(\text{OEt})=\text{CH}_2$  (2), the vinylic functionality is attached directly to the phosphorus of

Table 4.17

Copolymer system	Finemann-Ross method	Mortimer-Tidwell method	Reference
CPHVB-MA	$r_1(\text{MA}) = 0.04$ $r_2(\text{CPHVB}) = 1.55$	$r_1(\text{MA}) = 0.21$ $r_2(\text{CPHVB}) = 2.63$	Present work
CPHVB-EA	$r_1(\text{EA}) = 0.05$ $r_2(\text{CPHVB}) = 1.71$	$r_1(\text{EA}) = 0.09$ $r_2(\text{CPHVB}) = 1.11$	-do-
CPHVB-MMA	$r_1(\text{MMA}) = 0.03$ $r_2(\text{CPHVB}) = 2.48$	$r_1(\text{MMA}) = 0.11$ $r_2(\text{CPHVB}) = 3.41$	-do-
CPHVB-STY	$r_1(\text{STY}) = 0.63$ $r_2(\text{CPHVB}) = 1.20$	$r_1(\text{STY}) = 0.88$ $r_2(\text{CPHVB}) = 1.80$	-do-
$\sim$ 1-STY	$r_1(\text{STY}) = 1.35^{(a)}$ $r_2(\sim) = 2.20$	—	12
$\sim$ 2-STY	$r_1(\text{STY}) = 3.40^{(a)}$ $r_2(\sim) = 0.30$	$r_1(\text{STY}) = 3.04$ $r_2(\sim) = 0.19$	13
$\sim$ 3-STY	—	$r_1(\text{STY}) = 0.41$ $r_2(\sim) = 0.28$	14
$\sim$ 8-STY	$r_1(\text{STY}) = 0.33^{(a)}$ $r_2(\sim) = 0.26$	—	18
$\sim$ 8-MMA	$r_1(\text{MMA}) = 0.49^{(a)}$ $r_2(\sim) = 1.17$	—	18
HVB-STY	$r_1(\text{STY}) = 0.54^{(a)}$ $r_2(\text{HVB}) = 0.53$	—	31
HVB-MMA	$r_1(\text{MMA}) = 0.21^{(a)}$ $r_2(\text{HVB}) = 0.61$	—	31
HVB-MA	$r_1(\text{MA}) = 0.17^{(a)}$ $r_2(\text{HVB}) = 0.34$	—	31
p-HS-STY	$r_1(\text{STY}) = 0.79^{(a)}$ $r_2(\text{STY}) = 1.2$	—	32

(a) by using Mayo-Lewis method.

the inorganic heterocycle. Since, cyclophosphazene moiety has been shown to be  $\sigma$ -electron withdrawing in these two monomers the olefinic functionality suffers a depletion of electron density and hence reduced reactivities are observed. These are reflected in the reactivity ratios. Surprisingly in 1 although Allen observes an  $r_2$  of 1.35 with styrene no homopolymerization of 1 could be formed. Even in 3 ( $\text{N}_3\text{P}_3\text{F}_5-\text{C}_6\text{H}_4-\text{C}(\text{CH}_3)=\text{CH}_2$ ) where the vinyl functionality is separated from the cyclophosphazene moiety by a phenyl substituent, the  $r_2$  (3) is still low.

In comparison with the above cyclophosphazene monomers, in the present system it is seen that the biphenyloxy substituent is very effective in insulating the vinyl functionality from the electron withdrawing effect of cyclophosphazene ring. This accounts for the high  $r_2$  values. Secondly, all Allen's monomers are  $\alpha$ ,  $\alpha'$ -disubstituted olefins and are therefore sterically encumbered. In contrast, in CPHVB only one substituent is present on the olefinic group. Inoue and coworkers have recently reported the copolymerization studies of (10) with styrene. It is clear that the reactivity ratios they have obtained (Mayo-Lewis Method) are not very different from those seen in the present system. It is interesting to note that the copolymerization studies of HVB with styrene, methylacrylate, methyl methacrylate and acrylonitrile (Table 4.17) the  $r_2$  (HVB) values are much higher than  $r_1$  indicating that the HVB prefers to add on to itself. Thus the basic nature of HVB monomer is not altered by substitution on cyclophosphazene ring in CPHVB.

#### 4.3.7 Q-e Scheme

We have used the  $r_1$  and  $r_2$  values obtained from Mortimer-Tidwell method for calculating the Alfrey-Price parameters, Q and e. As discussed earlier in section 4.1.2.2.3; the e and Q values are empirical parameters which describe

the nature of the monomer with respect to the resonance stabilization and polarity of the olefinic centre. The  $e$  and  $Q$  values are summarized for each system in Table 4.18. Since for CPHVB-STY system,  $r_1 r_2 > 1$  we could not obtain the  $Q$  and  $e$  values from this study. It is expected that a given monomer would have unique set of  $Q$  and  $e$  parameters. However, because of the assumptions involved in copolymer equation and in evaluating  $r_1$ ,  $r_2$  values and the experimental errors, one does not obtain the same  $Q$ - $e$  values for given monomer in its copolymerization behaviour with different comonomers. Thus for example, Inoue obtained different  $e$  and  $Q$  values for (8) in its copolymerization with different comonomers.

It can be seen from the Table 4.18 that for CPHVB the  $e$  values are negative and  $Q$  values are positive and greater than unity. A comparison of the  $Q$ - $e$  values of CPHVB with that of HVB and p-hydroxystyrene reveals that the

**Table 4.18**  $e$ - $Q$  values of CPHVB and other cyclophosphazene monomers

Copolymer	$e$	$Q$	Ref
CPHVB-MA	-0.16	1.25	Present work
CPHVB-EA	-1.30	4.17	-do-
CPHVB-MMA	-0.59	4.49	-do-
1-STY	0.18	0.21	12
2-STY	-0.06	0.18	13
3-STY	0.72	0.72	14
8-STY	0.76	0.87	18
8-MMA	1.14	2.02	18
HVB-STY	-1.91	4.48	31
HVB-MMA	-1.03	1.98	31
HVB-MA	-1.05	2.59	31
pHS-STY	-1.03	1.52	32
pHS-MMA	-1.16	1.14	32

nature of the olefin functionality remains unaltered as was seen earlier in the discussion on reactivity ratios. High positive  $Q$  values indicate substantial mesomeric interaction of the olefin functionality with its substituent. It is difficult to comment whether the cyclophosphazene ring is also involved in any mesomeric interaction. However, in view of the similarity of the  $Q$  values of HVB and CPHVB, as well as the invariance of the phosphorus chemical shifts of cyclophosphazene in CPHVB and in the copolymers, it is reasonable to conclude that there is a negligible electronic interaction between the cyclophosphazene ring and the olefinic centre. This reluctance of the phosphazene unit to enter into significant mesomeric interaction with unsaturated organic units has been pointed out earlier<sup>12,33</sup>.

It is also appropriate to compare the  $Q$ - $e$  values of CPHVB with that of other cyclophosphazene monomers. It is quite clear that 1, 2, and 3 have positive  $e$  values which reflect the reduction of the electron density of the olefin functionality by the strong  $\sigma$ -electron withdrawing effect of cyclophosphazene moiety. The presence of an ethoxy substituents at  $\alpha'$ -position in the monomer (2), to some extent counter balances the electron withdrawing nature of the phosphazene ring.

In conclusion, it may be said that the reactivity ratios and the  $Q$ - $e$  values obtained for CPHVB in the various copolymerization studies indicate that the vinyl functionality of the monomer is electron rich and conjugatively stabilized. It is quite clear that the biphenyleneoxy group is very effective in insulating the olefinic centre from the  $\sigma$ -electron withdrawing effect of cyclophosphazene ring.



#### 4.3.8 Conclusions

The results obtained from the present investigation can be summarized as follows:

- CPHVB readily forms copolymers with methyl acrylate, ethyl acrylate, methylmethacrylate and styrene.
- The maximum incorporation of CPHVB in copolymers is as high as 90%, higher than observed in any other phosphazene copolymer.
- All the copolymers are stable and readily soluble in a wide range of organic solvents.
- In all the copolymers the cyclophosphazene group is intact structurally.
- All the copolymers are thermally very stable (char yield > 60 % at 600°C). Even a small percentage incorporation in the copolymer imparts good thermal stability.
- All CPHVB copolymers are fire retardant and act as self extinguishers.
- The molecular weight of the copolymers are in the range of  $10^4$  which is in good agreement with other cyclophosphazene copolymers known in the literature.
- The reactivity ratios and Q values of CPHVB show that it forms block copolymers indicating that the  $\sigma$ - electron withdrawing effect of cyclophosphazene is not felt at the olefinic centre. This is due to the biphenylyloxy group which separates the olefinic centre from the cyclophosphazene.

## REFERENCES

1. (a) "Comprehensive Polymer Science", the Synthesis, Characterization, Reaction and Applications of Polymer, V.1-7, Eds. Allen, G. and Bevington, J.C., Pergamon Press, Oxford(1989).  
(b) "Contemporary Polymer Chemistry", Allcock, H.R. and Lampe, F.W. Printice Hall, New Jersey (1990).
2. Allcock, H.R., *Chem. Eng.*, (1985), 63, 22
3. Rheingold, A. in "Encyclopedia of Polymer Science and Engineering" Eds. Mark; Bikales; Overberger; Menges. 2<sup>nd</sup> Ed., V.8, p 138, John Wiley & Sons, new York (1987). 4. Pittman, C.V.; Carraher, C.E.; Reynolds, J.R. in Ref 3, p 541.
5. Phosphorous-Nitrogen Compounds, Allcock, H.R. Academic Press, New York (1972).
6. (a) Allcock, H.R. and Kugel, R.L.; *J. Am. Chem. Soc.*, (1965), 87, 4216.  
(b) Allcock, H.R.; Kugel, R.L.; Valan, K.J. *Inorg. Chem.*, (1966), 5, 1709.  
(c) Allcock, H.R.; Kugel, R.C., *Inorg. Chem.*, (1966), 5, 1716.
7. Allcock, H.R. *Acc. Chem. Res.* (1979), 12, 351.
8. Potin, Ph. and De Jaegar, R. *Eur. Polym. J.* (1991), 27, 341.
9. (a) Allcock, H.R. ; Evans, T.L. ; Patterson, D.B. *Macromolecules* (1980), 13, 201.  
(b) Allcock, H.R.; Disorcie, J.L.; Harris, P.J. *J. Am. Chem. Soc.*, (1983), 105, 2814.  
(c) Evans, T.L.; Patterson, D.B.; Suszko, P.R.; Allcock, H.R. *Macromolecules*, (1981), 27, 341.
10. (a) Wisian-Neilson, P.; Neilson, R.H. *J. Am. Chem. Soc.* (1980), 102, 2848  
(b) Neilson, R.H; Wilsian-Neilson, P, *J. Macromol. Sci. Chem.* (1981), A16, 425.
11. Wisian-Neilson, P.; Neilson, R.H., *Chem. Rev.* (1988), 88, 541.
12. Du pont, J.G.; Allen, C.W., *Macromolecules*, (1979), 12, 169.
13. Allen, C.W.; Bright, R.P., *Macromolecules*, (1986), 19, 571.
14. Allen, C.W.; Shaw, J.C.; Brown, D.E., *Macromolecules*, (1988), 21, 2653.
15. Inoue, K.; Takagi, M.; Nakano, M.; Nakamura, H.; Tanigaki, T., *Makromol. Chem., Rapid Commun.* (1988), 9, 345.
16. Inoue, K.; Kaneyuki, S; Tanigaki, T., *Macromolecules*, (1989), 22, 1530.
17. Inoue, K.; nitta, H.; Tanigaki, T. *Macromol. Chem. Rapid Commun.*, (1990), 11, 467.
18. Inoue, K.; Kaneyuki, S.; Tanigaki, T., *J. Polym. Sci. Part A: Polym.*

*Chem.*, (1992), 30, 144.

19. (a) Inoue, K.; Nishikawa, Y.; Tanigaki, T. *Macromolecules*, (1991), 24, 3464.  
 (b) Inoue, K.; Nishikawa, Y.; Tanigaki, T.; *J. Am. Chem. Soc.*, (1991), 113, 7609.  
 (c) Inoue, K.; Nishikawa, Y.; Tanigaki, T.; *Solid State Ionics*, (1992), 58, 217.
21. (a) Mayo, F.R., and F.M. Lewis, *J. Am. Chem. Soc.*, (1944), 66, 1594.  
 (b) Mayo, F.R. and C. Walling, *Chem. Rev.*, (1950), 46, 1919.
22. Finemann, M. and Ross S.D. *J. Polymer. Sci.*, (1950), 5, 259.
23. Tidwell, P.W., and Mortimer, G.A., *J. Polym. Sci. Part A*, (1965), 3, 369.
24. Tudos, F. and Kelen, T. *J. Macromol. Sci., Chem.*, (1975), A9, 1.
25. (a) Garcia-Rubio, L.H.; Lord, M.G.; Mac Gregor, J.F.; Hamielec, A.E. *Polymer*, (1985), 26, 2001.  
 (b) Vande Meer, R.; Linssen, H.N.; German, A.L. *J. Polym. Sci., Polym. Chem. Ed.* (1978), 16, 2915.
26. Alfrey, T. Jr.; Young, L.J. "Copolymerization", 2<sup>nd</sup> Ed., Ed. Ham, G.E. Wiley, New York (1971).
27. Young, L.J. "Polymer Handbook", 2<sup>nd</sup> Ed.; Eds. Brandrup, J. and Immergut, E.H., Wiley, New York (1975).
28. Inoue, K.; Nakahara, H.; Tanigaki, T. *J. Polym. Sci. Part A, Polym. Chem.* (1993), 31, 61.
29. "Experiments in Polymer Science", Collins, E.A.; Bares, J.; Billmeyer, F.W. Jr., John Wiley & Sons, New York (1973).
30. Vogel's "Text book of Organic Chemistry", Furniss, B.S.; Hannaford, A.J.; Smith, P.W.; Tatchell, A.R. 5<sup>th</sup> Ed. ELBS/Longman, UK (1989).
31. Tanigaki, T.; Shirai, M.; Inoue, K. *Polymer J.* (Tokyo), (1987), 19, 881.
32. Kato, M. *J. Polym. Sci. A-1*, (1969), 7, 2175.
33. Allen, C.W.; Toch, P.L.; Perlman, M.; Brunst, G.; Green, J.C. *Int. Conf. Chem. Inst. Can. Am. Chem. Soc., Abstr. Inorg.*, 63, Montreal, (1977).